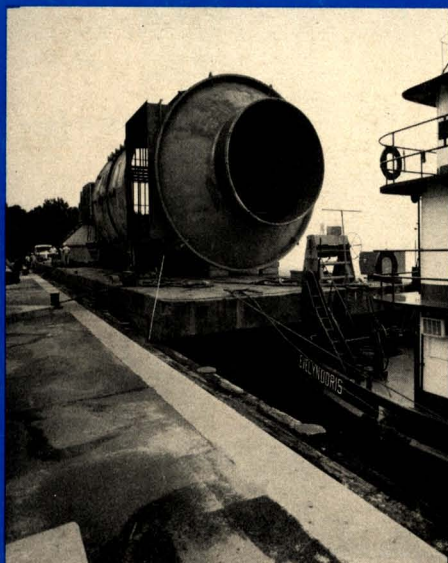


ENVIRONMENTAL PROGRESS

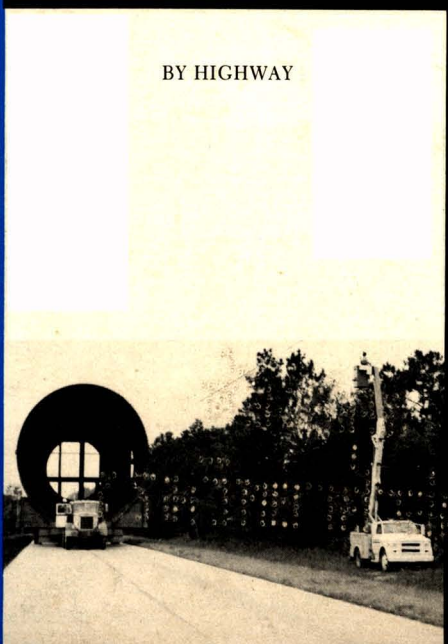
May 1984
Vol. 3, No. 2



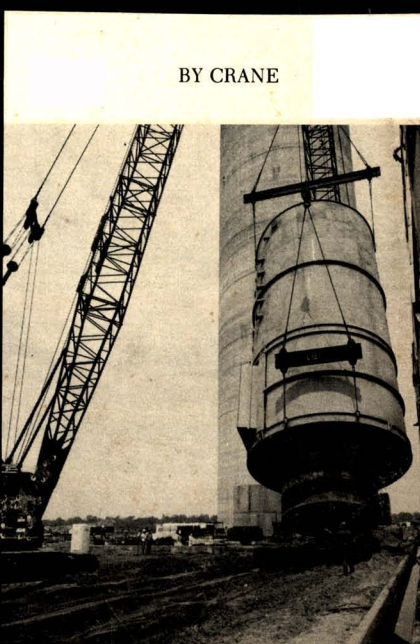
BY BARGE



BY FLAT-BED



BY HIGHWAY



BY CRANE

CONTENTS

Editorial	M2
Environmental Shorts	M3
Chemical Emissions from Surface Impoundments <i>Louis J. Thibodeaux, David C. Parker and Howell H. Heck</i>	73
Improved Estimates of Sulfate Dry Deposition in Eastern North America <i>Marvin L. Wesely and Jack D. Shannon</i>	78
Simultaneous Wastewater Concentration and Flow Rate Equalization <i>James W. Patterson and Jean-Paul Menez</i>	81
New Solutions to Industrial Waste Management	<i>Linda M. Curran</i> 88
Solving Environmental Challenges of Indirect Coal Liquefaction <i>Margaret M. Lobnitz and Michael G. Webb</i>	91
Reverse-Osmosis Membrane for Treating Coal-Liquefaction Wastewater <i>D. Bhattacharyya, M. Jevtitch, J. Ghosal and J. Kozminski</i>	95
In-Situ Biological Oxidation of Hazardous Organics <i>D. L. Michelsen, D. A. Wallis and F. Sebba</i>	103
Oil Shale—Potential Environmental Impacts and Control Technologies .. <i>E. R. Bates, W. W. Liberick and J. Burckle</i>	107
A Methodology for Predicting Fugitive Emissions for Incinerator Facilities	<i>G. A. Holton and C. C. Travis</i> 116
The Environmental Representative Program	<i>Bruce P. McLeod</i> 121
Recovery Process for Complexed Copper- Bearing Rinse Waters	<i>R. M. Spearot and J. V. Peck</i> 124
Surface Area of Calcium Oxide and Kinetics of Calcium Sulfide Formation <i>Robert H. Borgwardt, Nancy F. Roache and Kevin R. Bruce</i>	129
Mineral Processing Water Treatment Using Magnesium Oxide .. <i>Joseph E. Schiller, Daniel N. Tallman and Sanaa E. Khalafalla</i>	136
Environmental Division Newsletter	M5

Environmental Progress is a publication of the American Institute of Chemical Engineers. It will deal with multi-faceted aspects of the pollution problem. It will provide thorough coverage of abatement, control, and containment of effluents and emissions within compliance standards. Papers will cover all aspects including water, air, liquid and solid wastes. Progress and technological advances vital to the environmental engineer will be reported.

AICHE EXECUTIVE DIRECTOR
J. C. Forman

PUBLICATIONS DIRECTOR
Larry Resen
(212) 705-7335

EDITOR
Gary F. Bennett
(419) 537-2520

PRODUCTION EDITOR
Maura Mullen
(212) 705-7327

ASSOCIATE EDITOR
Claudia M. Caruana
(212) 705-7317

TECHNICAL EDITOR
Waldo B. Hoffman
(207) 729-3701

EDITORIAL REVIEW BOARD
D. Bhattacharyya
R. Lee Byers
S. L. Daniels
T. H. Goodgame
P. Lederman
R. Mahalingham
C. J. Touhill
Andrew Benedek
J. A. Scher
Leigh Short
R. Siegel
Andrew Turner

Publication Office, 215 Canal Street, Manchester, N.H. Published quarterly by the American Institute of Chemical Engineers, 345 East 47 St., New York, N.Y. 10017. (ISSN 0278-4491). Manuscripts should be submitted to the Manuscript Center, American Institute of Chemical Engineers, 345 East 47 St., New York, N.Y. 10017. Statements and opinions in *Environmental Progress* are those of the contributors, and the American Institute of Chemical Engineers assumes no responsibility for them. Subscription price per year: AIChE members \$20; others \$40. Single copies \$15. U.S. postage is prepaid. Outside the U.S. please add \$5 per subscription. Payment must be made in U.S. dollars. Second-class postage paid at New York, N.Y. and additional mailing offices. Copyright 1984 by the American Institute of Chemical Engineers.

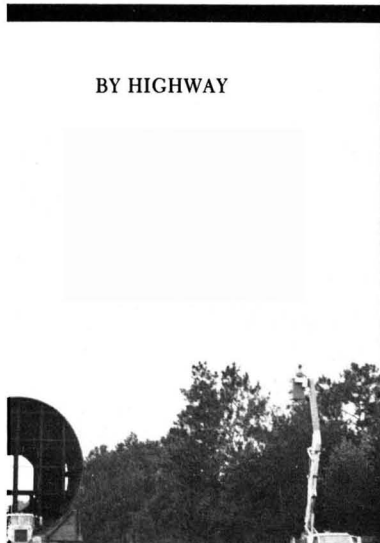
Postmaster: Please send change of addresses to Environmental Progress, AIChE, 345 East 47 Street, New York, N.Y. 10017.



BY BARGE



BY FLAT-BED



BY HIGHWAY



BY CRANE

Flue gas desulfurization system supplied by Peabody Process Systems to Seminole Electric Co-op included five absorbers 30 ft. in diameter and 80 ft. high.

Reproducing Copies

Authorization to photocopy items for internal or personal use, or the internal or personal use of specific clients, is granted by AIChE for libraries and other users registered with the Copyright Clearance Center (CCC) Transactional Reporting Service, provided that the \$2.00 fee is paid directly to CCC, 21 Congress St., Salem, MA 01970. This consent does not extend to copying for general distribution, for advertising or promotional purposes, for inclusion in a publication, or for resale.

Environmental Progress fee code: 0278-4491/84 \$2.00

ห้องสมุดกรมวิทยาศาสตร์บริการ

15.00000

Trends in Acid Rain Have Changed, New Research Shows

The acidity of precipitation has changed little in recent years in the Northeast, but appears to be increasing locally in other regions of the country, according to a new review prepared by the U.S. Geological Survey.

This report summarizes the findings of more than 200 published reports of acid rain research projects conducted by the USGS and other scientists over the past 30 years. The acidification of both precipitation and surface waters is discussed in three broad geographical areas—the midwestern-northwestern United States and southeastern Canada; the southeastern United States, and the western United States.

Author of the report, John T. Turk, a research hydrologist with the USGS in Denver, Colo., said that "When the results of the many individual studies are combined, they show that acidification of precipitation in the Northeast, which has the most damaging level of acidity on a regional basis, occurred primarily before the mid-1950s and has been largely stabilized since the mid-1960s."

Turk also concluded that surface waters in lakes and streams in the Northeast have followed a pattern of acidification similar to that of precipitation. The acidification of surface waters occurred before the mid-to-late-1960s. Since that time, some waters show a lack of further acidification, whereas other streams, which are monitored as part of a national USGS network, show a slight recovery.

Copies of the 18-page report, "An Evaluation of Trends in the Acidity of Precipitation and Related Acidification of Surface Water in North America," are available for \$2.75 each. They are available from the Branch of Distribution, Text Products Section, U.S. Geological Survey, 604 S. Pickett St., Alexandria, Va. 22304. Specify Water-Supply Paper 2240, and include a check or money order made payable to the Department of the Interior, U.S. Geological Survey.

CHEMICAL ENGINEERING PROGRESS

CEP, the official periodical of the American Institute of Chemical Engineers, circulates to over 58,000 subscribers every month.

This important publication has kept the chemical process industry apprised of the state-of-the-art and developing technologies since 1947.

Sample topics covered in the Scope section of 1983 issues included:

- Safety in Design: An Ethical Viewpoint.
- The Contractor's Marketing Effectiveness.
- The Future of the European Fertilizer Industry.
- Propylene Feedstock: Supply and Demand.
- Ammonia Plant Shutdowns.

Sample articles in 1983 issues included:

- New Radiant Coil Technology.
- Standardized Pilot Plant Procedures.
- Optimum Efficiency in the Recovery Area.
- Improved Evaporators for Radioactive Wastes.
- Recent Developments in Coal Gasification.
- Wastewater Rinse and Recycle in Petroleum Refineries.
- Automatic Humidity Control of Dryers.
- Technical Challenges to Heavy Oil Conversion.
- How to Reduce Costs in Amine Sweetener Units.
- Survey of the Incinerator Manufacturing Industry.
- Cost-Effective Mechanical Vapor Recompression.
- Profile of a Successful Computer Control Project.

Regular features include coverage of the Washington, D.C. scene, new books, future meetings, new equipment and materials, employment services, and Institute news.

1984 Annual Subscription: \$35. Foreign Postage Extra: \$10.

IMPORTANT: ALL DUES PAYING MEMBERS OF AIChE AUTOMATICALLY RECEIVE MONTHLY ISSUES OF CEP AS PART OF THEIR MEMBERSHIP DUES.

CEP SUBSCRIPTION ORDER FORM

Mail to: AIChE Subscription Dept.
345 East 47 Street
New York, NY 10017

Name _____

Company (if applicable) _____

Address _____

City _____ State _____ Zip _____

Check or Money Order drawn on a U.S. bank. U.S. \$ _____ enclosed.

Chemical Emissions from Surface Impoundments

A practical method for the field measurement of volatile-chemical emission rates from wastewater-treatment basins.

Louis J. Thibodeaux, David G. Parker, and Howell H. Heck, University of Arkansas, Fayetteville, Ark. 72701

Wastewater and other liquids placed in surface impoundments are often the source of volatile chemical emissions to air. The overall objective of this work was to determine the magnitude of the flux rate of organic compounds that are emitted into the air from selected wastewater-treatment facilities for the pulp and paper industry. In order to make these measurements, it was necessary to develop a field-sampling methodology, hereafter called the concentration profile method (CPM), and a laboratory-analysis methodology to trap and measure low-molecular weight, volatile organics in air.

Various organizations, including the chemical process industries, and federal and state agencies, are concerned about aspects of air emissions from wastewater-treatment basins. In some cases, efforts are aimed at odor control. In other cases, there is concern for the emission of hazardous substances, which originate from surface impoundments, into the air. There is also a general concern for emission of vapor-phase organics and inorganics from wastewater-treatment basins. The placement of organic compounds (non-sulfurous) in these basins gives rise to vapor-phase organic (non-methane) emissions that increase the quantity of hydrocarbons in the nearby air mass. In this regard, attention has been focused on wastewater-treatment basins as a source of potentially hazardous trace contaminants to air.

As a result of interest generated during an EPA demonstration project with Georgia Kraft Company, that evaluated the effectiveness of cooling towers as a combined wastewater cooling, biotreatment, and stripping operation, research was initiated at the University of Arkansas to develop an apparatus to quantify the air-strippable organic fraction in industrial wastewater [1, 2]. A mathematical simulation of air-stripping and natural desorption from aerated stabilization basins suggested that a significant quantity of volatile organic material is escaping treatment by the air route [3]. Further studies of raw wastewaters representing a broad spectrum of industrial operations including the wood-products industry suggested that a significant fraction of the discharged organic material was volatile and easily stripped by air [4]. Gas chromatograph/mass spectrometer analysis of organic compounds in treated Kraft-mill wastewater indicates that many of these compounds are know volatile chemicals (5).

There is no question that quantities of chemicals are escaping through the air-water interface of wastewater-treatment facilities. The question is how much of what chemicals are desorbing. Due to various sinks for chemicals in the facilities, which include water seepage, biochemical oxidation, adsorption upon the sediments and particulate matter, etc., a realistic approach to quantifying

the flux to the air is to perform measurements in the air boundary layer immediately above the water surface. The method presented is a variation of the "aerodynamic method" employed to measure the flux of pesticides from soil surface [6]. A similar technique was employed to measure the flux of a pesticide from a flooded alfalfa field [7].

THEORY OF METHOD

One prime objective of the science of micrometeorology is to study the atmospheric boundary layer to obtain tractable expressions for the fluxes of heat, momentum, water vapor, and other atmospheric constituents. The complexity of turbulence is such that so far only semi-empirical relationships have been developed, and micrometeorologists continue to work on refinements. However, from a practical standpoint, the science can be used in its present form, within proper limitations, to obtain chemical-flux estimates from surface impoundments.

In air flow over a large region, the effects of the Earth's frictional forces induce the creation of a boundary layer. The boundary layer extends, by definition, to the height at which velocity is about 99% of that in the free air above. The size of the atmospheric boundary layer depends, of course, on the wind speed and on the type of terrain, but it is usually of the order of 1000 m. Beyond this layer is an environment free of viscous or turbulent shear called the free layer. In the absence of shear stresses, the motion of the free layer is strongly governed by the rotation of the Earth and, consequently, is given the name of geostrophic layer, where the motion is called geostrophic.

Below the free layer is the outer layer or the Ekman layer, which is influenced by Coriolis, pressure, and Reynolds stresses. Near the surface, in a layer a few meters high, the mean velocities are small and, consequently, the inertia and the Coriolis forces, which depend on velocity, are negligible compared to the shear forces (viscous and Reynolds), which appear to be constant in this inner layer. Each mountain, building, levee, or surface feature of varying roughness or height has its effect on the air stream passing over it, and a local boundary layer equilibrated to each surface develops within the inner layer. Figure 1 illustrates the development of a local boundary layer above a surface impoundment. It is in this local boundary layer of the inner atmospheric layer that micrometeorological techniques can be utilized to obtain emission flux rates from surface sources.

The flux rate of chemical from the water surface in the re-established boundary layer is:

$$n_A = -(\mathcal{D}_{A1} + \mathcal{D}_{A1}^{(w)}) d\bar{p}_{A1}/dy \quad (1)$$

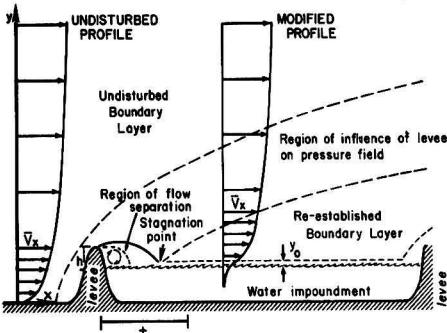


Figure 1. Boundary layers above a surface impoundment.

L (Obukhov scale length) in cm is given by:

$$L = -\rho_1 c_p v^3 T_1 / k g q \quad (5)$$

where: g is the gravitational acceleration 980.7 cm/s^2 . This length was conceived by Obukhov to be the height above the surface at which the mechanical energy production is equal to the buoyant energy production and serves as a characteristic height which determines the structure of the surface layer.

Businger [8] correlated wind-shear observations, ϕ_m , from micrometeorological measurements with dimensionless height, ζ , created from the Obukhov scale length. Several other investigators have developed diabatic correlations by relating ϕ_m directly to the Richardson Number, Ri . These efforts have been summarized by Rosenberg [9] and include the work of Holzman, Panofsky, Lumley, Dyer, Hicks, Webb, Oke, Swainbank, Businger, and Rider, and involve relations of the form

$$\phi_m = (1 \pm b Ri)^{-1/n} \quad (6)$$

where b and n are empirically determined constants and the sign relates to the stable or unstable case. Temperatures are necessary to compute the Richardson Number, which can be expressed in finite difference form:

$$Ri \approx \frac{g}{T_1} \frac{(\bar{T}_{12} - \bar{T}_{11})(y_2 - y_1)}{(\bar{v}_{x2} - \bar{v}_{x1})^2} \quad (7)$$

where subscripts denote elevation points 1 and 2. The correlations have limited Ri applicability stable, $|Ri| \leq 1.0$ and unstable $|Ri| \leq 4.0$.

In 1939, Thornthwaite and Holzman developed a gradient method for determining the flux of water vapor from land and water surfaces. Their procedure assumed $\mathcal{D}_{A1}^{(0)}/\nu_1^{(0)} = 1$, and was only reliable under near-adiabatic conditions. In the case we want to study, the transfer of a trace constituent to the atmosphere, it is advantageous to link it to the transfer of water vapor. Brooks and Pruitt [10] developed and presented the modified Thornthwaite-Holzman Equation for water-vapor flux above a crop surface:

$$n_A = \frac{k^2 (\bar{v}_{x2} - \bar{v}_{x1})(\bar{P}_{A12} - \bar{P}_{A11})}{\phi_m^2 Sc_{A1}^{(0)} [\ln[(y_2 - d)/(y_1 - d)]]^2} \quad (8)$$

where: n_A is the flux rate of water in $\text{g/cm}^2 \cdot \text{s}$
 $Sc_{A1}^{(0)}$ is the turbulent Schmidt number (i.e., $Sc_{A1}^{(0)} = \nu_1^{(0)}/\mathcal{D}_{A1}^{(0)}$)
 d (cm) is the zero displacement for the crop which replaces y_0 for flat surfaces.

Equation (8) requires two observations of velocity, concentration, and temperature at exactly the same heights and this somewhat limits its utility. It has been found that $Sc_{A1}^{(0)}$ was not unity but also related to Ri .

In the case of several closely spaced sensors and samplers positioned at unequal distances from the surface in the lower two meters of the boundary layer, Equation (8) is cumbersome to use for flux calculations. Relations involving profiles in this region, using up to six observations of concentration and velocity, are more flexible. Equation (2) can be integrated with the use of Equation (4) to yield the velocity-profile equation for neutral and non-neutral conditions:

$$\bar{v}_x = \frac{v_* \phi_m}{k} (\ln y - \ln y_0) \quad (9)$$

In a similar fashion Equation (1) can be integrated for trace constituent B with

$$\mathcal{D}_{B1}^{(0)} = (\mathcal{D}_{B1}/\mathcal{D}_{A1})^{2/3} k v_* y / \phi_m^2 m Sc_{A1}^{(0)} \quad (10)$$

where the molecular-diffusivity ratio, $(\mathcal{D}_{B1}/\mathcal{D}_{A1})^{2/3}$, corrects the turbulent diffusivity of water vapor for the chemical

where: n_A is the flux rate in $\text{g/cm}^2 \cdot \text{s}$
 \mathcal{D}_{A1} is the molecular diffusivity in cm^2/s
 $\mathcal{D}_{A1}^{(0)}$ is the turbulent diffusivity in cm^2/s
 \bar{P}_{A1} is the time-smoothed average atmospheric concentration of A in g/cm^3
 y is the distance from the water surface in cm.

With expressions for the gradient and diffusivities and field measurements of concentration and micrometeorology, Equation (1), in principle, can be used to estimate the flux rate. Similar phenomenological expressions apply for the transport of momentum:

$$\tau = \rho_1 (\nu_1 + \nu_1^{(0)}) d\bar{v}_x/dy \quad (2)$$

and sensible heat:

$$q = -\rho_1 c_p (\alpha_1 + \alpha_1^{(0)}) d\bar{T}_1/dy \quad (3)$$

in the re-established boundary-layer region,

where: τ is the shear stress in the surface layer in $\text{g/cm} \cdot \text{s}^2$

ρ_1 is the air density in g/cm^3
 ν_1 is the kinematic viscosity of air in cm^2/s
 $\nu_1^{(0)}$ is the turbulent viscosity in cm^2/s
 \bar{v}_x is the time-smoothed x -component of the wind velocity in cm/s
 q is the sensible heat flux from the water in $\text{J/cm}^2 \cdot \text{s}$
 c_p is the specific heat of air in $\text{J/g} \cdot \text{K}$
 α_1 is the thermal diffusivity in cm^2/s
 $\alpha_1^{(0)}$ is the turbulent thermal diffusivity in cm^2/s
 \bar{T}_1 is the time-smoothed air temperature in K.

The inner or surface layer is usually defined as the logarithmic layer and is the lowest part of the boundary layer where the fluxes may be considered independent of height. This is approximately the case in the lowest 10 to 20 meters. In this layer, the interaction with the water surface is very strong and adjustments to the surface conditions are relatively rapid. A quasi-steady state, with respect to the build-up of the surface boundary layer may, therefore, often be assumed. The logarithmic profile applies only to the pure turbulent region of the surface boundary layer, where the Reynolds stresses predominate. Neutral or near-neutral conditions exist only for short periods at sunrise and sunset or on overcast days when the air and soil are at or near the same temperature. The diabatic surface layer is different from the neutral surface layer because the turbulent structure is affected by the presence of a heat flux. When non-neutral conditions exist, the slope of the wind profile deviates significantly from the logarithmic ideal.

The correct form for the turbulent viscosity, for use under all stability conditions is:

$$\nu_1^{(0)} = k v_* y / \phi_m \quad (4)$$

where: v_* is the friction velocity in cm/s
 k is van Karman's constant (0.40)
 ϕ_m is a function of y/L

constituent of concern. Integration yields the concentration-profile equation:

$$\bar{p}_{B1} = \rho_{B1} \Big|_{y_0} - \frac{n_B \phi_m S_{C_{A1}}^{(0)}}{(\partial \bar{v}_x / \partial A_1)^{2/3} k v} (\ln y - \ln y_0) \quad (11)$$

where $\rho_{B1}|_{y_0}$ is the concentration of species B at $y = y_0$. It should not be inferred that Equations (9) and (11) are linear throughout the two-meter sample zone.

Field observations of \bar{v}_x and \bar{p}_{B1} may be displayed graphically (or analytically), according to Equations (9) and (11), as \bar{v}_x vs. $\ln y$ and \bar{p}_{B1} vs. $\ln y$ to yield profiles. With the control of up to six observations of each variable, straight lines may be fitted (least squares or visually) to portions of or the entire profile. The slopes of the velocity-profile line, S_p , in cm/s and the concentration-profile line, S_c , in g/cm³, can now be used to obtain an estimate of the flux rate of chemical B. Using the slope terms of the linear Equations (9) and (11) ...

$$n_B = -(\partial \bar{v}_x / \partial A_1)^{2/3} S_p S_c k^2 / \phi_m^2 S_{C_{A1}}^{(0)} \quad (12)$$

Ri should be calculated in the same region that S_p and S_c were extracted. It should be noted that a construction of velocity and concentration profiles under diabatic and neutral conditions requires a knowledge of y_0 and $\rho_{B1}|_{y_0}$; however, the effect of these variables is not felt when only gradients are considered. In reality, Equation (12) is a more flexible version of the modified Thornthwaite-Holzman equation (i.e., Equation (8)), and both employ gradients. S_p will be a negative number for the net loss of a trace constituent from a surface so that the flux is positive. If S_p is positive, then deposition at the water surface is indicated.

The diabatic velocity-profile correction factor, ϕ_m , and the turbulent Schmidt number, $S_{C_{A1}}^{(0)}$, are available for a limited range of Richardson numbers. The data on ϕ_m vs. Ri is rather exhaustive, but that for $S_{C_{A1}}^{(0)}$ is small and limited to observations on water vapor. The field data supporting these two empirical functions likely contain the highest degree of fluctuations and will cause a sizable range of uncertainty in flux computations. For example, under stable conditions at Ri = -1.0, the product $\phi_m^2 S_{C_{A1}}^{(0)}$ ranges from 5 to 10 [10]. This will cause a factor-of-two variation in n_B . Brooks and Pruitt [10] developed a correction factor that combines ϕ_m and $S_{C_{A1}}^{(0)}$:

$$(\phi_m^2 S_{C_{A1}}^{(0)})^{-1} = (1 \pm 50 Ri)^{-1/2} \quad (13)$$

where -50 and +1/2 apply for unstable and +50 and -1/2 apply for the stable case.

With respect to slope determinations from concentration and velocity logarithmic profiles, S_p will likely contain more variation than S_c , because of the difficulty of the atmospheric chemistry determinations at the low level of the trace constituents normally encountered. However, with methanol we have obtained five profile-slope observations from a surface impoundment with correlation coefficients of 0.964 or better. Long sample times up to two hours and/or larger samples will minimize the uncertainty in S_p and S_c .

Molecular diffusivities are known with a relatively high degree of accuracy (i.e., $\pm 5\%$). The 2/3 power of this correction factor is borrowed from turbulent boundary-layer evidence on flat plates.

Working Equations for the CPM

Field measurements of the concentration of the chemical in air, \bar{p}_{A1} , wind speed, \bar{v}_x , and temperature \bar{T}_1 , within the turbulent boundary, no more than two meters above the water surface, need be made. Six observations of each variable, distributed in a logarithmic fashion from the water surface, taken well downwind of any wind-velocity disturbances, should be made. See the report by Thibodeaux, et. al [11] for other limitations on the

sampling methodology. Based on these measurements, Equation (12) is used to determine the vertical flux of the chemical (i.e., species B) from the water surface.

Since the air sampling is done so close to the water surface, only the vertical flux is needed to assess the emission rate from the water surface.

The flux rate, n_B , is in grams of species B per second per square centimeter of water surface (g/s · cm²). S_p is the slope of a line from a graphical plot (or linear regression, computer-generated) of \bar{p}_{A1} (g/cm³) vs. $\ln y$, where y is the sample height above the water surface, in cm. Figure 2 is an example of such profiles. For the flux of chemical B from the water surface, the slope should be a negative number of units, g/cm³. S_c is the slope of a line from a similar relation between \bar{v}_x (cm/s) vs. $\ln y$. This slope should be a positive number and have units of cm/s. The combination of the units of S_p and S_c is the units of flux.

Only if the air boundary layer is neutral should the concentration and velocity vs. \ln -height profiles be linear over the entire range of the six observation heights. The profiles may be non-linear under stable and unstable micrometeorological conditions and may display some curvature. In this case, the slopes of tangent lines drawn to the profiles in the boundary-layer region nearest to the water surface should be used for S_p and S_c .

The stability category of the air boundary layer is obtained by determining the Richardson Number. The Richardson Number (i.e., Ri) is computed from temperatures and wind velocities in the boundary layer by Equation (7). The three equations (7), (12), and (13) are the working formulas of the concentrations-profile method.

Materials and Methods

Air samples were obtained within a two-meter height above the water surface from the prow of a boat facing into the wind. Six simultaneous samples, obtained from heights positioned in a logarithmic fashion, were obtained at a fixed location (i.e., at anchor) on the impoundment surface. Figure 3 illustrates the sample apparatus arrangement.

Air from each location was drawn through the extender tubing to a steel U-tube trap in a 300-ml Dewar flask containing liquid oxygen. Each trap was packed with 30-40 mesh glass beads. Water vapor, methanol, acetone, acetaldehyde, and other volatile organics were condensed and frozen onto the surface of the beads. One liter of air could be drawn through each trap before plugging problems developed. Rotameters were used to measure the air sampling rate.

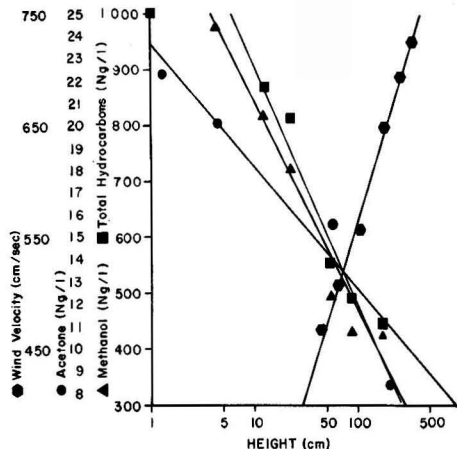


Figure 2. Field data from Mill 2. Sample trip 1.

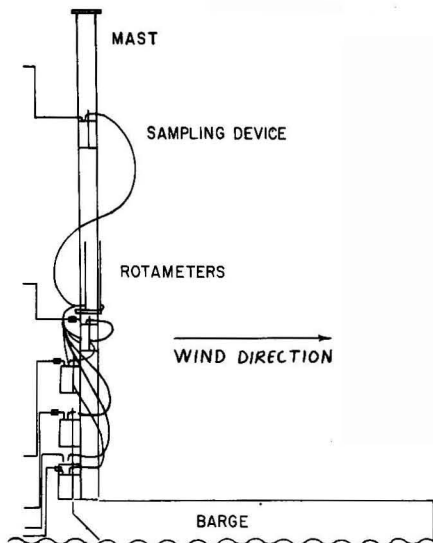


Figure 3. Concentration mast in place in barge.

The wind-profile system (Thorntwaite Associates Model) consisting of a 3.3-meter mast with six anemometers, a wind-direction unit, digital indicators, and recorder, was used to obtain the velocity profile during the sampling period. Temperature profiles, wet and dry-bulb, were obtained by traversing an aspirated, shielded thermocouple device (Atkins Technical, Inc. model) up and down a separate mast.

The concentrations of acetone, methanol, and acetaldehyde were determined using a microprocessor-controlled Perkin-Elmer Sigma 3 gas chromatograph (GC) fitted with a flame-ionization detector (FID). Sample U-tubes were thermally desorbed with a 2000-watt, 200°C heat gun. The condensables were transferred to a capillary trap prior to entering the GC. The column used was a "waterproof" Chromasorb 102 column 2 m long and 3.8 mm in diameter obtained from Supelco. Permeation tubes (Dynacalibrator Model 220-F) were used to calibrate the sampling tube-gas chromatograph system for methanol, acetone, and acetaldehyde. Further details of the sampling and analysis procedure are available [11, 12].

Field Studies

The field test program was performed over the period of February to June 1980. Four aerated basins adjacent to four pulp and paper mills in central and southeastern Arkansas were sampled. Table 1 contains some general in-

TABLE 1. MILL AERATED STABILIZATION BASIN DATA

Mill No.	1	2	3	4
Water flow (mgd)	50	30	4	10
Detention time (days)	12.5	13.8	4	25
Depth (feet)	7.5	10	7	10
Surface area (acres)	265	85	7	110
Surface aerators (No.)	25	32	10	8
Power per aerator (hp)	75	75	20	100
Water temperature (°C), Trip 1	25	28	34	36
Water temperature (°C), Trip 2	29	34	36	35
Air temperature (°C), Trip 1	24	20	28	30
Air temperature (°C), Trip 2	27	25	24	27
Wind speed (mi/hr), Trip 1	2.8	16	7.4	11
Wind speed (mi/hr), Trip 2	4.4-8.0*	13	7.5	6.2-12*
Methanol in water (mg/liter) -1	26	17	12	10
Methanol in water (mg/liter) -2	15	29	0	6.9

* Denotes morning and afternoon values.

formation for each surface impoundment. Each site was sampled twice. Mill No. 1 was an integrated, 1270 mt/d, bleached-Kraft mill processing pine and hardwood, No. 2 was also a bleached-Kraft mill producing 1820 mt/d, No. 3 was a un-bleached Kraft mill producing 320 mt/d, and No. 4 was a Kraft mill producing 420 mt/d. Mills 1, 2, and 3 are fifteen or more years old, while Mill 4 went on stream in 1979.

RESULTS AND DISCUSSION

It is of interest to establish the range of chemical concentrations observed in the aerodynamic boundary layers above the respective wastewater-treatment basins. Table 2 summarizes the concentrations of methanol, acetone, and total hydrocarbon (GC/FID) at each site and for each trip. With few exceptions, the maximum concentration was observed at the lowest sample point, which was usually a few centimeters above the water surface. The maximum reported concentration is that single high value observed for that chemical on that particular trip. The average value reported represents all samples at all heights. Average values of the concentration at the uppermost sample point, usually two meters above the water surface, are also given in the table. It is apparent from this table of concentrations that the water surface is the source of the volatile chemicals. Figure 2 is an illustration of a typical profile. This variation with height reflects the general characteristics of the thirty-eight profiles obtained in the field. Based on peak area, at least sixty to eighty-five percent of the total hydrocarbon fraction was methanol.

Graphs of each profile, similar to those shown in Figure 2, were prepared for each chemical. Data points reflecting obviously erroneous chemical analyses were discarded. Erroneous analyses were often due to improper GC integrator-peak separation, leaks in the sample line downstream of the U-tube traps, and inadvertent dipping of the extension tube into the water or the foam layer.

Each set of from 4 to 6 observations was processed on a statistical linear-regression computer program. The slope (with appropriate sign), standard error of the estimate, multiple-correlation coefficient (one dependent variable only), and the *t*-value for the slope (with appropriate sign) were extracted from the print-out.

TABLE 2. CONCENTRATIONS IN THE BOUNDARY LAYER

Site/Trip	Parameter	Methanol (ng/liter)	Acetone (ng/liter)	Total Hydrocarbon (ng/liter)
Mill 1, Trip 2	maximum	868	51.9	1020
	average	271	23.9	655
	at 2 meters	101	11.6	199
Mill 1, Trip 3	maximum	3400	81.6	3540
	average	1130	44.1	1360
	at 2 meters	522	22.6	543
Mill 2, Trip 1	maximum	1180	22.9	1260
	average	612	18.2	773
	at 2 meters	636	10.3	443
Mill 2, Trip 2	maximum	2090	52.6	3150
	average	768	35.3	902
	at 2 meters	48.5	8.5	66.9
Mill 3, Trip 1	maximum	366	26.0	569
	average	233	19.5	—
	at 2 meters	51.8	7.4	—
Mill 3, Trip 2	maximum	359	153	1280
	average	85.3	35.0	335
	at 2 meters	22.5	13.1	65
Mill 4, Trip 1	maximum	2030	43.6	2120
	average	807	33.1	1130
	at 2 meters	23.8	—	127
Mill 4, Trip 2	maximum	481	43.3	1260
	average	231	31.8	484
	at 2 meters	55.7	6.7	363

The slopes were based on all the selected data within the two-meter boundary layer. In almost all instances, the wind profiles (i.e., \bar{v}_x , vs. $\ln y$) were perfectly linear and this was the basis on which the decision to use all the data was made. Data scatter inherent in the chemical profiles precluded any detection of non-linearity from the respective graphs. The correlation coefficient for the wind profiles are very near unity in most cases, and always greater than that for the chemical profiles. On occasion, chemical-profile slopes were positive. This suggests that methanol is being absorbed by the water surface at this point on the basin.

The Richardson number was calculated from two dry-bulb temperatures and two wind-velocity observations at approximate heights of 20 cm and 200 cm above the water surface using Equation (7). All conditions of stability were encountered. No temperature profiles were taken at the Mill 3 site. The available boat at this site was too small to accommodate the temperature-profile apparatus. Neutral stability was assumed in making the flux calculation for Mill 3.

Individual flux calculations for Mill 2 appear in Table 3. The stability-correction factor in column 2 was obtained from Equation (13). Diffusivity corrections are as follows: $(D_{B1}/D_{A1})^{2/3} = 0.711$ for methanol, 0.626 for acetone and 0.711 for total hydrocarbon.

No major surface discontinuities were present on or near the lagoon surfaces upwind of the sample sites except on May 30 at Mill No. 3. Most profiles were obtained at locations where height-to-fetch ratios were at least 1 to 50. Profiles near the berm where this ratio was not present are noted by superscript in column 1 of Table 3.

TABLE 3. MEASURED CHEMICAL FLUX RATES FROM WATER SURFACE

Mill and Sample No.	Stability Correction $\{\phi_{sc}^{(0)}\}^{-1}$	Flux Rate, (ng/cm ² · s)		
		Methanol	Acetone	Hydrocarbon
2-1-S1*	1.21	1.7	.021	1.6
S2	1.32	5.2	.019	5.3
S3	1.30	3.2	.0039	3.5
S4	1.36	5.2	.063	4.9
S5*	1.14	2.3	—	2.7
2-S-S1*	1.11	1.2	—	1.5
S2	1.29	.16	-.011	-.14
S3	1.05	2.1	.029	2.2
S4*	1.17	2.7	.066	2.9
S5	—	2.0 ⁺	.082	5.5
S6	1.53	4.0	.13	2.4

* Denotes flux rate with stability correction factor of unity.

⁺ Denotes significant upwind surface discontinuity at sample site.

The individual flux measurements for all mills were reviewed and only those values meeting certain statistical, R_i , and height-to-fetch ratio criteria were used to obtain the selected observations summary results in Table 4. Chemistry data with correlation coefficients of less than 0.8 were excluded. Table 4 also contains a summary of all observations of the flux. The values for Mill No. 3 are only approximate because neutral stability was assumed. It appears that the methanol flux is roughly 2 ng/cm² · s (16 lbs/acre · day), acetone is .06 ng/cm² · s (0.46 lbs/acre · d), and total hydrocarbon is 3 ng/cm² · s (23 lbs/acre · day). Emission rates are summarized in Table 5.

The range of the respective fluxes reported in the selected observations column of Table 4 should not be interpreted as a confidence interval. The reported values in this table for a particular chemical in a particular basin reflect fluxes measured under drastically different environmental conditions. Point values of the flux are strong functions of chemical concentration in the water, water temperature, and wind speed. Concentration and water temperature change significantly from basin inlet to basin outlet. Wind regulates transport significantly.

Repeated observations at a single point on one basin were not made; however, some insight into the degree of reproducibility of the method can be obtained from studying the results for methanol for the first visit to Mill No. 2 (sample No. 2-1 in Table 3). High winds in the morning (white caps were present) likely mixed the water in the basin so that the entire surface was at a uniform methanol concentration and temperature. Brisk, steady winds were present when the five profiles were obtained at various

TABLE 5. ORGANIC CHEMICAL EMISSIONS

Parameter	Mill			
	1	2	3	4
Detention time (days)	12.5	13.8	4	24
Surface area (acres)	265	85	7	110
Surface aerators (number)	25	32	10	8
Methanol emission (tons/day)	2.7	1.2	.011	0.61
Methanol flux (lbs/day · acre)*	20	29	3.2	11
Acetone emission (lbs/day)	200	39	2.5	24
Acetone flux (lbs/day · acre)*	.77	.46	.36	.22
Total hydrocarbon† (tons/day)	4.4	1.1	.042	1.3
Total hydrocarbon† (lbs/day · acre)*	33	25	12	23

† GC/FID

* Flux rate ng/cm² · s = (lbs/day · acre) ÷ 7.70.

TABLE 4. VOLATILE CHEMICAL EMISSION FLUX SUMMARY

Mill Number and Chemical	Selected Observations			All Observations		
	n	Flux (ng/cm ² · s)	Flux Range	n	Flux (ng/cm ² · s)	Standard Error of Flux
1-methanol	7	2.6	.14-7.7	11	4.1	6.1
1-acetone	5	.10	.0076-.38	11	.11	.15
1-total hydrocarbon	7	4.3	.27-14.	11	3.2	4.7
2-methanol	4	3.8	2.1-5.2	11	2.7	1.6
2-acetone	4	0.060	.019-.13	9	.045	.044
2-total hydrocarbon	6	3.2	1.5-5.3	11	2.9	1.7
3-methanol	—	—	—	7	.41	.47
3-acetone	—	—	—	7	.047	.057
3-total hydrocarbon	—	—	—	8	1.5	2.0
4-methanol	5	1.4	.09-4.3	7	1.1	1.5
4-acetone	2	.028	.022-.034	8	.0096	.018
4-total hydrocarbon	6	3.0	.12-9.4	8	2.9	3.4

locations on the basin. Apparently GC chemical separation and air leaks were minimal for this sortie also. Considering all observations, the average flux was $3.4 \text{ ng/cm}^2 \cdot \text{s}$ with standard deviation of $1.7 \text{ ng/cm}^2 \cdot \text{s}$. Conditions were not as ideal on the second trip to this site, where the average flux was $2.0 \text{ ng/cm}^2 \cdot \text{s}$ with a standard deviation $1.3 \text{ ng/cm}^2 \cdot \text{s}$. When all doubtful data is disregarded, the average flux at the site combining both visits is $3.8 \text{ ng/cm}^2 \cdot \text{s}$, with a range of $2.1\text{--}5.2 \text{ ng/cm}^2 \cdot \text{s}$.

CONCLUSIONS

A field-sampling protocol and associated apparatus, referred to as the concentration-profile method (CPM) was developed and tested for volatile chemical emissions from surface impoundments. The method is based on obtaining samples of air, wind velocity, and temperature in a two-meter boundary-layer region above the water surface. Turbulent-transport theory coupled with concentration and micrometeorological measurements is used to develop the flux-measurement algorithm for these area sources.

Volatile chemicals in the wastewater are emitted into the overlying air boundary layer. Air samples in a two-meter region above the water surface had quantities of methanol, acetone, and total hydrocarbon in levels much higher than the background. Concentrations in the layer decreased significantly with height above the water. To make these measurements a method of trapping, concentrating, and analyzing low-molecular weight volatiles in the presence of excess water vapor was developed.

The flux rates of methanol, acetone, and total hydrocarbon, originating in aerated wastewater-treatment basins, were measured during field tests on the CPM.

Ranges of the average flux rates for the basins were: methanol, 1.4 to $3.8 \text{ ng/cm}^2 \cdot \text{sec}$ (11 to $29 \text{ lbs/acre} \cdot \text{day}$); acetone, 0.28 to $0.10 \text{ ng/cm}^2 \cdot \text{sec}$ ($.22$ to $0.77 \text{ lbs/acre} \cdot \text{day}$); and total hydrocarbon (FID), 3.0 to $4.3 \text{ ng/cm}^2 \cdot \text{sec}$ (23 to $33 \text{ lbs/acre} \cdot \text{day}$). Acetaldehyde was detected, but at extremely low concentration.

ACKNOWLEDGMENTS

Work reported above was presented as Paper No. 127a at the Annual Meeting of American Institute of Chemical Engineers, New Orleans, La, Nov. 1981. Financial support was provided by U.S. Environmental Protection Agency, Industrial Environmental Research Laboratory, Cincinnati, OH, under Grant No. R-805534. Mr. Paul dePercin served as Project Officer.

LITERATURE CITED

1. McAlister, J. A., B. G. Turner, and R. E. Estridge, "Treatment of Selected Internal Kraft Mill Wastes in a Cooling Tower," U. S. E. P. A., Water Pollution Control Res. Series, 12040 EEK 08/71 (August, 1971).
2. Thibodeaux, L. J., "A Test for Volatile Component Stripping of Waste Water," U. S. E. P. A., Environmental Protection Technology Series, EPA-660/2-74-044 (May, 1974).
3. Thibodeaux, L. J. and D. G. Parker, "Desorption Limits of Selected Industrial Gases and Liquids from Aerated Basins," Paper No. 30d, 76th National Meeting, AIChE, Tulsa, Okla. (March, 1974). (Published in *AIChE Symposium Series 156*, Vol. 72, 1976).
4. Thibodeaux, L. J. and J. D. Millican, "Quality and Relative Desorption Rates of the Air-Strippable Organics in Industrial Wastewater," *Env. Science Technology*, 11, No. 9, 879-882 (1977).
5. Keith, L. H., "Identification and Analysis of Organic Pollutants in Water," Ann Arbor Sci., Pub. Inc., Ann Arbor, Mich. p. 671 (1976).
6. Parmele, L. H., E. R. Lemon, and A. W. Taylor, "Micrometeorological Measurements of Pesticide Vapor Flux from Bare Soil and Corn Under Field Conditions," *Water, Air, and Soil Pollution* 1, 433-451 (1972).
7. Claitth, M. M., W. F. Spencer, W. J. Farmer, T. D. Shoup, and R. Brover, "Volatilization of S-Ethyl N, N-Dipropylthiocarbamate from Water and Wet Soil during and after Flooded Irrigation of an Alfalfa Field," *J. Agric. Food Chem.*, 28, 610-613 (1980).
8. Businger, J. A., "Turbulent Transfer in the Atmospheric Surface Layer," "Workshop on Micrometeorology," Duane A. Haugen, ed., American Meteorological Society, Boston, Mass. (1973), p. 76-100.
9. Rosenberg, N. J., "Microclimate—The Biological Environment," Wiley, New York, New York p. 108-111 (1974).
10. Brooks, F. A. and W. O. Pruitt, "Investigations of Energy, Momentum and Mass Transfer Near the Ground," Final Report, 1965, U.S. Army Electronics Command, Atmospheric Sciences Lab., Res. Div., Fort Huachuca, Arizona p. 39-42 (June 1966).
11. Thibodeaux, L. J., D. G. Parker, and H. H. Heck, "Measurement of Volatile Chemical Emissions from Wastewater Basins," Final Report, Research Project Grant No. R-805534, U.S. Environmental Protection Agency, Industrial Environmental Research Laboratory, Cincinnati, Ohio, (December, 1981).
12. Dickerson, Richard L., "A Technique for the Measurement of Certain Wastewater Volatiles," Unpublished M. S. Thesis, Chemical Engineering, University of Arkansas, Fayetteville, Arkansas, 1980.

Improved Estimates of Sulfate Dry Deposition in Eastern North America

Seasonable sulfate dry deposition, computed numerically with a Lagrangian regional-scale model, appears to be smaller than previous estimates.

Marvin L. Wesely and Jack D. Shannon, Argonne National Laboratory, Argonne, Ill. 60439

Early work on producing maps of deposition velocity (downward surface flux divided by local concentration) for sulfate in Eastern North America (Sheih *et al.*, 1979) [12] relied on very preliminary micrometeorological field-experiment data on the surface flux of particles less

than $0.1 \mu\text{m}$ in diameter (Wesely *et al.*, 1977) [14]. Since particles smaller than $0.1 \mu\text{m}$ are deposited relatively quickly compared to slightly larger particles, rather large deposition velocities were generated. These estimates, which yield daily averages of near 0.45 cm s^{-1} over a sum-

mer time landscape, have been used in a reduced form in regional Lagrangian statistical trajectory models (e.g., Shannon, 1981) [11]. However, the sulfate-deposition velocities are not universally regarded to be so large.

In his review, Sehmel (1980) [10] indicates that there is no general agreement on the behavior of sulfate-deposition velocities and that, in any case, the deposition velocity for submicron particles is a strong function of particle size, among other factors. On the basis of much theoretical and wind-tunnel work, Slinn (1982) [13] has challenged all work that give values much greater than 0.01 cm s^{-1} for submicron particle-deposition velocities. Garland and Cox (1982) [2] conclude that daily averages should not exceed 0.1 cm s^{-1} , partially based on their work with large wind-tunnel enclosures placed over grass in the field. The purpose here is to summarize some recent micrometeorological results on sulfate-deposition velocities, which are found to be smaller than the initial micrometeorological estimates, and interpret the results in terms of total sulfur deposition to large areas.

REVISED SULFATE-DEPOSITION VELOCITIES

A series of short-term intensive micrometeorological experiments designed to measure the dry deposition of sulfate over natural surfaces have been conducted. Hicks *et al.* (1982) [5] describe the first of these, which took place over a pine forest in 1977. In all experiments, the eddy-correlation technique was used with instruments placed at heights of 5-10 m, primarily over grass and forested surfaces. With the eddy-correlation technique, such as described by Wesely (1983) [15], a fast-response flame-photometric sensor was used in conjunction with a propeller anemometer, and half-hour averages of the vertical mass-flux density were measured, usually over several 24-hour periods at each site. Wesely *et al.* (1983) [16] have summarized most of these results, except for data collected at the 1982 Dry Deposition Intercomparison Experiment conducted over grass near Champaign, Illinois. The latter experiment produced results very similar to the 1981 pilot experiment at the same site, as described by Wesely *et al.* (1983) [16].

The eddy-correlation experiments produce a clear trend in deposition velocity for particulate sulfur. Minimum values are found in atmospherically neutral and stable conditions, which usually occur in the absence of substantial solar heating of the surface, and maximum values are detected during gusty unstable daytime conditions. It appears that the deposition velocities can be normalized by division by the friction velocity u_* , and that a parameterized deposition velocity can be given for atmospherically stable conditions as

$$v_d = 0.002u_*, \quad (1a)$$

and for unstable conditions as

$$v_d = 0.002u_*[1 + (-220L)^{-2/3}], \quad (1b)$$

where L is the familiar Obukhov length scale that indicates the state of atmospheric stability.

The formulation given by Equation (1) is most appropriate for deposition over surfaces such as grass that are moderately rough aerodynamically. The structure of the formula clearly reflects a micrometeorologist's point of view on scaling turbulent fluxes in the atmospheric surface layer. Use of the exponential numerical value of $2/3$ fits the data quite well and is an attempt to incorporate directly the effects of convective turbulence where large-scale eddies penetrate deep into vegetative canopies (e.g., Lewellen *et al.*, 1983) [7]. Admittedly, this is a great simplification of the nature of the large eddies in deep complex canopies. Further, there is no attempt to include directly the effects of changes in leaf area and number and

of various properties of microscale roughness on individual surface elements.

An interesting feature of Equation (1) is that it usually produces deposition velocities within the range of 0.05 to 0.1 cm s^{-1} for moderate to light winds in near-neutral and stable atmospheric conditions. These values are still considerably larger than some wind-tunnel estimates for unheated surfaces (e.g., Chamberlain, 1966; Sehmel, 1973) [1, 9], possibly because a significant fraction (over 10%) of the particulate sulfur is often found in particles larger than $1.0 \mu\text{m}$ in diameter (e.g., Loo *et al.*, 1978) [8], which can have relatively large deposition velocities (Garland, 1983) [3]. On the other hand, the present micrometeorological parameterization produces estimates of deposition velocity that roughly agree with values found by Ibrahim *et al.* (1983) [6] for deposition of radioactive submicron tracer particles to snow in the field.

SULFUR DEPOSITION OVER LARGE AREAS

With the assumption that the parameterization offered by Equation (1) is valid over most of the atmospheric and surface conditions that are normally encountered over eastern North America, calculations such as those by Sheih *et al.* (1979) [12] can be carried out to indicate typical values of particulate sulfur (here assumed to be in the form of sulfate) deposition velocities over the region. When this is done, the 24-hour daily average deposition velocity during summer is found to be near 0.25 cm s^{-1} over North America, with a large diurnal variation. The resulting diurnal pattern is similar to the curve shown in Figure 3, Shannon (1981) [11], only scaled by approximately one half.

The ASTRAP (Advanced Statistical Trajectory Regional Air Pollution) model of Shannon (1981) [11] has been rerun for the one test month of July, 1980, to study the effects of altered sulfate-deposition velocities on the integrated deposition of sulfur compounds over large regions of North America. Exactly one half the values of sulfate-deposition velocities used by Shannon in his Figure 3 were adopted here for the purpose of comparison. Daily averages of deposition velocity are now 0.225 cm s^{-1} instead of 0.45 cm s^{-1} . A major effect is that concentrations of airborne sulfate are increased over the entire region of interest. For example, in areas where the greatest surface air concentrations are normally found, such as in West Virginia, the calculated monthly averaged concentrations increase by over 30% from 12 to $16 \mu\text{g m}^{-3}$. In areas remote from sources, calculated concentrations often increase by 100%, such as from 1.5 to $3.0 \mu\text{g m}^{-3}$ in parts of New Brunswick.

Results on sulfur deposition computed both with the original and with the halved deposition velocities for particulate sulfur are shown in Table 1. The total of wet and dry integrated deposition is decreased by only 2-4% in the east-central United States, while increases of 1-4% are evident for remote areas. Clearly, increased wet deposition, associated with larger amounts of sulfate in aerosols available for scavenging by precipitation, tends to compensate for reduced sulfate by deposition. The extent of this compensation is dependent on the efficiency of the scavenging processes assumed. As discussed by Shannon (1981), [11], the efficiency assumed is rather high, though not necessarily unrealistically. If slower wet-removal rates were assumed, simulations would indicate smaller wet-deposition amounts, larger concentrations of sulfur dioxide and sulfates in aerosols, larger amounts of dry deposition, etc.

The most significant change shown in Table 1 concerning the halved sulfate-deposition velocities is that the total dry-deposition rates are reduced noticeably. With either choice of sulfate dry-deposition velocities, sulfur dioxide

TABLE 1. INTEGRATED AMOUNTS OF ELEMENTAL SULFUR (IN KILOTONNES) COMPUTED FOR THE MONTH OF JULY, 1980, FOR SELECTED STATES AND PROVINCES IN EASTERN NORTH AMERICA, AND COMPARISON OF RESULTS WHEN SULFATE-DEPOSITION VELOCITIES ORIGINALLY AVERAGING APPROXIMATELY 0.45 cm s^{-1} ARE HALVED.

Location*:	West MO	Center WV	South GA	NY	VT	ME	NB	NS	Remote NFLD
SO ₂ , dry:	4.5	8.3	12.2	11.3	1.0	2.6	1.4	1.2	1.2
B. Before, with larger v _d for sulfate.									
Total, wet:	5.2	15.1	12.4	13.7	1.8	5.0	3.9	3.2	5.6
SO ₄ ²⁻ , dry:	1.5	2.4	4.4	4.1	0.5	1.7	1.2	1.0	1.8
A. After, with halved v _d for sulfate.									
Total, wet:	5.4	15.5	13.0	14.3	1.9	5.4	4.3	3.5	6.5
SO ₄ ²⁻ :	1.0	1.5	2.8	2.6	0.3	1.1	0.8	0.7	1.3
Ratios, A/B.									
Total S:	0.98	0.98	0.96	0.97	0.98	0.98	1.01	1.01	1.04
Total dry:	0.91	0.91	0.90	0.90	0.88	0.87	0.86	0.87	0.84
SO ₄ ²⁻ , dry:	0.64	0.62	0.63	0.64	0.65	0.67	0.69	0.70	0.73

*MO is Missouri, WV is West Virginia, GA is Georgia, NY is New York, VT is Vermont, ME is Maine, NB is New Brunswick, NS is Nova Scotia, and NFLD is Newfoundland.

dominates the dry deposition of sulfur except in remote areas.

CONCLUSIONS

Recent eddy-correlation measurements of the dry deposition of particulate sulfur indicate that the associated deposition velocities have a strong diurnal trend and are quite small in near-neutral and stable atmospheric conditions. Daily averages of the deposition velocity in the summertime over Eastern North America are expected to be near 0.25 cm s^{-1} , nearly half the values thought earlier on the basis of preliminary micrometeorological experiments. However, the corresponding change in monthly total deposition of sulfur (wet plus dry, all forms) computed with the ASTRAP numerical model is quite small, within 5%, as a result of the compensation by increased wet deposition of particulate sulfur. The major effect of the lower deposition velocities is that computed airborne sulfate concentrations increase substantially, from 30% near source regions to 100% in remote areas.

It is evident that sulfur-dioxide dry deposition dominates the dry deposition of sulfur except in remote areas. Near major source regions, the former is now computed to be 4-5 times greater than the sulfate dry deposition, largely as a result of the relatively high concentrations of sulfur dioxide coupled with rather large deposition velocities. Even greater differences are found in the winter. Hence, small fractional changes in sulfur-dioxide deposition velocities chosen are relatively important. In terms of damage to vegetation, the effects of sulfur dioxide might be larger than that of sulfate for a reason in addition to contributing more to total sulfur deposition, namely, that sulfur dioxide penetrates more easily than particulate sulfur through leaf stomatal openings leading to sensitive inner leaf cells (e.g., Hällgren, 1978) [4].

If the sulfate-deposition velocities were assumed to be nearly zero at all times, the calculated total sulfur deposition would probably be decreased by less than 10% of that computed with large deposition velocities assumed earlier, while the calculated airborne sulfate concentrations would increase substantially. The latter increase would give maximum regional monthly sulfate concentrations in excess of $20 \mu\text{g m}^{-3}$, which is approximately 25% too large in comparison to actual measurements (Shannon, 1981) [11]. The present choice of deposition velocities, derived from extensive field studies and half that assumed

earlier from preliminary investigations, produces simulated concentrations that are within 10% of the observed values for this test case.

ACKNOWLEDGEMENTS

Dr. C.-M. Sheih of Argonne National Laboratory computed the deposition velocities averaged over inland areas of North America. Although the research described in this article has been funded wholly or in part by the United States Environmental Protection Agency (EPA) through Interagency Agreement DW930060-01-1 to the United States Department of Energy, it has not been subjected to EPA review and therefore does not necessarily reflect the views of EPA and no official endorsement should be inferred.

LITERATURE CITED

1. Chamberlain, A. C., "Transport of Lycopodium Spores and Other Particles to Rough Surface," *Proc. Roy. Soc. Ser. A* **296**, 45-70 (1966).
2. Garland, J. A. and L. C. Cox, "Deposition of Small Particles to Grass," *Atmos. Environ.* **16**, 2699-2702 (1982).
3. Garland, J. A., "Dry Deposition of Small Particles to Grass in Field Conditions," Paper presented at the 4th International Conference on Precipitation Scavenging, Dry Deposition and Resuspension, Nov. 29 - Dec. 3, 1982, Santa Monica, Calif., to be published in 1983.
4. Hällgren, J. E., "Physiological and Biochemical Effects of Sulfur Dioxide on Plants," in *Sulfur in the Environment, Part II, Ecological Inputs*, Ed. J. O. Nriaga, John Wiley & Sons, New York, pp. 163-209 (1978).
5. Hicks, B. B., M. L. Wesely, J. L. Durham, and M. A. Brown, "Some Direct Measurements of Atmospheric Sulfur Fluxes over a Pine Plantation," *Atmos. Environ.* **16**, 2899-2093 (1982).
6. Ibrahim, M., L. A. Barrie, and F. Fanaki, "An Experimental and Theoretical Investigation of the Dry Deposition of Particles to Snow, Pine Trees, and Artificial Collectors," *Atmos. Environ.* **17**, 781-783 (1983).
7. Lewellen, W. S., A. K. Varma, and Y. P. Sheng, "Dry Deposition Model Sensitivity," Paper presented at the 4th International Conference on Precipitation Scavenging, Dry Deposition and Resuspension, Nov. 29 - Dec. 3, 1982, Santa Monica, Calif. to be published in 1983.
8. Loo, B. W., W. R. French, R. C. Gatti, F. S. Goulding, J. M. Jaklevic, J. Llacer, and A. C. Thompson, "Large-Scale Measurements of Airborne Particulate Sulfur," *Atmos. Environ.* **12**, 759-771 (1978).

9. Sehmel, G. A., "Particle Eddy Diffusivities and Deposition Velocities for Isothermal Flow and Smooth Surface," *Aerosol Sci.* 4, 125-138 (1973).
10. Sehmel, G. A., "Particle and Gas Dry Deposition: A Review," *Atmos. Environ.* 14, 983-1011 (1980).
11. Shannon, J. D., "A Model of Regional Long-Term Average Sulfur Atmospheric Pollution, Surface Removal, and Net Horizontal Flux," *Atmos. Environ.* 15, 689-701 (1981).
12. Sheih, C. M., M. L. Wesely, and B. B. Hicks, "Estimated Dry Deposition Velocities of Sulfur over the Eastern United States and Surrounding Regions," *Atmos. Environ.* 13, 1361-1368 (1979).
13. Slinn, W. G. N., "Predictions for Particle Deposition to Vegetative Canopies," *Atmos. Environ.* 16, 1785-1794 (1982).
14. Wesely, M. L., B. B. Hicks, W. P. Dannevik, S. Frisella, and R. B. Husar, "An Eddy-Correlation Measurement of Particulate Deposition from the Atmosphere," *Atmos. Environ.* 11, 561-563.
15. Wesely, M. L., "Turbulent Transport of Ozone to Surfaces Common in the Eastern Half of the United States," in "Trace Atmospheric Constituents: Properties, Transformations, & Fates," Ed. S. E. Schwartz, John Wiley & Sons, New York, pp. 345-370 (1983).
16. Wesely, M. L., D. R. Cook, R. L. Hart, B. B. Hicks, J. L. Durham, R. E. Speer, D. H. Stedman, and R. J. Tropp, "Eddy-Correlation Measurements of the Dry Deposition of Particulate Sulfur and Submicron Particles," Paper presented at the

4th International Conference on Precipitation Scavenging, Dry Deposition and Resuspension, Nov. 29 - Dec. 3, 1982, Santa Monica, Calif., to be published in 1983.

Marvin L. Wesely is manager of the Atmospheric Physics Program of the Environmental Research Division of Argonne National Laboratory. He received his Ph. D. degree from the University of Wisconsin at Madison and joined Argonne in 1973. He is presently responsible for management of a group performing atmospheric research for the U.S. Environmental Protection Agency and the U.S. Department of Energy. His primary research interests involve experimental studies of dry deposition and transport in the planetary boundary layer.



Jack D. Shannon is a meteorologist and deputy manager of the Atmospheric Physics Program of the Environmental Research Division at Argonne National Laboratory. He received a Ph. D. degree in meteorology from the University of Oklahoma. His primary research interests are modeling of long-range transport and deposition of air pollutants and optimal design of networks.



Simultaneous Wastewater Concentration and Flow Rate Equalization

Simple models are developed and validated to predict the performance of waste-strength equalization basins.

James W. Patterson and Jean-Paul Menez, Illinois Institute of Technology, Chicago, Ill. 60616

One major problem encountered by the designers and operators of many wastewater treatment plants is extreme variations in mass loading, constituent concentrations, and flow rates of the wastewater entering the treatment plant. To reduce these variations and especially shock loads, the environmental engineer has available a very simple control technique: equalization. Equalization involves reduction in variability of the flow rate and/or strength of peak waste loads, by retaining wastes for a sufficient length of time to obtain an effluent from the equalization basin which is more uniform, in order to achieve a more consistent direct discharge or treated effluent quality, or a reduction of the complexity or cost of treatment of the wastewater.

Peak loads can have significant adverse effects on the performance of both biological and physical-chemical treatment systems, and several benefits have been suggested for equalization [1, 5]:

1. Dampen or suppress hydraulic surges to physical-chemical or biological treatment units and systems, thereby permitting operation compatible with economical selection.
2. Stabilize solids loading to primary and final clarifiers.
3. Dampen shock organic loadings on biological processes.
4. Provide continuous feed to biological systems over intervals when plant waste flow is interrupted.

5. Dampen mass loadings to chemical treatment processes, thereby improving chemical feed controller and treatment process reliability.

Equalization is widely employed for these reasons. In addition, equalization can be a cost-effective option to upgrade an overloaded treatment plant.

There are essentially two types of equalization used: flow equalization and waste strength equalization. The first is commonly used in both municipal and industrial wastewater treatment plants. Flow equalization is intended to dampen or suppress fluctuations in waste flow rate. Flow equalization can achieve some reduction in the variability of the strength of the waste, although this is not the primary objective. The second technique, waste strength equalization, is utilized to dampen, but cannot totally suppress, fluctuations in waste constituent concentration. This technique is a cost effective feature in many industrial wastewater treatment facilities. In this case, the volume of the liquid contained in the equalization basin is normally maintained constant, with the basin operated full. Thus, equalization for waste strength is achieved at the expense of unstable basin discharge flow rate, where flow rate also varies. For maximum efficiency, the waste strength equalization basin must be placed in line with the other treatment processes, and usually before them.

Design techniques for waste flow equalization are well established [7]. The design of a waste strength equalization basin is more complex, and the design criteria less well es-

tablished. Design should consider the type of treatment system following the equalization basin, the dispersion and mixing characteristics of the basin, the rate, extent, and pattern of fluctuation of raw wastewater character, and any biochemical, chemical, or physical reactions which might occur in the equalization basin [7]. Most designs for waste-strength equalization assume complete mixing, a condition difficult to achieve in itself. Further, the pattern of waste character fluctuation is often random [8], and a probabilistic design approach might be required.

In design for waste strength equalization, the designer attempts to relate the characteristics of the fluctuating basin influent to those of the equalized effluent as a function of basin volume (i.e., detention time). There is a trade-off between basin volume and degree of equalization achieved. The designer therefore is required to predict basin effluent variability as a function of basin size, and ultimately to size the basin to yield a cost-effective degree of equalization.

Various design methods have been proposed to size waste strength equalization basins. Some, based upon the probability of effluent concentration falling within a selected range of values (i.e., a confidence limit), are attractive, but become difficult to apply except for the case of constant basin influent flow rate [2, 4]. Most industrial wastes fluctuate, often independently, in both flow rate and waste strength.

The purpose of this work has been to develop and evaluate a simple design procedure for waste equalization, by correlating the characteristics of the fluctuating influents with the equalized effluents as a function of the instantaneous basin-detention time of the waste. To achieve this goal, a completely mixed equalization basin has been used to simulate the performance of a unit receiving an influent randomly varying in both flow and waste strength.

Design models were developed and validated against the results of a laboratory pilot-scale equalization unit. To select the optimum volume of basin, efficiency curves were constructed for both concentration and mass loadings. The design equations have been further evaluated by computer simulation, and the results indicate that the apparent disparate objectives of simultaneous equalization of waste concentration and waste flow rate can be economically achieved.

DESIGN MODEL DEVELOPMENT

The objective of the models presented in this section is to correlate the effluent concentration of the equalization basin as a function of the influent concentration and the retention time of the basin.

Waste-Strength Equalization

Data collection for waste characterization, for the purpose of design of equalization basins, is usually performed by continuous monitoring (e.g., flow rate, pH) or collection of frequent grab or one-hour composite samples for analysis.

In the following development, the equalization basin is assumed to be completely mixed, to have a constant liquid volume, and waste-characterization data is collected on a continuous or extremely frequent grab basis. When data collection is on a continuous basis, the data base must be digitized to provide data values at discrete time intervals.

The mass balance of the system represented in Figure 1 is:

$$VdX = Q(X_i - X)dt \quad (1)$$

where

V = volume of the equalization basin

X = concentration of the waste in the equalization basin and effluent

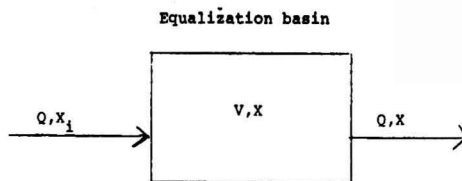


Figure 1. Mass balance diagram for a completely mixed system.

X_i = influent concentration of the waste

Q = flow rate of the waste

Equation (2) can be integrated to yield:

$$X(t) = X_i + (X(O) - X_i) \exp(-t/\tau) \quad (2)$$

where

$X(t)$ = concentration of the waste in the equalization basin at time t

= instantaneous hydraulic detention time ($\tau = V/Q(t)$)

Actual influent-waste cycles with varying flow rate and concentration can then be represented by a succession of intervals of time length T , each interval having constant influent flow rate and concentration. T can be selected for convenience; for example, the interval between two grab samples. Using this simplified representation of an actual cycle consisting of a series of time intervals, the effluent concentration of the basin can be calculated for each time interval using the following expression obtained from Equation (2):

$$X^j(t) = X_i^j + (C_0^j - X_i^j) \exp(-t/\tau^j) \quad (3)$$

where the superscript j represents the j^{th} time interval and

C_0^j = concentration of the waste in the equalization tank at the beginning of the j^{th} interval ($C_0^j = X^{j-1}(T)$)

Alternately, the operation of the equalization basin may be more simply described with a sequential time-interval mass balance around the system. This simplification is possible when the effluent concentration is almost constant during one time interval, which is the operational objective of waste-strength equalization basins. At constant basin volume, the expression of this mass balance over time interval T is:

$$X_i^j Q^j T + X^{j-1} V = X^j Q^j T + X^j V \quad (4)$$

By rearranging, we obtain X^j , the value of the effluent concentration:

$$X^j = \frac{X_i^j T + X^{j-1} \tau^j}{T + \tau^j} \quad (5)$$

The two models whose Equations (3) and (5) are the predictive design equations for the effluent concentration of the equalization basin will be referred to, respectively, as Models 1 and 2, and are derived from simple mass balances around the equalization facilities.

In order to measure the effectiveness of the equalization basin in damping waste fluctuations, a new dimensionless parameter has been introduced: the peaking factor (PF), which is the ratio of the maximum to minimum value of the waste characteristic over a cycle of operation. To obtain an uniform basis to evaluate the performance of equalization basins of different sizes, an additional parameter is introduced: the relative retention volume, (V_r). V_r is the ratio of the retention volume of the basin to the total inflow of one cycle.

Example Application

The application of Models 1 and 2 is easily demonstrated using the example data of Table 1. The data represent a series of eight one-hour time intervals, constituting a

TABLE 1. EXAMPLE INFLUENT AND CALCULATED EFFLUENT DATA FOR APPLICATION OF MODEL 2

Time Interval	Flow Rate gpm $\times 10^3$	Influent Conc., mg/l ⁻¹	Effluent Concentration at V_r of	
			1.0	0.5
1	1.6	245	187	198
2	0.2	64	185	193
3	1.0	54	173	169
4	1.2	167	172	169
5	1.6	329	194	208
6	2.0	48	169	162
7	1.2	55	157	141
8	1.0	395	179	181
Average	1.225	178	178	178
PF	10.0	8.2	1.2	1.5

cycle of operation (e.g., one work shift). With additional monitoring the time interval can be shortened, or the cycle of operation easily extended to a day, week, or longer. In Table 1, flow rate and waste concentration are independently varying. PF for flow rate is 10.0, and is 8.2 for influent-waste concentration.

Using either Model 1 or 2, various basin volumes are evaluated to determine the degree of equalization achievable. For example, for a full cycle of equalization, incorporating the eight time intervals of Table 1, V_r is 1.0, and a basin volume of 588,000 gallons would be required. The basin-effluent concentration is then calculated for each interval condition. Calculated effluent values for V_r of 1.0 and 0.5, using Model 2, are given in Table 1.

Initial basin concentration is assumed to be represented by the average flow-weighted concentration, equaling 178 mg/liter, the flow of one cycle. If the final calculated basin concentration at the end of the cycle is not equal to the assumed initial concentration, the calculated final concentration is taken as a new estimate of the initial concentration and the calculations repeated. That is, an iterative technique is employed until the assumed initial and calculated final basin concentrations converge. Convergence is generally quite rapid, requiring only one to three iterations. The calculations are easily performed on a programmable calculator. After the influent conditions are predicted for the selected basin size, a new basin size is then evaluated. Following evaluation of alternative basin sizes, the designer can then select a basin size based upon the trade-offs between size and degree of equalization achievable.

EXPERIMENTAL EQUIPMENT AND PROCEDURE

Experimental Equipment

To test the validity of the models developed above, an experimental equalization apparatus was constructed. The equalization unit was simulated by a ten-stage, 60-liter total capacity, cylindrical Plexiglas column. With this unit, equalization experiments could be performed at equalization volumes representing 6-liter increments. To ensure good mixing, Plexiglas blades were mounted on an aluminum shaft (Figure 2). The design criteria for the mixing column and blades were obtained from Nagata [6].

The rotational speed of the blades was set at 40 rpm. Before starting the equalization study, the mixing conditions were checked for complete mixing by using the step-response method [6]. The response was satisfactory, as shown in Figure 3. The shape of the actual curve representing the measured data is identical to the shape of the theoretical curve. The relative error between the experimental and theoretical results is about 5 percent.

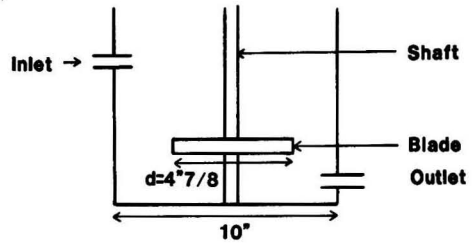


Figure 2. Schematic of the bottom stage of the test tank.

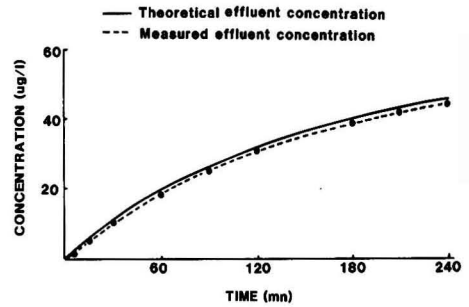


Figure 3. Response of the completely mixed column to a step input.

The influent solution simulating a waste stream was pumped from feed tanks to the column, using peristaltic pumps. The flows were measured using four manometers. A schematic of the experimental set-up is presented in Figure 4. To achieve precision in the control of the flows, separate manometers were used to measure flows between 20 and 50 ml/mn and flows between 50 and 250 ml/mn.

The simulated waste stream was tap water containing a tracer. The tracer used was a green dye, fluorescein, (water soluble, Aldrich Chemical Co.), and sample concentrations were measured by a fluorometric technique.

Experiments

A series of experimental runs were performed to compare the measured and predicted performance of the equalization system. Each experiment consisted of one or more cycles of operation, each cycle consisting of either five or ten forty-five-minute intervals. The values of flow rate and influent concentration and their sequence of occurrence were randomly generated. The possible range of variation of both flow rate and concentration was 10-fold. The smallest interval flow rate value was 20 ml/mn and the highest was 200 ml/mn. The design range for the dye concentration was 5 to 50 ppb. The actual range was slightly larger. The random combination of 10-fold variation in both flow rate and dye concentration yields a maximum influent mass-loading range of 100-fold. Samples were taken at the inlet and outlet of the column, every fifteen minutes. The initial dye concentration in the column, which was intended to be the theoretical mean con-

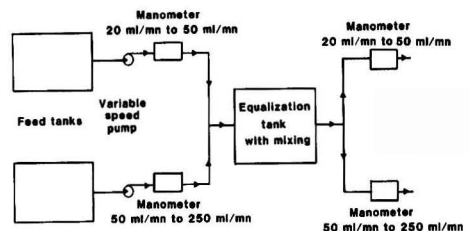


Figure 4. Schematic diagram of the experimental apparatus.

centration of the cycle, was also measured. Both Models 1 and 2 were used to predict the basin-effluent concentrations, based only upon the basin volume tested and its influent conditions.

The model-validation study was divided into four phases. During each experimental phase, the equalization basin was operated at a constant volume.

In Phase I the basin volume used was 18 liters. During this phase, ten runs, numbered from one to ten, were performed. Each run consisted of ten intervals. Runs 1 and 2, 3, and 4, and so forth were intended as replicates. However, due to difficulty in replicating the dye concentrations in the feed, only the flow rates were duplicated and the actual dye influent concentrations varied between replicates. Thus, for evaluation of the Models, the runs were considered different. In Phase I, V_r varied from 0.34 to 0.48.

The second phase was designed to run the same cycle twice, sequentially. Each cycle was composed of five intervals. The same basin volume was used as in Phase I. These runs were numbered 11 through 15, and V_r varied from 0.56 to 0.77. In the third phase, Runs 1, 3, and 5, already evaluated in Phase I, were repeated. The basin volume was increased from 18 to 24 liters. The three runs of this phase were numbered 16 to 18, and V_r was 0.45, 0.52, and 0.63, respectively. In the fourth and last phase, the three cycles previously run in Phases I and III were again repeated, but with a basin volume of 12 liters. These runs were numbered from 19 to 21 and V_r ranged from 0.23 to 0.31.

RESULTS AND DISCUSSION

For each run, and using the influent data values, effluent concentrations were predicted by both Models 1 and 2. These predicted values were then compared with the measured effluent concentrations. The performance of both models was quite good. Example results are presented in Figures 5 through 7.

From the plots of the measured and predicted concentrations of the effluent of the equalization tank (See Figures 5-7) it appears that these concentrations are approximated by a succession of straight lines. The slope of each straight line is essentially constant during each time inter-

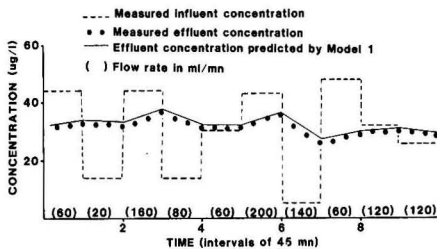


Figure 5. Experimental data vs. values predicted by Model 1 for Run 3.

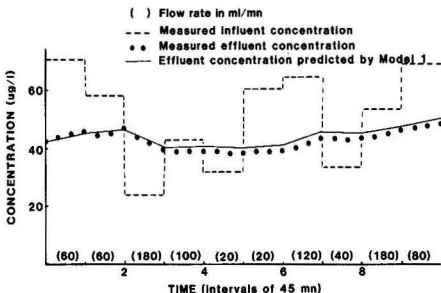


Figure 6. Experimental data vs. values predicted by Model 1 for Run 18.

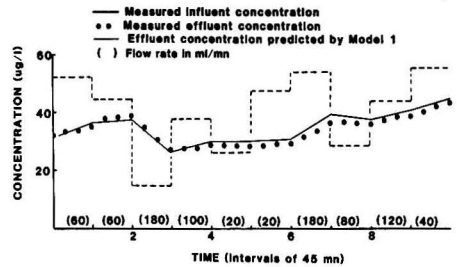


Figure 7. Experimental data vs. values predicted by Model 1 for run 21 ($V_r = 0.23$).

val, but shifts from one time interval to the next. Figure 5 shows that, if the concentration in the tank at $t = 0$ is the average flow-weighted concentration of the cycle, the concentration at the end of the tenth interval will be very close to the starting point of the cycle.

As demonstrated in Figure 8, the predicted values of the two models were very close. In order to quantitatively compare the two models the relative mean error was computed for each cycle and for each model, using the expression:

$$E^j = \sum_{i=1}^{30} [e_i(t)]/30 \quad (7)$$

where,

$e_i(t)$ = relative error at time t for the i^{th} data point

E^j = relative mean error for the j^{th} run

The calculated values of the relative mean errors are summarized in Table 2. The relative mean error is usually 5 percent or less, although in Run 6 the relative mean errors are in excess of 10 percent. However, Run 5 replicated Run 6 for flow rate and was an approximate replicate for influent concentration. As seen in Table 2, the relative mean error for Run 5 is quite low. The analytical results for Run 6 were rather erratic, and it is believed that the poor predictions in Run 6 reflect analytical error. For most runs, the relative mean error was negative, which means that the values computed by the models are slightly greater than the actual effluent values. Thus, both models are conservative. The prediction of the experimental values is very good by both models. Neither model gives a consistently better prediction than the other. However, for data representing very short time intervals, Model 1 would be most accurate.

In Table 3, the influent and effluent peaking factors, for both concentration and mass loading, are presented to show the efficiency of the process in damping fluctuations of the waste. Influent concentration peaking factors, ranging from near 3 to above 13, were reduced to effluent peaking factors generally below 1.5. Influent mass-loading peaking factors ranging up to 63.6 were also significantly reduced in the effluent. For Runs 11 and 14, the effluent mass-loading peaking factor was higher than the influent peaking factor. This phenomenon occurs whenever the interval of highest flow rate coincides with

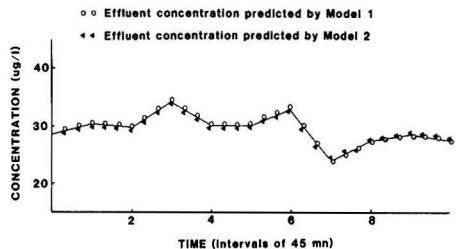


Figure 8. Values of predicted effluent concentrations for Run 1.

TABLE 2. RELATIVE MEAN ERRORS

Phase	Run Number	Relative Mean Error for	
		Model 1	Model 2
I	1	6.3	7.2
	2	3.1	2.8
	3	1.9	2.1
	4	3.9	3.5
	5	1.3	1.9
	6	11.4	11.4
	7	2.4	2.4
	8	3.5	3.5
	9	5.8	4.5
	10	3.8	2.7
II	11	8.6	9.3
	12	5.0	5.0
	13	4.0	4.2
	14	4.6	4.7
	15	5.2	5.5
III	16	5.5	5.8
	17	4.4	4.5
	18	3.3	3.6
IV	19	6.3	6.3
	20	5.2	5.2
	21	4.4	4.6

a period where the basin contents are near their cycle-maximum concentration and the interval of lowest flow rate coincides with a period where the basin contents are near their cycle-minimum concentration. The timing and values of these maxima and minima are a function of V_r plus basin-influent conditions.

The data of Table 3 reveal the high degree of equalization efficiency achievable, even at the relatively low V_r values tested. This efficiency is further demonstrated in Figure 9, through a frequency distribution diagram of the influent and effluent-waste streams of one typical run. The slope of the line for the effluent concentration is

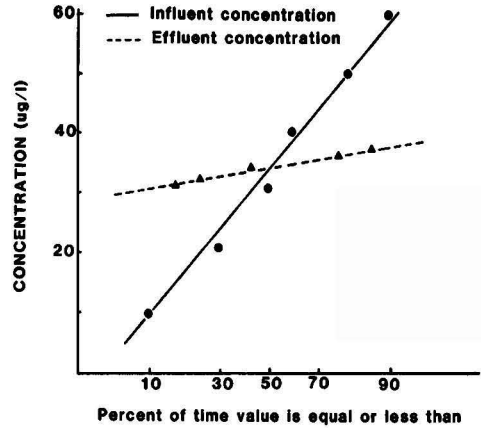


Figure 9. Frequency distribution diagram for Run 7.

smaller than the slope for the influent concentration. The former, near horizontal, is representative of a more consistent-quality effluent.

APPLICATION

The two design models presented above are useful to predict the effluent concentration of the equalization tank, but also help the designer of a new basin in the selection of its volume.

In order to evaluate the influence of an increased retention time (i.e., increased basin size) of the waste in the equalization basin, several hypothetical cycles were run using Model 1 to predict the basin-effluent concentration. The results of these simulations are plotted in Figure 10 for the effluent-concentration peaking factor and in Figure 11 for the effluent mass-loading peaking factor. V_r values evaluated ranged from zero (no equalization) to 1.1.

TABLE 3. PEAKING FACTORS OF THE 21 EXPERIMENTAL RUNS

Run Number	Influent concentration peaking factor	Effluent concentration peaking factor	Influent mass-loading peaking factor	Effluent mass-loading peaking factor
1	8.2	2.2	40.5	9.2
2	12.4	2.1	50.2	10.0
3	10.0	1.4	31.1	11.2
4	13.4	1.4	28.4	11.0
5	3.5	1.4	14.5	11.8
6	4.1	1.5	21.1	13.0
7	8.2	1.3	16.0	9.6
8	10.5	1.4	21.2	9.6
9	7.1	1.7	43.0	13.1
10	9.2	1.7	37.7	13.5
11	3.1	1.3	2.6	4.9
12	10.3	1.3	10.7	3.2
13	4.0	1.4	6.7	4.5
14	9.6	1.5	7.9	14.0
15	5.5	1.6	9.7	4.0
16	9.3	1.5	23.5	9.6
17	8.5	1.8	41.3	9.2
18	2.9	1.3	15.1	10.9
19	13.1	2.6	63.6	9.5
20	12.9	1.7	24.5	12.0
21	3.7	1.6	15.0	12.3
Range	2.9-13.4	1.3-2.6	2.6-63.6	3.2-14.0

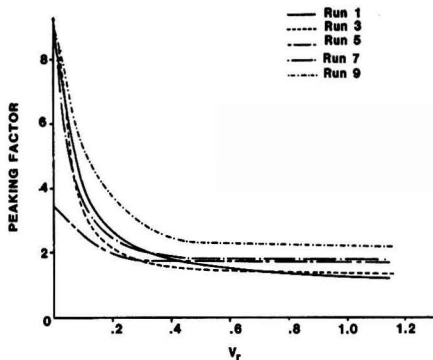


Figure 10. Concentration peaking factor vs. relative retention volume for waste equalization.

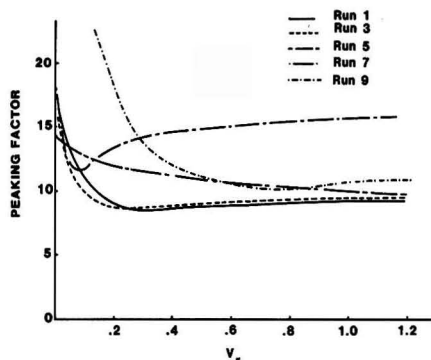


Figure 11. Mass-loading peaking factor vs. relative retention volumes for waste equalization.

The cycles studied had influent-concentration peaking factors which ranged from 3.5 to 10.0. Usually, as can be seen in Figure 10, for a retention volume of one-third, the inflow of one cycle (e.g., eight hours detention time for a 24-hour cycle), the effluent peaking factor has been damped to about 2.0 or less. This simulation demonstrates that the greatest extent of equalization is achieved at relatively low values of V_r , and there is little or no gain if an increased retention volume is utilized. Many existing waste-strength equalization basins incorporate a V_r equal to one-day detention, or longer.

For the cycles evaluated, the influent mass-loading peaking factors ranged from 14.5 to 43.0. From Figure 11, the minimum effluent peaking factor was usually obtained for a retention volume of less than 0.3. Beyond this basin size, little reduction is obtained in the effluent

mass-loading peaking factor. For Run 5, after reaching a minimum at V_r of 0.1, the effluent mass-loading peaking factor increased significantly with higher relative retention volumes. As V_r is changed for a particular influent-waste stream, the pattern and extent of fluctuation of the basin-content concentrations also changes. At V_r values where maximum flow coincides with basin concentrations higher than the flow-weighted average and minimum flow coincides with basin concentrations lower than the average, effluent mass-loading peaking factors are exacerbated. From Figure 11, the range of the minimum effluent mass-loading peaking factor is from 7 to 16, largely due to the flow-rate peaking factors, which ranged from 9 to 10.

SIMULTANEOUS FLOW AND WASTE STRENGTH EQUALIZATION

As previously mentioned, the flow-rate equalization technique also achieves a partial reduction in waste-strength fluctuations. The minimum volume required to achieve in-line flow equalization was computed for each of the five flow-rate-paired runs of Phase I. The values of this flow-equalization volume were found to be between 12 and 17 percent of the total inflow of one cycle (see Table 4). The effluent concentrations and the effluent mass loadings were calculated, with the basin operated full, and with the basin allowed to fill and empty as required for flow equalization. In the same way as before, and to compare both equalization methods, the influent and effluent peaking factors were computed. For the same relative retention volume, flow equalization is indicated to be nearly as efficient as waste-strength equalization in reducing the variations of the waste concentrations, as shown by Table 4. Further, flow equalization is much more efficient than the alternative technique to reduce fluctuations of mass loadings. The reason for this efficiency, for a relatively small retention volume (about 15 percent of the total inflow of one cycle), is that flow equalization achieves a complete equalization of the flow-rate variation, and a substantial reduction of the waste-concentration variation.

However, effluent-concentration variations after flow equalization may still be large, as seen in Table 4 where effluent-concentration peaking factors ranged up to 4.0. To achieve a further reduction, the volume of the flow-equalization tank may be increased. In this case there is no complete draw-down of the basin, in order to always provide some basin contents to dampen waste-strength fluctuations.

A simulation was therefore performed for the same runs presented in Table 4, at V_4 of 0.33. In this analysis, a portion of the basin volume is allocated for flow equalization, and the remainder is utilized solely for waste-strength equalization. For example, using Run 1 at a total

TABLE 4. PEAKING FACTORS AT A RELATIVE RETENTION VOLUME REQUIRED FOR FLOW EQUALIZATION

Run	$V_r^{(1)}$	Influent concentration peaking factor	Influent mass-loading peaking factor	Effluent concentration peaking factor for waste-strength equalization ⁽²⁾	Influent mass-loading peaking factor for waste-strength equalization ⁽²⁾	Effluent peaking factor for flow equalization ^(3, 4)
1	0.12	9.0	45.0	3.6	10.5	4.2
3	0.13	9.0	26.7	2.7	9.3	2.3
5	0.17	3.3	14.4	2.1	12.2	2.4
7	0.15	10.0	21.3	2.8	12.7	4.2
9	0.17	9.0	45.0	4.0	20.7	3.2

⁽¹⁾ V_r is value calculated to provide flow equalization only.

⁽²⁾ Basin operated full at all times; no flow equalization.

⁽³⁾ Basin fills and empties as necessary for flow equalization.

⁽⁴⁾ This is both the concentration and mass-loading peaking factor, since effluent flow rate is constant with flow equalization.

TABLE 5. EFFLUENT PEAKING FACTORS AT A MAXIMUM RELATIVE RETENTION VOLUME OF 0.33

Run	Concentration peaking factor for waste-strength equalization ($V_r = 0.33$)	Peaking factor ⁽¹⁾ for flow equalization ($V_r, \text{max} = 0.33$)	Mass-loadings peaking factor for waste-strength equalization ($V_r = 0.33$)
1	2.0	1.9	8.5
3	1.7	1.4	8.5
5	1.8	1.4	11.5
7	2.0	1.6	14.2
9	2.8	2.0	13.0

⁽¹⁾ This is both the concentration and mass-loading peaking factor, at constant basin-effluent flow rate.

V_r of 0.33, the flow equalization V_r required is only 0.12 (Table 4) and the remainder is available for waste-strength equalization.

The simulation showed (Table 5) that, for a total retention volume of 0.33 (which appeared to be close to the optimum retention volume for waste-strength equalization from Figure 10, and to about twice the minimum volume required for flow equalization alone), the range of the effluent peaking factors is 1.4 to 2.0, and better than with simple waste-strength equalization at $V_r = 0.33$, whose PF is from 1.7 to 2.8 (for concentration). Mass-loading peaking factors also are greatly reduced. The superiority of this new technique to equalize waste strength while simultaneously equalizing flow rate is clear, in comparison to the traditional approaches involving either flow rate or waste-strength equalization.

CONCLUSIONS

From the experimental results, and from the calculations performed using the validated models, the principal conclusions of this investigation are as follows:

1. Both models developed accurately predict the effluent concentration from the waste strength equalization basin. Thus, it is simple to determine the size of the equalization facility, based upon the maximum acceptable variation of the effluent concentration of the waste;
2. Waste-strength equalization, when accomplished with a constant liquid volume in the equalization basin, is an efficient method to dampen the concentration and the mass loading of the waste;
3. Large retention volume to equalize waste-strength fluctuations does not appear to be necessary, because there is little or no efficiency gained by such an increase in the volume of the basin;
4. For the cycles studied, a retention volume of about one-third of total cycle inflow was usually sufficient to achieve economical waste-strength equalization;
5. Contrary to the flow-equalization technique, by which it is possible to totally suppress flow variations, there is a practical limit to the equalization of waste-strength fluctuations, and it is not feasible to completely suppress waste-strength variations; and
6. An increase in the minimum basin volume required for flow equalization, up to about one-third of the total inflow of one cycle, stabilizes flow rate and produces a substantial decrease in the fluctuations in both waste concentrations and mass loadings. This new technique appears to be more efficient than waste-strength equalization alone, using a constant-volume tank.

NOMENCLATURE

- $C(O)$ = $X(O)$
- d = column diameter
- dt = time interval
- dX = change in wastewater constituent concentration

- e = relative error at time t
- E = relative mean error
- PF = peaking factor and is the ratio of the maximum to minimum constituent concentrations over a cycle of operation
- Q = wastewater flow rate
- t = time
- T = time interval
- X = wastewater constituent concentration
- $X(O)$ = wastewater constituent concentration in equalization basin at time interval preceding time t
- $X(t)$ = wastewater constituent in equalization basin at time t
- V = volume
- Y = basin instantaneous hydraulic detention time

Subscripts

- i = influent condition
- r = ratio of basin retention volume to total flow volume of one cycle of operation

Superscripts

- j = j^{th} interval

LITERATURE CITED

1. Adams, C. E. and W. W. Eckenfelder (ed.), "Process Design Techniques for Industrial Waste Treatment," Enviro Press, Nashville, Tenn. (1974).
2. DiToro, D. M., "Statistical Design of Equalization Basins," *ASCE Journal of the Environmental Engineering Division*, EE6 (1975).
3. Humenick, M. J., "Water and Wastewater Treatment," Marcel Dekker, Inc., New York, N.Y. (1975).
4. Humenick, M. J. and R. D. Taylor, "Functional Design of Equalization Basins," Report EHE-7501, CRWR-120. Center for Research in Water Resources, University of Texas at Austin (1975).
5. Metcalf and Eddy, Inc., 1979. "Wastewater Engineering: Treatment, Disposal, Reuse," McGraw-Hill, New York (1979).
6. Nagata, S., "Mixing Principles and Applications," John Wiley and Sons, Inc., New York, N.Y. (1975).
7. Ouano, E. A. R., "Developing a Methodology for Design of Equalization Basins," *Water and Sewage Works* 124, 48-52 (1977).
8. Wallace, A. T. and D. M. Zollman, "Characterization of Time Varying Organics Loads," *ASCE, Journal of the Sanitary Engineering Division* 97, SA3 (1971).

James W. Patterson is Professor of Environmental Engineering and Chairman of the Pritzker Department of Environmental Engineering, at Illinois Institute of Technology, Chicago, Ill. He also serves as Director of the Industrial Waste Elimination Research Center of IIT. In addition, he is the founder and President of the firm of Patterson Associates, Inc.



He is an internationally recognized expert on industrial pollution control, and he is the author of one book and over seventy other publications. He has served as a consultant to numerous government agencies and industries. He has also just completed a six-month assignment as Executive Director of the Illinois Hazardous Task Force, which developed state policy for the long-term management of hazardous waste in Ill.

New Solutions to Industrial Waste Management

The modification of existing processes must be considered in the search for cost-effective solutions in the treatment of hazardous wastes.

Linda M. Curran, Battelle Columbus Division, Columbus, Ohio 43201

Most of the hazardous waste generated in the U.S. is land-disposed without prior treatment. In a survey of ten states, industrial wastes were among the most frequently reported sources of groundwater contamination [1]. Yet, valuable materials are contained in the millions of tons of industrial waste that are discarded each year. Rather than disposing of these wastes in landfills, changing the process to reduce reuse, or eliminate the waste is often a more attractive and cost-effective solution. With the increasing costs of waste-disposal options, as well as long-term liabilities associated with containment methods, process modifications should be considered a primary method for waste control.

The options available for waste management are illustrated in Figure 1. Up to 80 percent of waste currently generated in the U.S. is directly landfilled [2]. Volume-reduction methods can be employed to increase the landfill space available for other wastes or render the waste easier to handle. Hazard-reduction methods are treatment techniques that break down hazardous constituents into non-hazardous compounds, reduce the level of hazardous constituents, or substitute a less hazardous component. The process-modification approach employs both methods of volume and hazard reduction.

Process changes are not a new concept. Industry has been effectively using process modifications to reduce operating costs and increase operating efficiencies, but generally, waste control has not been a primary incentive. Reduced operating costs have been achieved through changes in raw material, energy, and labor requirements. In some cases, equipment changes have resulted in reduced capital requirements as well.

The purpose of this paper is to review technologies that can lead to the implementation of cost-effective process changes for hazardous-waste reduction.

Process Modification Approaches

Volume reduction of waste can be achieved through four methods of process modification: 1) improved reactor designs; 2) process-chemistry changes; 3) improved separa-

tions methods; and 4) advanced sensing and control technology. Both recent and historical examples of these approaches will be described.

New Reactor Designs

New reactor designs offer promising ways of improving process efficiency, as well as reducing wastes. The chlor-alkali industry is a good example of an industry that historically has incorporated process changes to increase efficiencies and reduce operating costs. At the same time, waste has been reduced through the implementation of these changes. Two different electrolysis processes were developed to produce chlorine and sodium hydroxide at about the same time. One, the mercury-cell process, yields high concentrations of sodium hydroxide, but generates a waste containing mercury.

The other process, the diaphragm-cell process, uses naturally available salt brines and generates a waste containing chlorinated hydrocarbons, but no mercury. Modification of the latter, the replacement of the graphite anode with a dimensionally stable anode, has reduced the quantity of chlorinated hydrocarbons in the waste.

In a more recent modification of the diaphragm cell, involving replacement of the asbestos diaphragm with a polymeric membrane, the process has been improved to generate a higher sodium-hydroxide product concentration, similar to that generated in the mercury cell. On a total industry basis, the volume of waste generated potentially could be reduced. Through the phase-out of mercury-cell units and the adoption of this latest process modification, both elimination of mercury-contaminated waste and a reduction in waste contaminated with chlorinated hydrocarbons could result [3].

Advances in fluidized-bed designs offer opportunities for volume/hazard reduction in a number of applications. An example of fluidized-bed technology that has been applied to the conversion of wastes in the Multisolid Fluidized Bed (MSFB) process developed by Battelle [4]. The MSFB process uses a fluidized bed of relatively dense material such as gravel and a circulating bed of lighter material (sand). The system operates at relatively high velocities (20-40 ft/sec) and is capable of achieving high conversion efficiencies (95%) at these high throughput rates. A commercial system (5,000 lb fuel/day) has been operated by Conoco in Uvalde, Texas, to generate steam for secondary recovery of oil. The unit is designed to burn both coal and petroleum coke, a waste material from the refining process that is difficult to burn with conventional systems because of its low volatile content. The wastes and other materials shown in Table 1 have been successfully tested in smaller-scale MSFB units. Most waste materials can be burned to generate steam for process use or heating re-

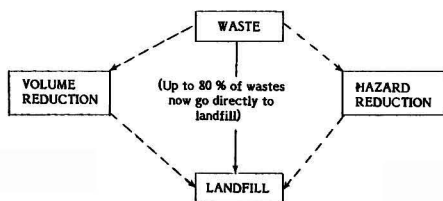


Figure 1. Waste management options.

quirements. In some cases, a medium-Btu gas is a preferable conversion product, and a gasification system based on the MSFB technology has also been developed.

Another example of improved operation, waste reduction, and emissions control resulting from redesign of a reactor system is in the manufacture of Supertropical Bleach, a decontamination chemical used in the U.S. Army. The desired product is a mixture of double salts of limited solubility such as $\text{CaCl}_2 \cdot \text{Ca}(\text{OH})_2 \cdot \text{H}_2\text{O}$ and $\text{Ca}(\text{OCl})_2 \cdot 2\text{Ca}(\text{OH})_2$. Prior process designs such as a fluidized-bed chlorination process have emitted chlorine levels above the allowable limits and did not consistently generate a product that met specifications. A modified system was designed based on chlorinating hydrated lime in an aqueous solution. Chlorine gas or liquid is bubbled into the solution; the solids are decanted and spray-dried, and then finished-dried in a fluidized bed. Old, inactivated, bleaching powders also can be processed in the system and regenerated. The primary advantage, in addition to improved product quality, is control of chlorine emissions by reuse within the process without the need for additional scrubbing systems.

Process-Chemistry Changes

Of the four categories, process-chemistry changes generally require the most substantial equipment changes and, therefore, the largest capital investment to make the modifications. However, in most cases, this approach offers the greatest potential for reduction or elimination of hazardous waste. The electroplating industry has incorporated many modifications to reduce the hazard level of the waste generated, as well as the quantity of waste. Generally, the modifications are waste-stream treatments, as opposed to process-chemistry changes. For example, acidic solutions are neutralized with caustic soda and hexavalent-chromium wastes are converted to the trivalent state to reduce toxicity. However, significant quantities of waste can be eliminated through process-chemistry changes. One example can be cited in the manufacture of printed circuit boards. The conventional process uses acid solutions to chemically etch circuits in copper-coated plates. Waste solutions from the process are corrosive and toxic due to contaminant metals. A better method involving a process-chemistry change substitutes a fast-rate electrodeposition (FRED) technique to electroform the circuit elements to final shape so that chemical etching is not required. Scrap copper, waste heat, acid spray, and air (or oxygen) are used in a separate reactor to produce a copper-sulfate solution for the electrodeposition bath. The only waste products to be disposed of are low-grade heat and used photoresist material [5].

The same technology has been coupled with an injection-molding process to plate plastic parts. Current practice involves the molding of plastic parts in one operation, then chemically etching activating, metallizing, and plating them in an entirely separate production line. The in-mold plating process deposits the metal on the mold, then the part is injection-molded. The new process is claimed to be fifty times faster and 30 percent cheaper than the conventional method, and does not produce waste acidic solutions.

TABLE 1. WASTE MATERIALS PROCESSED IN MSFB PROCESS

Materials	Conversion Process
Sewage sludge	Combustion
Municipal solid waste	Combustion
Pulping liquor	Combustion
Peat	Gasification
Wood chips	Combustion/Gasification
Coal	Combustion/Gasification
Petroleum coke	Combustion

A process improvement developed to reduce waste from the electroless nickel-plating process has been shown to stabilize the plating bath to avoid decomposition of the bath. With the conventional process, the bath decomposes after a few days and must be discarded. Thousands of gallons of nickel-containing solutions must be treated and dumped annually. Treatment methods to remove nickel from the waste include reduction to metal, precipitation to metal sulfides with sodium hydrosulfite or ferrous sulfide, alkaline precipitation by caustic, lime, or potassium permanganate followed by calcium-chloride, or ion-exchange purification. All treatment methods are expensive and not completely effective. By adopting a dual-anode process, where the soluble anode controls bath composition and the insoluble anode controls bath pH and stability, a bath results which can be used indefinitely, hence avoiding frequent dumping. The new plating process generates surface finishes that are bright and hard, and at least as good as the electroless equivalents, all for a lower cost.

Separation Technologies

Integrating a separation step into a process rather than as an add-on processing step can be an effective way to reduce the waste volume or hazard as well as reducing downstream processing costs. Traditionally, separation technologies have been applied to waste streams as an end-of-pipe control technology. As an example, primary wastewater-treatment systems are based on physical separation methods. Component-separation methods, e.g., ion exchange, ultrafiltration, reverse osmosis, electrolysis, and resin adsorption are increasing in importance in commercial applications, particularly in systems requiring removal of metal ions from solutions. Chemical transformation, e.g., precipitation followed by settling, has been effectively employed for the separation of salts and metals from solutions. Thermal oxidation has been used not only to destroy wastes, but also for recovery of materials from the combustion products.

Some advanced separation technologies have been applied to reduce the volume of wastes. Advanced separation techniques include ultrasonic methods, supercritical extraction, dual-solvent extractions, thermal leaching, high-performance liquid chromatography, electrophoresis, and affinity separations. These technologies are emerging as potential methods for waste reduction where high-cost materials can be recovered and reused.

Some examples of separation techniques that have been successfully implemented as process changes and have resulted in both waste and operating-cost reductions are shown in Table 2.

Sensors and Control Technology

Process-control technology has historically led to reduced waste through improved operational efficiency. Recent advances in microelectronics have led to new capabilities in control systems. The functional elements of control technology are illustrated in Figure 2. Sensor needs may be identified during the development of the process-control strategy. Based on the needs identified, new sensors may be required. Sensor-location strategy implies the importance of locating the sensors in the appropriate position in the system and the control logic. Diagnostics represents the process of interpretation of sensor information. All three elements are critical functions in process-control strategy.

One example of the application of a sensor that has led to process modification and waste reductions is in combustion systems. Measurements of oxygen partial pressure have been related to incomplete mixing of fuel and combustion gases as well as localized corrosive environments. The result is redesign of fuel feed systems that has led to

TABLE 2. APPLICATIONS OF SEPARATION TECHNOLOGIES FOR WASTE REDUCTIONS

Application	Technology	Result
1. Separation of PCBs from [7] hydraulic fluid	Vacuum distillation	Operation in commercial plant —Recycle of hydraulic fluid —Destruction of concentrated PCB waste stream
2. Titanium ore processing [6]	Thermal leaching	Elimination of slime formation—restart of closed plant
3. Separation of plastic resins	Air classification	Recycle of resins —Reduced raw material cost
4. Recovery of gold from black [8] sands	Selective flocculation	Reduced operating cost

reduced gas emissions of carbon monoxide and hydrogen sulfide and improved fuel usage [9].

A second example is a sensor developed to control a rotary-kiln incinerator used for disposing of ammunition. The sensor was designed to automatically measure where detonations were occurring in the incinerator. The sensor was integrated into the control system to control the detonation position in the kiln, thereby limiting the emissions of the unburned gases generated by the detonation.

Similar technology has been used to design remote sensors for detecting chlorine, fluorine, iodine, sulfate, iron, uranium, plutonium, and ammonia, as well as sensors for pH and temperature. The sensors are designed to operate on-line in hazardous and explosive environments and are low in weight, chemically inert, and made of non-strategic materials. These sensors could be applied to increase the understanding of process systems that may lead to improvements for the reduction in volume and/or hazard of wastes.

CONCLUSIONS

Significant improvements in waste control have been demonstrated through process modifications that result in waste volume and hazard reduction, as well as recovery of valuable feedstock. Hazardous-waste management is a complex problem and, unfortunately, process modification does not represent a single solution to all waste-disposal problems. Different processes require different modifications to avoid or reduce the amount and/or hazard or waste generated.

Progressive companies are using waste control as an opportunity to identify modifications that will improve

efficiencies and reduce costs as well as reduce or eliminate disposal liabilities.

LITERATURE CITED

1. Pye, V. I. and R. Patrick, "Groundwater Contamination in the United States," *Science*, **221**, 713-718 (August 19, 1983).
2. "Technologies and Management Strategies for Hazardous Waste Control," Office of Technology Assessment, Congress of the United States.
3. Colaruotolo, J. F., "An Environmentally Acceptable Alternative to the Asbestos Diaphragm Cell," A.I.Ch.E. National Meeting, Houston, Texas, March 27-31, 1983.
4. Curran, L. M., H. Nack, and B. C. Kim, "Battelle's Multi-Solid Fluidized-Bed Process—An Advanced Concept in Energy Conversion Processes," presented at the International Congress on Technology and Technology Exchange, Pittsburgh, Pennsylvania, May 3-6, 1982.
5. Schaer, G. R. and T. Wada, "Electroformed Flexible Printed Circuitry," *Plating and Surface Finishing* (July, 1981).
6. Stambaugh *et al.*, U.S. Patent, "Processing for Beneficiating Titaniferous Materials," Patent Number 4,321,236, March 23, 1982.
7. Mink, W. H., R. K. Smith, H. E. Carlton, and J. R. Longanbach, "Separation of PCB's from Hydraulic Oil," *Environmental Progress*, **2**, No. 4 (November, 1983).
8. Attia, Y., "Process and Apparatus for Producing Metalliferous Concentrate from a Particulate Feed Material," U.S. Patent Application applied for June, 1983.
9. Holt, C. F., A. A. Boirarki, and H. E. Carlton, "The Gas Turbine Heat Exchanger in the Fluidized Bed Combustion," ASME Paper No. 82-GT-225.

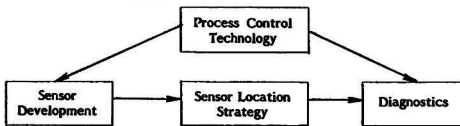


Figure 2. Elements of control technology.



Linda Curran, a registered professional engineer in the state of Ohio, holds B.S. Ch.E. and M.S. Ch.E. degrees from Ohio State University. She has been with Battelle's Columbus Laboratories since 1974 and is presently associate manager in the Chemical and Biochemical Processes Section. She recently completed a 1-year congressional fellowship with the Office of Technology Assessment and contributed to the study on "Technologies and Management Strategies for Hazardous Waste Control."

Solving Environmental Challenges of Indirect Coal Liquefaction

Despite the current oil glut, worldwide oil resources are finite and dwindling. Long-term research and development on coal-liquefaction are still imperative.

Margaret M. Lobnitz and Michael G. Webb, Engineering-Science Co. Arcadia, Calif. 91006

The W. R. Grace & Co. CMG process design produces consumer grade unleaded gasoline from high sulfur, agglomerating, Western Kentucky coal. Air pollution emissions are from materials handling, desulfurization, process heat generation, and catalyst regeneration. The major advantage of this gasoline synthesis route over other coal conversion approaches is that only barely detectable amounts of polynuclear aromatic compounds are present in either the process or product streams, substantially reducing the potential threat to the health and safety of workers and local communities. Another advantage is that most of the feedstock is converted to gasoline; a single, readily marketable commodity. One notable environmental innovation is an acid gas removal unit capable of removing carbon dioxide and hydrogen sulfide while minimizing release of carbon monoxide and volatile organic compounds. Another innovation is a rail-based solid waste handling system that automatically differentiates between three different solid byproduct trains utilizing the same transport corridor, thus eliminating potential disposal errors as it diminishes the land area disturbed during transport activities. Because this process involves only three major conversion steps, product yields are high and waste product types are fewer in number, minimizing areas requiring implementation of pollution control and simplifying disposal system design and operation.

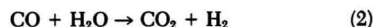
INTRODUCTION

America possesses more than a trillion tons of recoverable coal which contain as much as five times the total energy available in our domestic petroleum resources [1]. A basic impediment to using this coal is that the typical American consumer is on a liquid, rather than solid energy diet, mostly because of transportation requirements. The economic costs and time delays of converting transportation to a nonpetroleum fuel, whether it be hydrogen, micronized coal, electricity, or even alcohol, make it expedient to develop systems for producing synthetic gasoline from coal, even if the energy penalty is 50 percent or more.

Four coal liquefaction facilities were recently proposed for construction in Western Kentucky [2]; the W. R. Grace & Co. Coal-to-Methanol-to-Gasoline (CMG) Plant was one of those four.

This article introduces the reader to coal liquefaction as it is approached in the CMG plant and will discuss the technology approach taken in solving potential environmental issues regarding flue gas desulfurization, acid gas removal and material handling.

Coal exists as a solid because of the complexity of its carbon structures, and its low hydrogen-to-carbon ratio. Liquefaction can be effected by breaking the structures into smaller units, and/or by adding hydrogen (see Figure 1). When hydrogenation is employed, part of the carbon is usually sacrificed in side reactions with water to generate the hydrogen.



Coal can be liquefied by either of two systems: "direct liquefaction," which is partial hydrogenation or reformation to lower the melting points of the carbonaceous compounds, or "indirect liquefaction," which is total hydrogenation, reformation, or hydrolysis to generate gaseous compounds that are then converted to liquids via additional chemical treatment.

Direct liquefaction is semi-selective in product formation and, depending upon the degree of treatment, can be used to produce synthetic crude oil, light liquid hydrocarbons, or even synthetic natural gas [3]. Indirect liquefaction converts all the usable carbon to a single chemical species, then uses known reactions to form a pure liquid such as methanol. Further processing of the methanol can be employed to produce other organic liquids or solids.

The CMG Plant proposed near Baskett, Kentucky, is an indirect liquefaction plant designed to convert 24,300 tonnes per day (tpd) of high sulfur agglomerating coal into 16,200 tpd of methanol. The methanol is further processed to yield 50,000 barrels per day (8000 cubic meters) of consumer grade unleaded gasoline, and 7,000 bpd (1110 m³) of iso-butane and LPG. In addition, 900 tpd of sulfur are recovered for commercial use in other facilities.

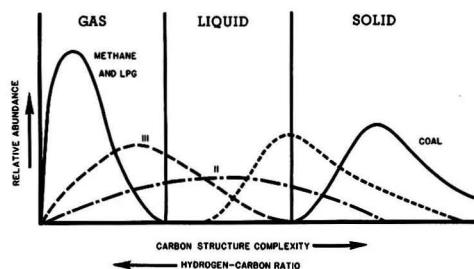
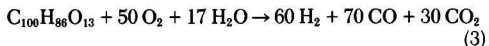


Figure 1. Direct liquefaction of coal, stages I, II, and III, and gasification to fuel gases.

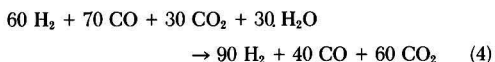
THE PROCESS

Figure 2 is a block flow diagram of the CMG Plant. Coal is fed to the gasifiers at the rate of 720 tonnes per hour MAF (moisture and ash free), giving an energy input of approximately 24×10^9 Btu/hr (25×10^{12} Joules/hr). Nearly 810 tonnes per hour (tph) of oxygen and 153 tph of water are also fed to the gasifier. Equation 3 shows part of the gasification reaction.



Sulfur in the feed coal is converted into hydrogen sulfide (H_2S) and carbonyl sulfide (COS). Based on the design coal input, approximately 34 tph of H_2S and 4 tph of COS exit the gasifier, totaling approximately 1/3 percent of the synthesis gas stream [4].

To attain the desired two-to-one ratio of hydrogen-to-carbon monoxide needed for methanol synthesis, part of the raw gas stream is reacted catalytically with additional water in a shift reactor. Equation 4 shows the main reaction.



At the same time, half of the COS is shifted to H_2S , for a resultant production rate of 35 tph H_2S and 2 tph COS.

The shifted gas stream contains approximately 75 percent of the heat value of the coal directed to the gasifier (and approximately 67 percent of the heat value of the total coal consumption of the plant).

An Acid Gas Removal (AGR) unit removes CO_2 , COS, and H_2S from the synthesis gas. Removal efficiencies are 94 percent, 99.5 percent, and 99.99 percent, respectively, resulting in a gas stream composition of approximately 68 percent H_2 , 29 percent CO, and 3 percent CO_2 .

In the methanol synthesis unit, 98 percent of the carbon oxides are converted to methanol. This represents a 41 percent conversion of the carbon fed to the gasifiers, or approximately 37 percent of the total carbon consumed at the facility. The methanol contains 15×10^9 Btu/hr (16×10^{12} Joules/hr) or approximately 62 percent of the heat energy fed to the gasifiers.

The process used for converting the methanol to gasoline is the M-Gasoline Process developed by Mobil Research and Development Corporation. It is a fixed-bed catalytic process which produces compounds predominately in the gasoline boiling range, from C_4 to C_{10} . The hydrocarbon products are highly branched paraffins, highly branched olefins, naphthenes, and aromatics. Due to the selective nature of the catalyst, almost no compounds are formed containing more than ten carbons, resulting in a

polynuclear aromatic content of less than 0.25 ppm in the finished gasoline [5].

During conversion, each 100 tonnes of methanol produces 56 tonnes of water, 42 tonnes of raw gasoline, and two tonnes of methane and other light gases. The raw gasoline is prepared for sale by fractionation to remove LPG, alkylation of butenes and pentenes, and reduction of durene. Ninety percent of the carbon fraction of the methanol is contained in the finished gasoline, 4.5 percent is converted to salable LPG, and 4.5 percent leaves the plant as isobutane. Heat content of these three products is approximately 45 percent of the heat input to the gasifiers, or approximately 40 percent of the total received at the plant. Figure 3 shows an overall energy schematic for the process.

THE PROBLEMS

The CMG plant was designed specifically to demonstrate the feasibility of converting high sulfur coal to a clean fuel. Therefore, use of the coal in an on-site steam generation unit was preferred to other options such as the importation of special, low sulfur boiler fuel, or direct purchase of electrical power from utilities using low sulfur fuels. Unfortunately, direct burning of the high sulfur coal gives rise to large quantities of SO_2 .

The process selected for flue gas desulfurization (FGD) was Research-Cottrell's proprietary Double-Loop™ limestone process. The system uses two limestone slurries of different pH's to react with the SO_2 and oxidize 95 percent of the resulting calcium sulfite to calcium sulfate, a conveniently disposable solid, which, with proper management, can be sold as gypsum board feedstock.

Of the 6.6 tph of sulfur dioxide formed in the steam boilers, only 0.5 tph, or 8 percent is released to the atmosphere, the rest is contained in 36 tph of stabilized FGD solid waste, which is landfilled on an adjoining site.

Sulfur in the coal that passes through the gasifiers and shift reactors results in H_2S and COS contaminants in the synthesis gas stream. This stream, which is 47 percent H_2 , 20 percent CO, 32 percent CO_2 , 1.1 percent H_2S , and 0.03 percent COS, presents unique problems for acid gas removal. The first problem is that of magnitude. The installation is larger than any other of its kind in the world [6]. In order to avoid mechanical and installation problems, the system has been divided into four parallel trains, each with capacities in the range of currently available equipment.

The high partial pressures of CO_2 and H_2S in the feed gas result in high absorption rates, and possibly large solvent temperature increases. A system employing selective absorption of H_2S by cold solvent, presaturated with CO_2 , is used to minimize heating and solvent circulation rate.

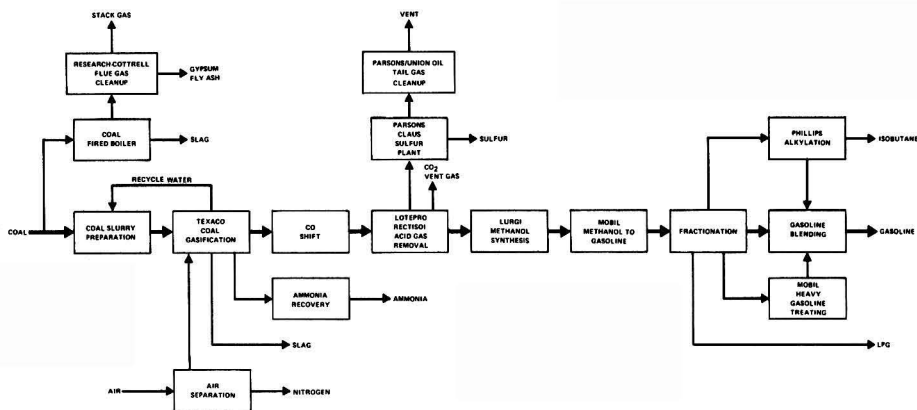


Figure 2. Block flow diagram.

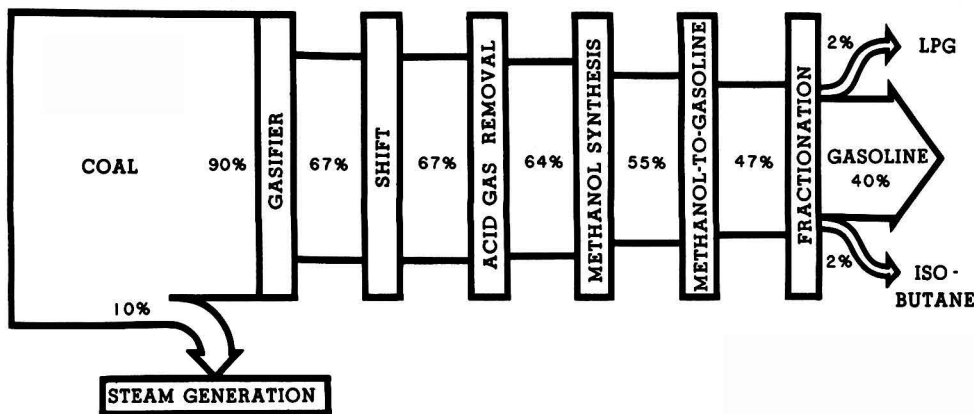


Figure 3. Overall energy schematic.

Two AGR systems were evaluated for use on the synthesis gas: Selexol, which uses the dimethyl ether of polyethylene glycol as a solvent, and Rectisol, which uses methanol at subzero temperatures. Selexol, which is often employed to remove CO_2 and H_2S on deeply shifted gases streams that contain no COS, cannot adequately separate COS from the CO_2 vent stream, and its use would result in high COS emissions from the CMG Plant [7]. A corrective procedure is to precede the AGR with a hydrolysis unit capable of converting 98 percent of the COS to H_2S , a compound easily handled by Selexol.

The Rectisol process is able to remove COS from the synthesis gas stream and desorb it into the H_2S fraction of the acid gases, allowing little of it to escape in the CO_2 vent gas. However, the solvent also absorbs some of the carbon monoxide from the synthesis gas and releases it with the CO_2 , adding to overall CO emission levels. Also, the solvent has a relatively high vapor pressure, and contributes to the amount of volatile organic compounds (VOC) released from the plant.

The Rectisol process was favored for the CMG Plant due to economics, availability of the solvent (methanol, an intermediate of the CMG process) and because of its superior control of COS. The potential environmental problems of excessive CO and VOC emissions were solved by adding flash drums on specific solvent streams to remove these gases. Flash gases high in methanol were then routed to water wash towers, and those high in CO were sent to four parallel trains of catalytic oxidizers. These procedures reduced potential CO emissions by 93 percent, and potential VOC losses by 87 percent.

The sulfur recovery unit processes 104 tph of acid gas containing up to 33 percent by weight of reduced sulfur compounds. Two Claus units convert 95 percent of the sulfur compounds to elemental sulfur, and produce 160 tph of tail gas containing 1.7 percent CO, 1 percent H_2S , 0.03 percent COS, and 0.5 percent SO_2 . The tail gas is treated by the Beavon Sulfur Removal Process which reduces CO emissions by 93 percent and total reduced sulfur compound emissions by 99 percent.

There are two unique sources of liquid pollutants in the CMG Plant. Gasification is the first source. Coal is introduced into the gasifiers in a water slurry, and the synthesis gas produced is quenched and scrubbed by water sprays. Excess water from the slurry and sprays contains fluoride, sodium salts, trace metals, and possibly some heavy organics. The second source of liquid pollutants is nascent water from the methanol synthesis reaction, which contains some water soluble organics.

Effluent from these sources, and other more common effluent streams such as cooling tower blowdown, clarifier underflow, and precipitation runoff are treated

using technologies that include aerobic digestion, trickling filters, pressure filtration, ion exchange, reverse osmosis, and evaporation (see Figure 4). These operations result in zero liquid discharge from the plant, and two solid wastes: one containing compounds known to be non-hazardous and a waste stream whose composition cannot be accurately predicted at this time. This waste will be handled in the same manner as a hazardous waste stream until its composition can be accurately determined.

In addition to the two solid waste streams produced by water treatment, the plant produces gasifier slag, boiler bottom ash, and FGD solids. The slag and ash will be landfilled together in an area which allows recovery if the material can be successfully marketed. Process water treatment solids that are of uncertain composition are combined in a second landfill area designed and operated in accordance with the hazardous waste landfill regulations. All other solid wastes are combined in a third landfill.

The three landfills are located two miles from the process area on a contiguous parcel of land. In order to assure proper disposal of each waste, and at the same time to minimize the environmental impact of the transportation facilities, three separate train systems are employed which share portions of the trackage (see Figure 5). Each waste has a dedicated set of cars: bottom dump cars for slag and ash, right-side dump cars for waste presumed to be hazardous, and left-side dump cars for other solid waste.

Each of the three types of waste has a separate loading facility in the process area. The facilities are automatic, and can be activated only by the cars specified for that particular waste. If a train of bottom dump cars intended for slag and ash is inadvertently pulled into a loading area for waste water solids, the facility will not operate, and no waste will be loaded into the cars. The same is true for other incorrect positioning of cars.

Once the train is loaded at the proper area, it moves onto the common rail system shared by all waste trains. These tracks lead from the process area to the waste disposal areas. By sharing the corridor, land use is minimized. As the train approaches the landfills, unique signaling devices in the cars cause the track switches to automatically direct the train to the correct disposal area. At the unloading site, automatic triggers similar to those at the loading areas unload the cars only if they are the specific type dedicated to that particular landfill. These automatic interlocks assure that the three waste streams will be kept separated at all times.

CONCLUSIONS

Following the transition from the Carter to the Reagan Administration, a decline began in the government's interest in coal conversion. The U.S. Department of Energy

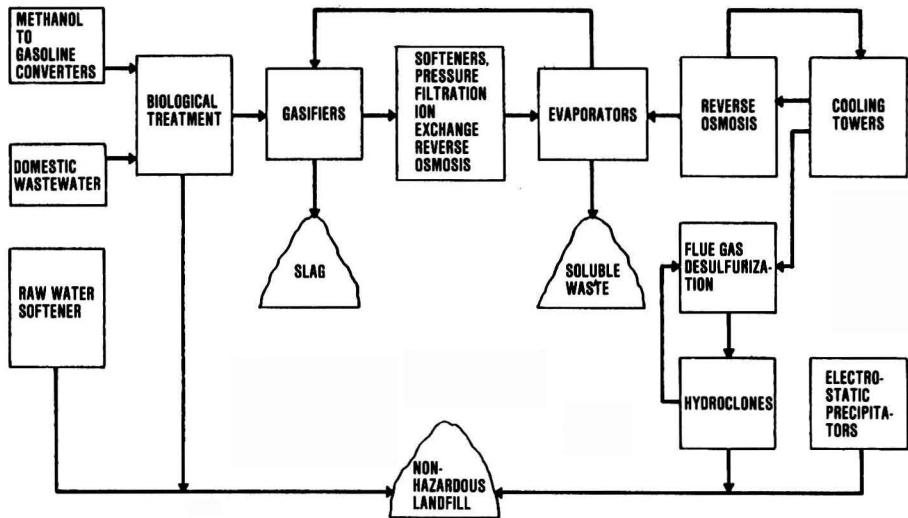


Figure 4. Liquid and solid-waste handling scheme.

relinquished its responsibility for developing coal conversion technology to the Synfuels Corporation. In early 1983, W. R. Grace & Co. participated in solicitation hearings with the Synfuels Corporation regarding their coal conversion project. Grace proposed a joint venture between itself and the Synfuels Corporation to construct the CMG Plant—the proposal was rejected. Currently, there are no plans to construct any of the four synthetic fuels facilities originally proposed for development in Kentucky.

A worldwide surplus of petroleum and correspondingly lower oil prices have caused alternate fuels to appear less financially attractive. Despite the current oil glut, worldwide oil resources are finite and are dwindling. Coal conversion projects ensure a long-term and reliable energy supply but additional research is necessary to confirm their environmental acceptability.

Coal conversion research should continue and full-scale demonstration facilities should be built and tested before the time when the need for this technology becomes critical.

LITERATURE CITED

1. Moore, J. W. and E. A. Moore, "Environmental Chemistry," Academic Press, New York (1976), p. 74.
2. Jones, J. E., Jr. and H. G. Enoch, "The Kentucky Synfuel Industry," Kentucky Department of Energy (March, 1981).
3. Jahng, C. E. and R. R. Bertrand, "Environmental Aspects of Coal Gasification," *Chemical Engineering Progress*, 127-132 (August, 1976).
4. U.S. Department of Energy; "Process Engineering and Mechanical Design Reports for a 50,000 BPD Coal-to-Methanol-to-Gasoline Plant" (August, 1982).
5. W. R. Grace & Co., "Prevention of Significant Deterioration Analysis of a 50,000 BPD Coal-to-Methanol-to-Gasoline Plant," Vol. I (1982).
6. R. M. Parsons Company, "Process Selection Study Report: Gas Purification Alternatives" (July, 1981).
7. Riesenfeld, F. C. and A. L. Kohl, "Gas Purification," Gulf Publishing Co., Houston, Second Edition, pp. 693-733.

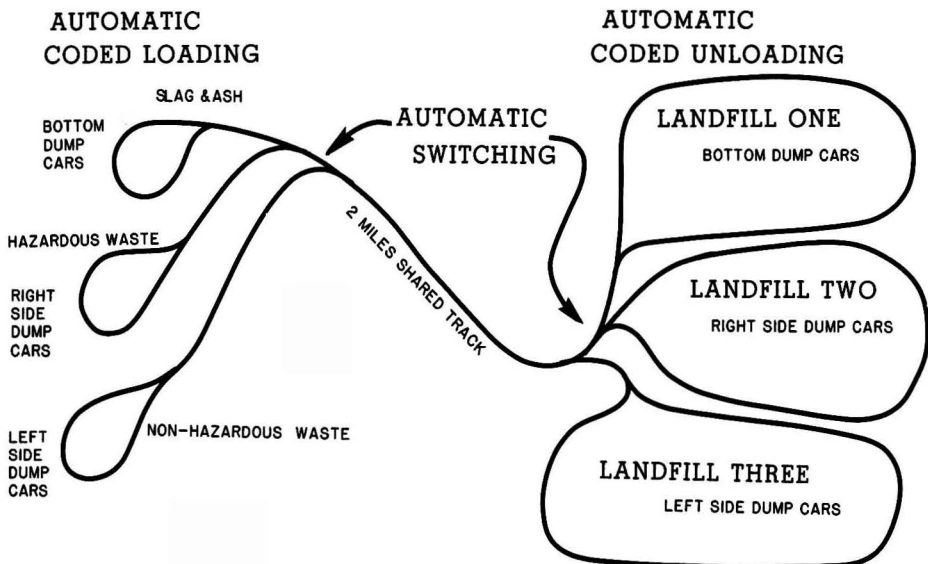


Figure 5. Solid-waste disposal system.



Margaret M. Lobnitz is a senior environmental scientist with Engineering-Science, Inc. She holds a doctorate in Environmental Science and Engineering from U.C.L.A. and has 4 years experience in the energy field.



Michael G. Webb is a senior environmental engineer with Engineering-Science, Inc. He is a Registered Professional Engineer in Calif., with 12 years experience in the energy field.

Reverse-Osmosis Membrane for Treating Coal-Liquefaction Wastewater

Low-pressure membrane separation processes are taking on importance for the purpose of permeate-water reuse.

D. Bhattacharya, M. Jevtitch, J. K. Ghosal, and J. Kozminski, University of Kentucky, Lexington, Ky. 40506-0046

The development of a low-pressure membrane separation process for the simultaneous removal of organics, salts, and scale-forming compounds from coal-liquefaction process wastewaters will minimize surface-water pollution and decrease water consumption by permeate recycling to cooling towers. Inherent to the operation of all coal-conversion facilities is the production of large amounts of highly contaminated wastewaters. For example, H-Coal liquefaction-process wastewater [1] contains as much as 3000 mg/liter phenol, 7000 mg/liter NH_3 , 8000 mg/liter H_2S , 1000-2000 mg/liter NaCl, and a variety of other compounds, organic and inorganic, which make extensive wastewater treatment a necessity for water discharge or in-plant reuse.

The use of membrane processes for water reuse and concentrate-volume reduction is gaining considerable attention in many industries. The recent industrial development of non-cellulosic thin-film composite membranes has provided treatment techniques with high solute (salts and organics)-separation characteristics (even at low pressures of 15×10^5 to 20×10^5 N/m^2 pressure range) and insignificant compaction problems. The low-pressure (commonly used for brackish-water treatment) membranes have definite advantages in terms of energy savings, and lower capital cost [2].

The work reported in this paper was conducted with actual wastewater obtained from the H-Coal liquefaction pilot plant (220 tons/day capacity), operated in Catlettsburg, Kentucky, by Ashland Synthetic Fuels, Inc. As part of an overall coal-liquefaction wastewater-treatment scheme (Figure 1), low-pressure membrane processes would be preceded by H_2S , NH_3 stripping, phenol extraction, followed by the powdered activated carbon-assisted biological process (PACT), for the removal of 92-99% of the organics, H_2S , and NH_3 . The effluent from the PACT process would still contain 80-200 mg/liter COD, and all the influent chloride (500-2000 mg/liter depending on the chloride content of coal) and other inorganic salts.

The overall objective of this investigation was to evaluate the separation and water-flux characteristics (with biotreated coal-liquefaction wastewater) of two types of low-pressure membranes: a spiral-wound module containing a thin-film composite (aromatic polyamide) membrane and a hollow-fiber module of high packing density

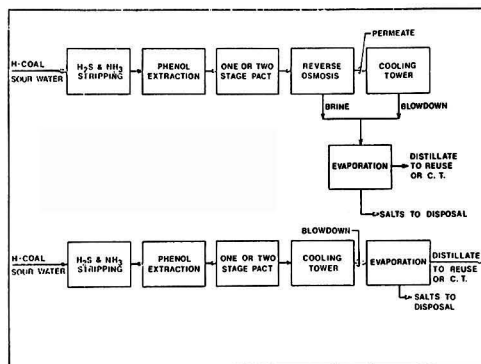


Figure 1. Possible treatment techniques for coal-liquefaction wastewater reuse.

containing asymmetric (aliphatic-polyamide) membranes. The membrane-separation characteristics are evaluated in terms of pretreatment requirements (Silt Density Index, SDI), flow rates, pressures (14×10^5 to 24×10^5 N/m^2), and extent of water recovery. In addition to conventional analysis, high pressure liquid chromatography (HPLC) was used to provide a preliminary characterization of feed and permeate quality.

COAL LIQUEFACTION WASTEWATER AND TREATMENT STEPS

As part of the H-Coal Pilot Plant data-collection effort, extensive characterization was performed on the plant-generated wastewater streams and has been reported by Churton and Skrylov [1]. Process wastewaters result from the washwater-injection system and the condensation of stripping streams used in the atmospheric stripper, the fractionator, and the vacuum tower. The combined wastewaters contained high concentrations of H_2S , NH_3 , phenolics, alkalinity, and NaCl. A typical composition of the major components of the raw wastewater stream resulted from the Kentucky #9 Coal liquefaction is shown in Table 1.

TABLE 1. H-COAL LIQUEFACTION WASTEWATER [1]

Parameter	Concentration, mg/liter	
	Mean	Standard Deviation
Phenol	2300	460
Cresol (para and meta)	1200	180
Cresol (ortho)	410	55
Resorcinol	240	28
TOC (total organic carbon)	4900	1400
H ₂ S	8900	2300
NH ₃	7600	2400
Alkalinity	22000	8100
Cl ⁻	1000	280
CN	27	18
pH	9.4	0.4

In an effort to obtain design information for a full-scale treatment plant (Figure 1), Ashland Synthetic Fuels, Inc. conducted H₂S and NH₃-stripping studies, followed by dephenolization studies by Chem-Pro, Inc. (New Jersey) and biological treatment by Zimpro, Inc. (Wisconsin). The biotreated water was then used for the membrane studies.

Stripping of the raw waste (shown in Table 1) resulted in H₂S and NH₃ concentration reduction to less than 3.0 mg/liter and alkalinity reduction to about 400 mg/liter. Dephenolization (by Chem-Pro, Inc.) of stripped water by solvent extraction showed about 92% removal of phenol and TOC. Samples of the stripped, phenol-extracted water were treated [3] by the powdered activated carbon-assisted biological process (PACT) in single-stage and two-stage systems. The influent contained 1900 mg/liter COD, 830 mg/liter BOD, 9000 APHA color units, etc. A detailed analysis [3] of a typical PACT effluent is shown in Table 2. It should be noted that, although the BOD value was reduced to <10 mg/liter, the effluent still contained high concentrations of COD, TOC, organic color compounds, and the inorganic salts.

TABLE 2. PACT EFFLUENT ANALYSES (H-COAL WASTEWATER)

Parameter	PACT Effluent	Parameter	PACT Effluent
BOD ₅	<10*	Silicon	<10
BOD ₂₀	<10	Barium	0.1
COD	200	Strontium	0.01
DOC or TOC	40	Iodine	N/A
Total phenols	2	Bromine	N/A
Color	1000 APHA units	Calcium	10
TKN	5	Magnesium	5
NH ₃ -N	1	Iron	1
NO ₃ -N	150	Total sulfur	<30
NO ₂ -N	2	SO ₄ -S	20
CN	1	Chlorides	1500
SCN	1	Sodium	2400
Total P	20	Manganese	N/A
Ortho P	20	Fluorides	N/A
Grease & oils	<0.1	CO ₂	150
Phenolphthalein alkalinity	N/A	Vanadium	0.05
Total alkalinity	N/A	Cobalt	0.1
Methyl alkalinity	N/A	Beryllium	<0.01
CO ₂	N/A	Copper	0.01
HCO ₃	N/A	Titanium	0.02
Total hardness	50	Zinc	0.1
Total solids	4000	Arsenic	0.01
Total ash	3000	Chromium	0.02
TDS	3750	Cadmium	<0.01
Suspended solids	15	Antimony	<0.01
Suspended ash	2	Silver	0.02
Turbidity	10 NTU	Lead	0.08
pH	7.5	Nickel	0.04
Free chlorine	N/A	Mercury	N/A
Boron	N/A		

* All units mg/liter unless otherwise specified.

MEMBRANE SEPARATION CONCEPTS AND SELECTED APPLICATIONS

General Concepts

Membrane processes are generally evaluated in terms of three parameters: membrane rejection (R), permeate-water flux (J_w), and extent of water recovery (r). The membrane rejection parameter, R , is a measure of the extent of solute separation,

$$R = 1 - \frac{C_p}{C_i} \quad (1)$$

in which C_p and C_i are the permeate and feed-stream solute concentrations, respectively. Primary separation of solutes occurs at the thin-film (skin) barrier layer. Thin-film results in a higher flux at pressures considerably less than asymmetric cellulose-acetate membranes.

A number of models have been developed to describe the transport of solute and solvent through membranes. Recently, Soltaneih and Gill [4] provided an excellent review of various models. The most commonly used model is the solution-diffusion model. The water and solute fluxes (under a chemical-potential driving force) are given by

$$J_w = \frac{D_w C_w V_w}{RT \Delta X} (\Delta P - \Delta \pi) = A(\Delta P - \Delta \pi) \quad (2)$$

and solute flux,

$$J_s = B(\Delta C) \quad (3)$$

in which D_w is the diffusivity of water in the membrane, C_w is the water concentration in the membrane, V_w is the partial molar volume of water, R is the gas constant, T is the absolute temperature, ΔX is the membrane thickness, $(\Delta P - \Delta \pi)$ is the net trans-membrane pressure, and "A" is the membrane-permeability (function of temperature) constant. "B" and "ΔC" in Equation 3 are solute permeability (function of solute-distribution coefficient between solution phase and membrane phase) and concentration gradi-

ent between the membrane surface and the permeate, respectively. In the case of negligible concentration polarization, ΔC and $\Delta \pi$ become the concentration and osmotic pressure difference between the bulk solution and the permeate, respectively.

Water Recovery

The water recovery, r , is defined as

$$r = \frac{\text{permeate flow rate } (F_p)}{\text{feed flow rate } (F_i)} = \frac{J_{avg} A'}{F_i} \quad (4)$$

in which J_{avg} = average permeate flux from a module and A' = membrane area. As water recovery increases, the bulk solute concentration in the membrane increases and, thus, the dependence of solute rejection upon concentration must be determined experimentally.

For semi-batch (where permeate is discharged and concentrate stream is returned to feed tank) operation with $F_p \ll F_i$, the following equations can be derived to predict the average concentration of permeate, as a function of " r ". If " V " is the feed-solution volume at any instant,

$$-VdC = CRdV \quad (5)$$

If R and C are related by,

$$1 - R = KC^n \quad (6)$$

in which K, n are functions of solute type and membrane characteristics. Combining Equations 5 and 6 and integrating between the concentration limits:

$$\int_{C_i}^{C_{concentrate}} \frac{dC}{C(1 - KC^n)} = \int_{V_i}^{V_{concentrate}} \frac{dV}{V} = \ln \left(\frac{1}{1 - r} \right) \quad (7)$$

Using Equation 7 and the solute material-balance relationship, the following two equations can be derived to compute the average solute permeate concentration, C_p , at any " r ";

Case 1: $n = 0$ (constant rejection)

$$C_p = \frac{C_i}{r} [1 - (1 - r)^n] \quad (8)$$

Case 2: $n \neq 1$ (variable rejection)

$$C_p = \frac{C_i}{r} (1 - M^{-\frac{1}{n}}) \quad (9)$$

in which

$$M = 1 - KC_i^n + K(1 - r)^{-n} C_i^n \quad (10)$$

Selected Applications

Reverse-osmosis membranes have been used to treat a variety of wastewaters [5-9]. Reviews of the development of membrane technology include works by Lonsdale [9], Sourirajan [10], Matson [11], Scott [12], and Strathman [8]. Bhattacharyya *et al.* [13-15] have done extensive work on membranes involving the separation of metals, oil, and permeate reuse of mine water and coal-conversion wastewater.

The rejection behavior of coal-conversion wastewater constituents (phenol, 0-cresol, 2,3-dimethyl phenol, catechol, resorcinol, etc.) with thin-film composite membranes has been reported [13]. Solute rejections for individual components ranged from (at $\Delta P = 14 \times 10^5 \text{ N/m}^2$) 70% to 90% at pH 5 (solutes nonionized), and from 93% to 97% at pH = 11.5 (solutes ionized). Recently, Campbell *et al.* [16] reported the use of polyamide and cellulose-triacetate membranes for demineralization of coal-conversion condensates (Hygas quench water). Tests with ac-

tual wastes showed that the polyamide membrane provided somewhat higher product-water quality (COD rejection = 90%, and conductivity rejection = 98%), while the cellulose-triacetate membranes provided greater water-flux rates. Asylova *et al.* [7] successfully removed dissolved organics and salts from refinery wastewater, using a treatment system consisting of ultrafiltration followed by reverse osmosis (cellulose-acetate membrane). Water quality, after membrane treatment, was sufficient to allow on-site reuse.

EXPERIMENTAL

Pretreatment of Wastewater (PACT Effluent)

As an estimate of the membrane-fouling tendency of a given wastewater, the Silt Density Index (SDI) [17] was measured by passing a sample of the wastewater through a $0.45\text{-}\mu\text{m}$ filter at $2.1 \times 10^5 \text{ N/m}^2$. The rate at which the filter became plugged was observed, and a 5-minute SDI (SDI₅) or a 15-minute SDI (SDI₁₅) was calculated. For example, the SDI₁₅ was calculated by noting the time to collect the first 500 cm³ of filtrate (t_i) and then, after filtering for 15 minutes, the time to collect a second 500 cm³ of filtrate was noted (t_f). From the SDI values of the raw and various pretreated wastes, sand filtration followed by cartridge ($5 \mu\text{m}$) filtration was chosen as the pretreatment scheme.

Membrane Unit Operation

Process Description. Twenty drums (55 gallons) of biotreated H-Coal wastewater effluent (as received from Zimpro, Inc.) was stored at 5°C in a refrigerated truck. For specific membrane experiments the temperature of selected amounts of water was adjusted to 25°C-38°C depending on the operating conditions. The membrane system and pretreatment schemes are shown in Figure 2. The wastewater was pumped through the sand filtration column (at $0.12 \text{ cm}^3/(\text{cm}^2 \text{ s})$) and $5\text{-}\mu\text{m}$ cartridge filter. SDI tests were run on the cartridge filtrate to check for SDI₁₅ values. If SDI₁₅ < 3, the water was pumped at high pressure through a stainless-steel heat exchanger to the membrane modules.

Membrane Modules. The modules used in the experiments were manufactured by DuPont (Delaware) and Film Tec (Minnesota) Corporations. The DuPont module, Permasep B9-0410-014N, consisted of polyamide hollow fibers and contained in a module 43 cm in length and 12.7 cm in diameter. The fibers had an inside diameter of $40 \mu\text{m}$. The Film Tec module, MBWHP-2521-1, consisted of a thin-film composite membrane supported on microporous polysulfone, in a spiral-wound configuration. The module was 6.4 cm in diameter, and 53.3 cm in length, with 0.076-cm spacings between membrane layers. The total membrane surface area was 9290 cm².

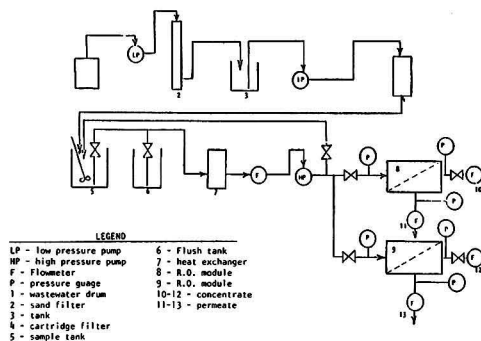


Figure 2. Schematic of membrane-treatment unit.

Membrane Unit Operating Procedure. The modules were first flushed with cartridge-filtered dechlorinated (by adding 10 mg/liter sodium bisulfite) tap water (designated as DTW) for several hours, and then standard NaCl (1500 mg/liter) rejections were established. Prior to each run, DTW was passed through the membrane modules at the same pressure, flow rate, and temperature, as desired for the actual experiment.

The operating conditions for the DuPont module were: temperature $\leq 40^\circ\text{C}$, pressure $\leq 2.8 \times 10^6 \text{ N/m}^2$, and flow rate 1.9-6.4 liter/min. For the Film Tec module, the operating conditions were: temperature $\leq 45^\circ\text{C}$, pressure $\leq 2.8 \times 10^6 \text{ N/m}^2$, and flow rate ≤ 19 liters/min. The conductivity and pH of permeates were continuously monitored.

For all runs, concentrate was recycled to the feed tank. Permeate may be collected or recycled to the feed tank. When permeate was collected, water recovery was taking place, and the feed necessarily became more concentrated. For example, when the feed was reduced to one half its original volume, it is known as "2X" feed. Likewise, when feed volume was reduced to one quarter its original volume, a "4X" feed remained. Various steady-state runs (8-36 hours duration) were conducted with 1X-10X feed wastes.

After the completion of a run, the module was flushed with DTW at low pressure ($3.5 \times 10^5 \text{ N/m}^2$) and high flow for a minimum of 1 hour. Next, the pressure and flow rate were adjusted to the original experimental levels, and the resultant permeate flow was compared to that measured prior to the run. Flushing was complete when these DTW permeate flows matched within 5%. A detailed description of all membrane experiments has been reported by Kozminski [18].

Analytical Procedures

Extensive analyses were conducted with the permeate, feed, and the concentrate streams. Total solids, total dissolved solids, hardness, and alkalinity were measured according to standard methods [19]. For the feed and concentrate samples, the color of the samples was first removed by activated-carbon adsorption prior to hardness and alkalinity determinations. Chloride was analyzed by Orion ion-selective electrodes. Metals were analyzed by Varian AA-575 Atomic Absorption Spectrophotometers.

Liquid-chromatography analysis was also conducted with selected samples. A Varian 5000 HPLC with a Vista 401 data-handling system was used for the analysis, utilizing a reverse-phase column (octyldecylsilane C_{18} bonded to 10- μm silica gel). The separation was obtained with a mobile phase acetonitrile/water. A 40-minutes gradient of 10% acetonitrile to 90% acetonitrile gave an optimum organics separation at a flow rate of 1 cm^3/min . A Varian variable UV detector was used for the peak determinations. Total organic carbon (TOC) was analyzed with a Beckman 915 TOC Analyzer.

RESULTS AND DISCUSSIONS

A summary of the results (from 20 different drums), compiled for the analysis of biotreated H-Coal wastewater (before membrane separation), is given in Table 3. Some variability between the drums was observed, as indicated by the concentration ranges. The second column in Table 3 indicates the average concentration values. Prior to the membrane experiments, several pretreatment studies were conducted to reduce the suspended-solids content of the feed wastewater.

Silt Density Index Test Results

The Silt Density Index (SDI) was used to estimate the possible membrane-fouling tendency of the feed wastewater. The possible range of SDI values are: $0 \leq$

$\text{SDI}_{15} \leq 6.7$, $0 \leq \text{SDI}_5 \leq 20$. A 15-minutes SDI_{15} values of 6.7 or a 5-minutes SDI_5 values of 20 indicates severe membrane fouling is likely to occur, unless the wastewater is pretreated.

The pretreatment schemes were: 0.45- μm Millipore filtration; Amicon PM-10 (10,000 molecular weight cut-off) ultrafiltration membrane; 5- μm cartridge filtration; sand filtration followed by 5- μm cartridge filtration. Table 4 shows the results of the raw waste and pretreated wastes. The high values of the raw wastes indicate the need for pretreatment. Sand filtration followed by cartridge filtration was chosen as the most practical treatment method. SDI values less than 3.0 are considered sufficient for processing by hollow-fiber membranes.

Membrane Separation Results

The membrane studies were conducted in a parallel system to evaluate the separation and flux characteristics of both hollow-fiber and spiral-wound (thin-film composite membrane) modules simultaneously. A total of 75 independent experiments were conducted. Most of the experiments were conducted at 32°C and a ΔP of $2.2 \times 10^6 \text{ N/m}^2$. Since both membranes could be operated at pH 4-11, feed-waste pH adjustments were not necessary.

Prior to the start of experiments with the actual wastes, pure-water permeate-flux behavior and standard NaCl (1500 mg/liter) rejections were established. The average membrane-permeability constant "A" at 32°C in Equation 2 was found to be: $2.7 \times 10^{-5} \text{ cm}^3/(\text{s})(\text{N/m}^2)$ for the DuPont module and $5.63 \times 10^{-10} \text{ cm}^3/(\text{cm}^2)(\text{s})(\text{N/m}^2)$ for the Film Tec module. The standard NaCl rejections for the DuPont and Film Tec modules were 92.7% and 97.4%, respectively.

Permeate-Water Flux Characteristics. Most of the steady-state membrane runs were made with complete recycle of

TABLE 3. ANALYSIS OF BIOTREATED H-COAL LIQUEFACTION WASTEWATER USED FOR MEMBRANE EXPERIMENTS

Parameter	Concentration, mg/liter	
	Range	Average
TDS (total dissolved solids)	3424-4193	3652
SS (suspended solids)	15-50	32
pH	7.4-7.9	—
Conductivity ($\mu\text{mho}/\text{cm}$)	3500-4250	3961
Hardness	35-80	63
Alkalinity	244-365	293
COD	131-200	158
TOC (total organic carbon)	35-87	61
Color Absorbance (at λ peak = 375 nm)	0.85-0.90	—
Chloride (Cl^-)	1135-1610	1347
Na	1160-1470	1292
Fe	0.2-1.0	0.70
Cu, Zn	0.1-0.2	0.16
Si	8-10	9.4
Nitrate (NO_3)	140-190	162

TABLE 4. SDI VALUES OF RAW AND PRETREATED WASTEWATER

Pretreatment Type	SDI_5	SDI_{15}
None	19.8	6.6
0.45- μm filter	—	1.3
Ultrafiltration (Amicon PM-10)	3.2	1.1
5- μm cartridge filter	3.5	1.2
Sand filter + 5- μm cartridge filter	2.5	1.0
Lexington tap water	2.5	0.9

the permeate and concentrate streams. In this way, the feed concentration remained constant and, if the feed was not concentrated prior to the run, it may be designated as "1X" run. A series of preliminary experiments were first conducted with various concentrate flow rates in order to establish possible concentration polarization effects. In the flow-rate range of 43-98 cm³/s (DuPont) and 60-195 cm³/s (Film Tec), only 3%-8% increase in permeate flux and slight (1-2%) increase in rejections were observed. These results thus indicate negligible polarization. Thus, for all the subsequent experiments the concentrate flow rates of 82 cm³/s (4.9 liter/min) for the DuPont module and 183 cm³/s (11.0 liter/min) for the Film Tech module, were selected.

The permeate flow rates of a typical "1X" run for the two modules are shown in Figures 3 and 4. After the initial drop, the permeate flow rates remained steady throughout the 36-hour run. The pure water (DTW) permeate rates before and after the run are also shown (open circles) in the figures for comparison. For example, with the DuPont module a 20% drop in permeate flow (compared to DTW) was observed. Part of the flux drop was due to the osmotic-pressure effects. The flux drop due solely to $\Delta\pi$ effects can be computed (by assuming $\pi_{wall} \approx \pi_{bulk}$) by Equation 2. The osmotic pressure (at 32°C) of the feed "1X" waste was calculated to be 1.06×10^6 N/m². The osmotic-pressure difference $\Delta\pi = (1.06 \times 10^6)$ (module concentration factor) (conductivity rejection). For the operating conditions used the concentration factors were: 1.67 (for DuPont module with 40% single-pass recovery) and 1.11 (for Film Tec module with 10% single-pass recovery). The water fluxes that will result due to $\Delta\pi$ effects are shown in Figures 3 and 4 as dotted lines ($J_{w,osm}$). The figures also show high conductivity rejections for both modules. The Film Tec composite membranes gave higher rejection and lower flux drops compared to the hollow-fiber module.

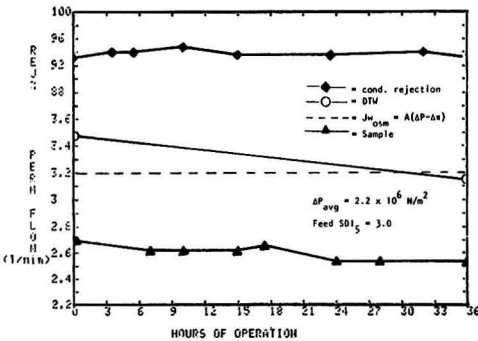


Figure 3. Effect of operating time on permeate flow and conductivity rejection with the Dupont-B9 membrane for a 1X H-Coal feed ($T = 32^\circ\text{C}$).

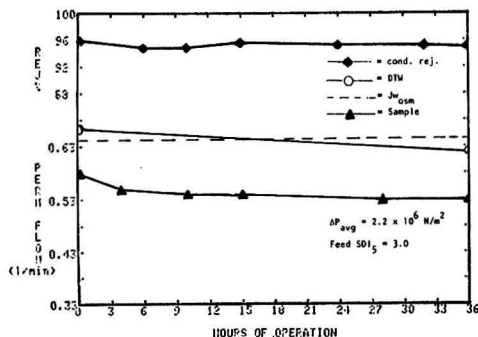


Figure 4. Permeate flow and conductivity rejection characteristics for a 1X H-Coal feed using a Film Tec-MB membrane ($T = 32^\circ\text{C}$).

For optimum membrane process-design, high water recovery is essential; thus, the flux behavior with the higher feed concentrations must be evaluated experimentally. During recovery runs, permeate flow from the module was collected separately, until the feed waste became concentrated by a factor of 2, 3, 4, 5, 8, or 10. Feeds concentrated in this manner are referred to as 2X, 3X, etc. After the attainment of proper feed concentration, steady-state runs were made with the concentrated wastes. For example, with the DuPont module, a 50% drop in permeate flow occurred as the feed concentration increased from 1X to 8X. Of course, one would expect partial flux drop due to an increase of $\Delta\pi$ with concentration.

At "8X" feed concentration, although the initial flux drop was considerably higher than the "1X" run, the flux remained constant during the 8-hour run. A considerable portion of the flux loss is due to osmotic-pressure effects. From the extensive number of experiments conducted with the 1X-10X feeds, the following correlations (correlation coefficient 0.92-0.95) are developed from the steady-state flux data (for $\Delta P = 2.2 \times 10^6$ N/m²):

For the DuPont hollow-fiber module,

$$\frac{J_w}{J_w} \text{waste} / \frac{J_w}{J_w} \text{DTW} = 0.78 (X)^{-0.41} \quad (11)$$

For the Film Tec spiral-wound module,

$$\frac{J_w}{J_w} \text{waste} / \frac{J_w}{J_w} \text{DTW} = 0.82 (X)^{-0.27} \quad (12)$$

In Equations 11 and 12, "X" refers to concentration factors (range 1-10). The powers of 0.41 and 0.27 indicate higher flux drops with the hollow-fiber module. At high concentrations, the flux drop due solely to the $\Delta\pi$ effects (which is a natural phenomenon) is quite significant. For example, with the Film Tec module, the actual value of $(J_w)_{waste} / (J_w)_{DTW}$ (Equation 12) at "10X" is 0.44; if the drop is due only to $\Delta\pi$ effects, the value would be 0.58. The difference in the two values indicates possible organic-solute accumulation on the membrane surface and/or organic solute-membrane interaction. It should also be noted that, at the end of each run, simple flushing with DTW resulted in complete recovery of initial flux values.

Solute Rejections and Permeate Quality. According to the solution-diffusion model, solute flux (J_s in Equation 3) is independent of operating pressure, and thus, rejection would be expected to increase to an asymptotic value as pressure is increased. Figure 5 (top) shows the TDS rejection of "1X" waste as a function of operating pressure. Above a ΔP of 2.0×10^6 N/m², rejected was found to be pressure-independent. The effect of temperature on rejection was also studied at a constant pressure of 2.2×10^6 N/m² (Figure 5, bottom). According to the solution-diffusion model, an increase in temperature would be expected to result in a decrease in solute rejection. This was found to be true with NaCl solution, where a 1% to 2% drop in rejection was observed between 25°C-38°C. With the "1X" waste, rejections were found to be independent of temperature (Figure 5). It should be noted that, although rejection was constant with temperature, a 10°C temperature rise from 25°C resulted in a 31% rise in permeate flux, which is important from the point of view of membrane-area savings. A 32°C temperature was selected for all subsequent runs.

Table 5 shows the ranges (from various 1X feeds) of permeate concentrations obtained with the two modules. Although the TOC concentration was similar for both modules, the spiral-wound module consistently gave a lower permeate concentration of other solutes. In order to establish the rejection behavior of solutes as a function of feed-concentration levels, extensive analyses of permeates were conducted for 1X-10X wastes. As the feed concentration increased, the permeate concentrations also in-

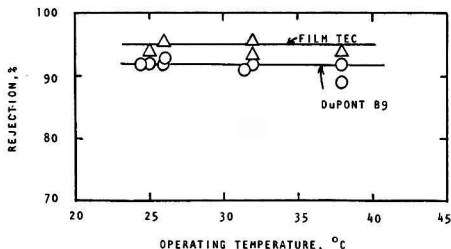
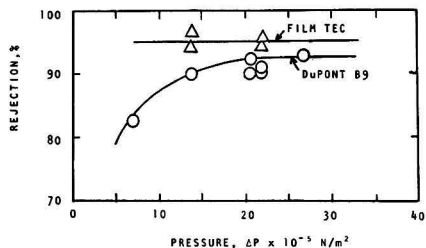


Figure 5. Effect of pressure and temperature on TDS rejection.

creased; for example, the rejections of chloride for 1X → 8X wastes dropped from 97.5% to 94% for the Film Tec module and 94% to 89% for the DuPont module. But these rejections are still quite high from the point of view of permeate-water reuse.

The typical permeate (shown in terms of $1 - R$, where R is fractional rejection) qualities in terms of TDS, conductivity, hardness, and chloride are shown in Figure 6 for the Film Tec module. The experimental data points shown in the figures are the average of three to five individual experiments. The data points are correlated by power functions (Equation 6) of the form shown below:

For the DuPont Module,

$$\text{Chloride: } 1 - R = 0.062(X)^{0.29} \quad (13)$$

$$\text{TDS and Conductivity: } 1 - R = 0.076(X)^{0.24} \quad (14)$$

For the Film Tec Module,

$$\text{Chloride: } 1 - R = 0.024(X)^{0.29} \quad (15)$$

$$\text{TDS and Conductivity: } 1 - R = 0.038(X)^{0.49} \quad (16)$$

The rejection of solutes by the Film Tec membrane was consistently higher than the DuPont module. For $X = 1$,

TABLE 5. TYPICAL PERMEATE CONCENTRATION RANGES OBTAINED WITH 1X FEED

Parameter	Concentration, mg/liter	
	DuPont B9 Hollow-Fiber	Film Tec Spiral-Wound
TDS	190-396	120-230
Conductivity ($\mu\text{mho/cm}$)	250-420	130-250
Hardness	2-10	2-10
Alkalinity	10-28	8-20
COD	10-20	<10
TOC	1-6	1-5
Chloride (Cl^-)	45-150	30-75
Na	60-120	25-58
Fe, Cu, Zn	<0.01	<0.01
Si	<2	<2
NO_3	35-40	15-20

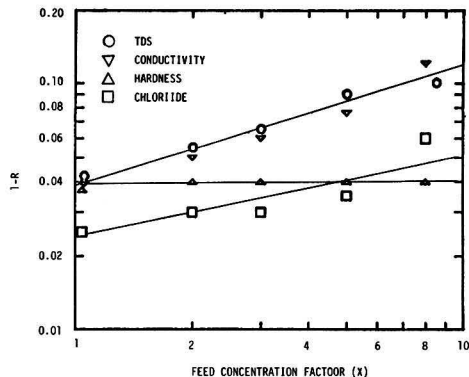


Figure 6. Effect of feed concentration on permeate quality for Film Tec spiral-wound module.

the above equations give the rejections of "1X" feed wastes. The permeate concentrations of TOC was a function of feed concentration. Concentrate-stream analysis of TOC showed membrane adsorption above 3X concentration levels and thus rejections were correlated with C_i values rather than "X". The relationship to calculate TOC rejections for both modules is:

$$1 - R = 0.017(C_i)^{0.24} \quad (17)$$

Utilizing Equations 13-17 and Equation 9, overall removals of selected parameters at high water recovery are computed and shown in Table 6. Even at 90% water recovery, the solute removals are sufficient for permeate reuse in cooling towers. Actual experimental removal data obtained at 90% water recovery, showed calculated removals to be within 1-2% of the experimental values. The alkalinity removals (not shown in Table 6) at $r = 0.9$ were 83% (DuPont) and 88% (Film Tec).

Liquid Chromatography (HPLC) Analysis of Feed and Permeate Samples

All chromatographic analyses were conducted with a reverse-phase column and a variable (210-280 nm) UV detector. Prior to the analysis of the biotreated water, the influent ($\text{H}_2\text{S-NH}_3$ -phenol-stripped water) waste to the biological unit was also analyzed for phenolics and carboxylic acids. The major detected peak (at 280 nm) was phenol (171 mg/liter). Other phenolic compounds, such as catechol, resorcinol, and hydroquinone, were also detected. If low-molecular weight organic acids were present, one would expect peaks (at 220 nm) at fast elution times 2.0-4.0 minutes with the reverse-phase column, but no such peaks were observed, indicating the absence of such acids in the nonbiotreated feed.

During the biological oxidation process, most of the phenolic compounds are oxidized and the oxidation products are expected to be mostly low-molecular-weight carbox-

TABLE 6. SOLUTE REMOVALS AT HIGH WATER RECOVERY

Fractional Water Recovery	Module	% Solute Removal		
		TDS and Conductivity	Chloride	TOC
0.75	DuPont Hollow-Fiber	84	87	96
0.90	DuPont Hollow-Fiber	77	80	94
0.75	Film Tec Spiral-Wound	90	94	96
0.90	Film Tec Spiral-Wound	84	91	94

ylic acids. Before and after the biological treatment, the water always shows an intense color that can be attributed to organic trace compounds having various functionalities.

The analysis of a "1X" biotreated H-Coal feed showed a broad peak in the region 2.0-3.1 minutes (Figure 7) that can correspond to several organic carboxylic acids overlapping (such as maleic, formic, fumaric, etc.) as well as nitrate salts. The presence of organic nitrogen and ammonia nitrogen will form nitrates during the biological oxidation that adsorb at 220 nm and elutes in the same time range (2.3 min). It should be noted that the peak (2.0-3.1 min) of the biotreated feed totally disappears above a scanning wavelength of 235 nm; thus, it can not be attributed to any aromatic benzene-ring compounds that would adsorb at wavelengths of 254 nm or 280 nm.

In order to differentiate the area-count contribution due to nitrates from one of the acids, the biotreated feed was analyzed before and after treatment by activated carbon (Filtrisorb 400). At low pH (≈ 2.5), an excess of activated carbon will remove all organic acids and leave inorganic salts in water. The chromatographic spectra of the "1X" feed before and after organic-acids separation are shown in Figures 7 and 8. The organic-acids removal dropped the area count (μ volts-sec) from 5.1×10^6 to 3.2×10^6 . Thus, the peak shown in Figure 8 is due solely to NO_3 and corresponds to about 190 mg/liter NO_3 . The equivalent maleic acid in "1X" is computed to be 47 mg/liter TOC.

By the same procedure, organic acids and NO_3 were analyzed for a typical permeate (Film Tec) from an "1X" run.

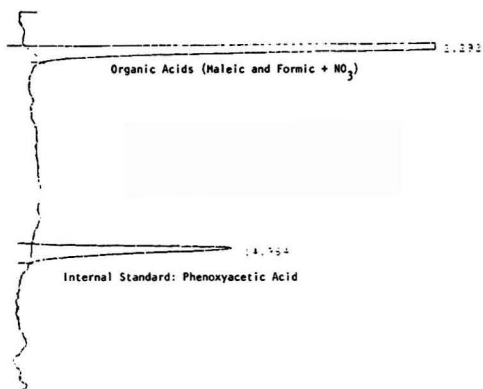


Figure 7. HPLC Spectrum of 1X H-Coal biotreated wastewater.

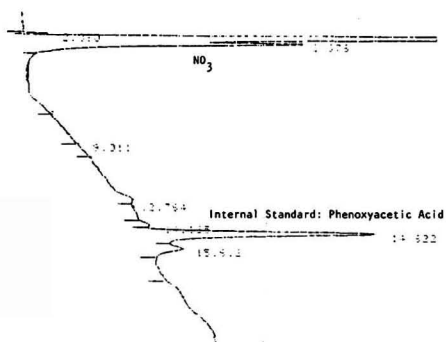


Figure 8. HPLC Spectrum of 1X H-Coal biotreated wastewater after removal of organic acids.

The permeate spectrum (after organic-acids separation) is shown in Figure 9. The analysis of the spectrum (by area-count drops) showed at least 91% rejection of NO_3 and permeate TOC in the range of 4-6 mg/liter. This TOC agrees well with the direct analysis shown in Table 5. It should be noted that the permeate TOC is primarily organic acids, since the color compounds (identified as isomers of methylpiperidinone, methylpyrrolidone, etc.) were rejected almost 100% by both membranes.

CONCLUSIONS

The development of low-pressure membrane-separation processes for the purpose of permeate-water reuse is gaining considerable importance because of the feasibility of simultaneous removal of organics and inorganics dissolved solids. The treatment scheme for the coal-liquefaction (H-Coal) wastewater consisted of: $\text{H}_2\text{S}-\text{NH}_3$ stripping, phenolics extraction, powdered activated carbon-assisted biological process, followed by a low-pressure membrane-separation process. Two types of membranes were evaluated: a polyamide hollow-fiber module and a spiral-wound module containing a thin-film composite membrane. The membranes were evaluated in terms of water flux, specific rejections of solutes, and extent of water recovery.

A pretreatment scheme consisting of sand filtration followed by 5- μm cartridge filtration was found to be sufficient for reducing the Silt Density Index (SDI) values of membrane feed streams. The flux drops with the hollow-fiber module was higher than for the spiral-wound module, particularly at "10X" feed-concentration levels. A significant part of the flux drop was due to the osmotic pressure of the solutions. Both membranes showed excellent rejections (at $\Delta P = 2.2 \times 10^6 \text{ N/m}^2$) of organics and inorganic salts. The rejections of total dissolved solids and salts were consistently 4-10% higher with the spiral-wound module, depending on the water-recovery levels. Both membranes removed 94-98% organics at zero to 90% water-recovery levels. At low water-recovery levels the chloride rejections were: 98% with the spiral-wound module and 94% with the hollow-fiber module. At 90% water recovery, 91% chloride removals were obtained with the spiral-wound module compared to 80% removal with the hollow-fiber module.

An extensive liquid-chromatography (HPLC) analysis was also conducted with the feed and permeate samples. More than 95% of the organics in the biotreated water were found to be aliphatic carboxylic acids (such as maleic, fumaric, and formic). Since, at a feed-water pH of 7-8, the acids were completely ionized, high rejections were obtained with both modules. The permeate quality (low salts

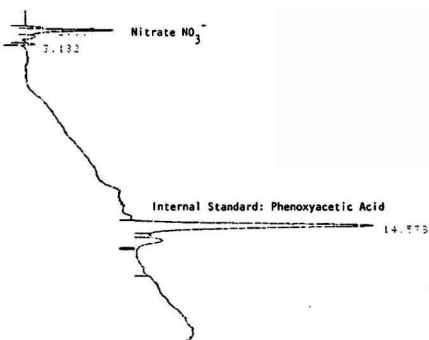


Figure 9. HPLC Spectrum of Permeate (after organic-acids separation) from the Film Tec spiral-wound module.

and organics) obtained is highly suitable for multiple-pass reuse in cooling towers, particularly in terms of the elimination of chloride-corrosion problems. Since these membranes also provide efficient removals (particularly with ionized phenolics) of phenolics and salts, it is possible that the direct use of membranes (without prior biological treatment) may be feasible to produce adequate permeate quality for reuse.

ACKNOWLEDGMENTS

This investigation was supported by Ashland Synthetic Fuels, Inc., Kentucky Energy Cabinet, and Institute of Mining and Minerals Research. The authors gratefully acknowledge the valuable suggestions of B. Churton and S. Shelton.

LITERATURE CITED

- Churton, B. M. and V. Skrylov, "Studies to Treat Process Wastewater from a Coal Liquefaction Plant," presented at AIChE Summer National Meeting, Cleveland, Ohio (1982).
- Mattson, M. E. and M. Lew, "Recent Advances in Reverse Osmosis and Electrodialysis Membrane Desalting Technology," *Desalination* 41, 1 (1982).
- Zimpro, Inc., "Biophysical Treatment of H-Coal Wastewater," Final Report for Ashland Synthetic Fuels, Inc., Zimpro, Inc., Rothschild, Wisconsin (1982).
- Soltanieh, M. and W. N. Gill, "Review of Reverse Osmosis Membranes and Transport Models," *Chem. Eng. Commun.* 12, 279 (1981).
- "Proceedings of First World Congress on Desalination and Water Reuse," *Desalination* 46, 3-181 (1983).
- Petty, P. E., S. D. Eliason, and M. M. LaGreid, "Treatment of Biomass Gasification Wastewater Using Reverse Osmosis," Report from Pacific Northwest Lab., Richmond, Wash. (1981).
- Asylova, K. G., V. I. Nazarov, and I. L. Taslik, "Properties of Cellulose Acetate Membranes for Purifying and Desalting Refinery Wastewater," *Chemical Technology* 16 (1980).
- Strathman, H., "Membrane Separation Processes," *J. Memb. Sci.* 9, 121 (1981).
- Lonsdale, H. K., "The Growth of Membrane Technology," *Journ. of Memb. Sci.* 10, 81 (1982).
- Sourirajan, S., "Reverse Osmosis and Synthetic Membranes, Theory—Technology—Engineering," National Research Council of Canada, Ottawa (1977).
- Matson, M. E., "Significant Developments in Membrane Desalination," *Desalination* 28, 207 (1979).
- Scott, J., "Membrane and Ultrafiltration Technology: Recent Advances," Noyes Data Corp., Park Ridge, New Jersey (1980).
- Bhattacharyya, D., R. I. Kermode, and R. L. Dickinson, "Coal Gasification Process Wastewater Reusability: Separation of Organics by Membranes," *Environmental Progress* 2, 38 (1983).
- Bhattacharyya, D., S. Farthing, and C. S. Cheng, "Multiple Pass Water Reuse: Use of Low Pressure Membranes with Metal Processing Wastewaters," *Environmental Progress* 1, 65 (1982).
- Bhattacharyya, D., A. B. Jumawan, R. B. Grieves, and L. R. Harris, "Ultrafiltration Characteristics of Oil-Detergent-Water Systems," *Separation Sci. and Tech* 14, 529 (1979).
- Campbell, J. R., R. G. Luthy, and D. A. Dzombak, "Deminceralization for Reuse of Coal Conversion Condensates," *Ind. Eng. Chem. Process Des. Dev.* 22, 496 (1983).
- Potts, D. E., R. C. Ahlert, and S. S. Wang, "A Critical Review of Fouling of Reverse Osmosis Membranes," *Desalination* 36, 235 (1982).
- Kozminski, J. D., "Removal of Organics and Salts from Coal Liquefaction Wastewater by Low Pressure Reverse Osmosis Membranes," M.S. Thesis, University of Kentucky (1983).
- "Standard Methods for the Examination of Water and Wastewater," 14th Ed., Am. Public Health Assoc. (1975).

D. Bhattacharyya is Ashland Professor of Chemical Engineering at the University of Kentucky. He received his M.S. degree at Northwestern University and Ph.D. degree at the Illinois Institute of Technology. He has published over 75 papers in the area of separation processes and pollution control. Currently, he is the Program Chairman of AIChE Environmental Division.

M. Jevtich is a graduate student of Chemical Engineering at the University of Kentucky. He received his B.S. degree at ESCIL, Lyon, France and M.S. degree at the University of Kentucky.

J. K. Chosal is assistant professor at Lexington Technical Institute, University of Kentucky. He received his Ph.D. degree at the University of Kentucky. He has published several papers in the area of foam separation and pollution control.

J. Kozminski is a research associate at the Albany International Membrane Development Venture, Norwood, Massachusetts. He received his B.S. degree at Michigan Technological University and M.S. degree at the University of Kentucky. At Albany International, he is currently involved in exploring the commercial applicability of composite hollow fiber membranes for gas and liquid separations.

In-Situ Biological Oxidation of Hazardous Organics

Colloidal gas aphanes show good adhesion and retention in unconsolidated saturated soil matrices.

D. L. Michelsen, D. A. Wallis, and F. Sebba, Virginia Tech., Blacksburg, Va. 24061

In order to appreciate the application of colloidal gas aphanes ("CGA") technology to *in situ* biological degradation, focussing on hazardous waste treatment, one must appreciate the implications of both CGA's and *in situ* treatment.

In Situ Hazardous Waste Treatment

This background discussion on *in situ* hazardous organics waste treatment is limited primarily to subsurface releases where land treatment or excavation with proper destruction or disposal is not practical or safe. Under these circumstances, treatment of organics is essentially limited to 1) injection/recovery techniques with above ground treatment, or 2) *in situ* treatment (destruction) techniques for the most part limited to biodegradation.

In the field, the use of injection/recovery techniques has become an accepted practice. For example, according to an EPA survey completed by Neeley *et al.* [1], of 180 remedial actions (on 169 sites), recovery wells and French drains (with and without surface treatment) were used in fifteen situations to prevent ground water contamination from landfills. On the other hand, only two instances were noted in which *in situ* treatment was used. In one case, lime was added to phenol, and in another, phosphates were added to accelerate biodegradation of a gasoline spill. In each of these applications, treatment was carried out above ground.

A survey had been completed of the contaminants found at the 114 top priority Superfund sites [2]. At these sites, 64 incidences were noted where slightly soluble organics occurred, including aromatics and halogenated hydrocarbons. Most of these would be amenable to injection/recovery techniques, but many organics would be biodegraded if *in situ* biooxidation techniques were developed and accepted as "state-of-the-art."

In a recent update of the remedial action survey, USEPA [3] has reported that O. H. Materials and the State of New Jersey conducted spray irrigation with draw down wells to remove contaminants from ground water at the Goose Creek site in Plumstead Township. Treatment, again, was completed above ground.

Captain Gross [4] of the U.S.A.F., Environics Branch, Tyndall AFB, Fla., has been conducting a ground water decontamination project at Wurstmith AFB, Michigan, which included pumping up contaminated ground water, air stripping to remove most of the TCE, and activated carbon processing for final treatment. The processing has been quite successful and a U.S.A.F. report to be issued shortly. Similarly, a number of other well systems have been installed around the country to remove and treat

ground water contaminated with chlorinated solvent (e.g., TCE, PCE) using air stripping. Dr. M. D. Cummins [5] of U.S. EPA-CINC has been conducting and monitoring tests at several sites to determine the effectiveness of air stripping for removing contaminants. However, little effort is apparently being expended to enhance recovery of hazardous materials from contaminated sites or from ground water. Recent articles in *Ground Water Monitoring Review* have documented other direct recovery and injection/recovery studies.

Occasionally, spills of hazardous waste have been treated in place. Harsh [6] documented the *in situ* neutralization of acrylonitrile by first raising the pH of the area above 10 with lime, and then spraying sodium hypochlorite over the area. Winn and Schulte [7] reported the clean-up of 14,000 pounds of phenol by treating a total of 1 million gallons of diluted waste with hydrogen peroxide. In addition, Zitrides [8] from Polybac Corporation has provided a bibliography of a number of spill situations at which full-scale applications of selected mutant microorganisms, as well as mixed microorganisms from waste treatment plants have been used for biodegradation of surface spills. Again the citations emphasize above ground treatment.

Perhaps the only field effort to conduct *in situ* biodegradation is being conducted by Biocraft Laboratories at its Waldwick, (Bergen County) N.J., site by its subsidiary, Ground Water Decontamination Systems (GDS). The technology developed has been patented and GDS was formed to sell the biostimulation process to other firms with similar groundwater problems. Their processing consists of two delivery trenches (4 ft × 100 ft × 10 ft (1.5 m × 30 m × 3m) long), up-gradient of a contamination source, with a subsurface drain trench (4 ft × 10 ft × 80 ft (1.5 m × 3m × 24 m) long) for primary collection located down gradient. Their innovation comes in the injection of air at several points into a 12-ft (3.5 m) thick contaminated layer of glacial till and stratified drift located 3 ft (1 m) underground. According to an earlier soil summary, three basic soil types were found to occur in the area: Merrimac gravelly loam, Papakating silt loam, and muck. In addition to some *in situ* biodegradation, above ground biological degradation of the contaminated ground water was also conducted before it was recycled back into the reinjection trenches. Nutrient and microorganism population was closely controlled. The subsurface horizontal flow rate was estimated to be 0.4 ft/day (0.12 m/day), and it takes an estimated year and a half for reinjected water to traverse from delivery to drain trench. Permeabilities (hydraulic conductivities) have been estimated to be 0.02 to 36 gallons per day per square foot (9.4×10^{-9} - 1.7×10^{-5} m/s

from slug tests [3]. A review of these activities was recently presented at the "Management of Uncontrolled Hazardous Waste Sites" Conference [9].

With regard to research and development, injection/recovery techniques seem limited to enhanced recovery of slightly soluble organics released to high permeability subsoils as shown by investigations completed by Texas Research Institute [10, 11] with some recent laboratory effort completed by JRB Associates.

The Texas Research Institute [10] has conducted several laboratory column and two dimensional modeling tests on the use of surfactants to enhance gasoline recovery from high permeability sand. These results indicated that, with a surfactant combination of an anionic (Richonate-YLA) oil soluble surfactant and a nonionic (Hyonac PE-90) surfactant, effective recovery was achieved.

JRB Associates has been testing similar techniques to those of Texas Research Institute for recovering a simulated mixture of hazardous materials using a representative soil from Superfund sites. The first report of this work is planned for the Oil and Hazardous Waste Spills Conference in Spring 1984. More recently, U.S. EPA MERL at Edison, N.J., has initiated efforts to enhance removal of hazardous materials using a larger test facility to be located at the OHMSETT site (Earle Naval Station, N.J.).

The development and testing of techniques for *in situ* biological oxidation of underground releases of organics, or within uncontrolled hazardous waste sites are very limited. Biodegradation techniques have been applied extensively to land treatment of refinery wastes and other organics, and have proven to be very effective. The large number of citations on land treatment and results presented at the Annual Research Symposium on Land Disposal: Hazardous Waste, and at other recent conferences have been very encouraging. In addition, research is being conducted on the use of mixed cultures and mutant microorganisms for biodegradation of hazardous organic materials, with a good review of the field recently completed by Kobayashi and Rittman [12]. Finally, several papers on field application of these techniques to hazardous release spills have been noted by Zitrides [8] of Polybac Corporation. In all of these efforts, treatment was conducted at or near the surface where the availability of oxygen for biooxidation is not limited.

The biological degradation of buried organics from releases of gasoline underground is an area where limited study has been conducted. The Texas Research Institute [13] has conducted studies on the microbial degradation of underground gasoline by increasing oxygen availability. The American Petroleum Institute has also initiated research on the use of hydrogen peroxide to provide oxygen for gasoline degradation [14].

In summary, *in situ* biological degradation of organics seems very feasible, but efforts to date have been quite limited.

Colloidal Gas Aphrons

The applications of Colloidal Gas Aphrons (CGA's) in the past have been focused on the removal of very fine suspended or precipitated particles. The separation can range from a combination of ion flotation and precipitation flotation to floc flotation, according to Sebba and Barnett [15]. Barnett and Liu [16] were able to float hydrophilic colloidal particles such as found in fish wastes from aqua-culture systems. Sebba and Yoon [17] demonstrated that CGA's were able selectively to float coal wetted with kerosene from ash, and, in limited tests, were able to separate minerals by selective bubble entrained floc-flotation. A recent study by Auten and Sebba [18] has explored the ability of fine CGA bubbles, to be entrained in a phosphate slime and to separate by flocculation/flotation these very finely divided particles. For many separations, it is the distinctive characteristics of

CGA's which make the applications technically feasible. Sebba and Barnett [15] have discussed the use of CGA's for a wide range of liquid/liquid and liquid/solid separations.

What are colloidal gas aphrons? In a CGA, gas bubbles are encapsulated in thin "soap" films that are so tenacious that the bubbles do not coalesce, even when pressed together. Hence, the bubbles remain very small (on the order of 25 μm) and present an enormous surface area. CGA's can be generated using virtually any water soluble surfactant, and any gas of limited solubility (e.g., nitrogen, oxygen, carbon dioxide), and, with selected surfactants, dispersions can be generated which contain 65% gas by volume. CGA's must be clearly distinguished from the so-called "bubbles" produced by dissolved air precipitation, sparging, or electrolysis, all of which are 2 to 1000 times larger and rise to the surface rapidly where they quickly coalesce. Recent papers by Auten and Sebba [18] and Sebba [19, 20, 21] provide a good background on the surface characteristics of CGA's.

Because CGA's are so stable and small that they remain suspended in solution they can flow through channels such as exist in a sand bed. Larger, unstable "bubbles" would be filtered out in such a situation. Another important characteristic is that CGA's can be pumped by conventional methods without deterioration.

A description of CGA production has been given by Sebba and Barnett [15]: "CGA's can be made very simply by passing a very rapid stream of dilute (about $2 \times 10^{-3}\text{M}$ surfactant solution through a Venturi throat, at which point there is a very restricted orifice through which gas (usually air) under an excess pressure of about one atmosphere is sucked into the stream. Because of the turbulent jet and the slow entry of gas, it enters in the form of microbubbles. A requirement for the generation of a shell encapsulated bubble is that the gas break through an aqueous-gas surface, with a surfactant monolayer at the surface, at least twice. The turbulence ensures that. In contrast, if a so-called "bubble" is introduced by sparging through a fitted disc or by gas precipitation, this is likely to be gas surrounded by the bulk water and have only one interface, and therefore, is effectively a gas-filled hole. To obtain a high concentration of CGA bubbles, the suspension is recycled a few times through the CGA generator. The method described for generating CGA's is excellent for laboratory production, and a generator of this type can operate for many years." In the laboratory, CGA's have been generated using a spinning disk with baffles. In generating CGA'S, care must be taken to get a homogeneous mixture with a minimum of large bubbles. In the short term, large bubbles tend to distort the control and flow of CGA's. In the long term, they may create cavitation problems in a centrifugal pump and thereby create delivery problems, particularly if used at other than modest pressures.

Because of their unique characteristics, several laboratory tests were conducted to explore their application to organic hazardous waste treatment. The limited test demonstrated the high propensity of CGA's made from anionic, cationic, and nonionic surfactants to adhere to most soil matrices and to restrict their flow through porous beds. CGA's tended to plug up the sand bed and flowed with more pressure drop than either pure water or air. Furthermore, we observed good compatibility between CGA's and microorganisms when flushed into and through sand matrices. The viability of the microorganisms was maintained. Because of these very preliminary findings, the thrust of this work was to explore the possibility of using CGA's plus microorganisms (and nutrients) for *in situ* biological degradation of organics in a saturated unconsolidated (normally anaerobic) matrix. For example, these laboratory tests would simulate the treatment of contaminated sediments found in either surface impoundment, or a buried matrix being contaminated by ground water.

EXPERIMENTAL AND RESULTS

CGA Retention Tests in Various Matrices

The adhesion and retention laboratory studies were conducted in a 500 ml wide mouth Erlenmeyer Flask. The procedure was to add 400 g of "as is" golf course sand (or material being tested) to a series of these flasks. Then water was added to completely saturate the unconsolidated matrix and raise the level in the flask to the 500 ml mark. This weight was recorded approximately and the water level was then lowered to 400 ml by decanting off a portion of the water covering the unconsolidated matrix.

The CGA's were generated and a FMI positive displacement pump was used to deliver the CGA's to the Erlenmeyer Flask until the level rose again in the 500 ml mark. A three-prong fork (rake) made using 1/16" stainless steel tubing was used to inject the aprons into the submerged matrix. Injection took 2 to 4 minutes. The rake was moved through the soil while injection was occurring. In several runs, a 100-ml graduated flask was filled with CGA's and allowed to destabilize in order to determine the quality of CGA's delivered to the flask (% air in the CGA mixture).

After careful adjustment of the water level to 500 ml, the flask was reweighed and the difference in weight from the original flask before sparging represents the cc of air (aprons) adhering to or retained within the matrix. Knowing the cc of CGA's retained and the quality of CGA's produced and injected, the fraction (or percentage) of CGA bubbles retained can be determined from the following relationship.

$$\% \text{ CGA Retention} = \left\{ \frac{\text{cc of Hold-Up Gas}}{\text{cc of Hold-Up Liquid} \left(\frac{\text{CGA Quality}}{\text{I-CGA Quality}} \right)} \right\} 100$$

The Erlenmeyer flasks were weighed, allowed to stand uncovered, and reweighed intermittently after bringing the water level back to the 500 ml mark. Some surface evaporation occurred.

A series of runs was made using the golf course sand (as is) and injecting CGA's generated from sodium dodecyl benzene sulfonate (SDBS) and also Tergitol 15-S-12. These tests were completed by the first author for the Envirionics Branch, Engineering and Services Laboratory, Tyndall AFB, Fla. (Captain T. Stoddart). The results are shown on Figures 1 and 2. The amount of air adhesion (pick-up) and also its retention compared favorably with the total water volume in the sand, measured between 80 and 90 cc. Some expansion of the bed also occurs but, if 50 cc is picked up, the air to water volume ratio is somewhere between 0.56 to 1.25 (50/(90 + 50) to 50/90). About 70% of the CGA's originally retained in the sand matrix were still present in the sand matrix, either as CGA's or somewhat

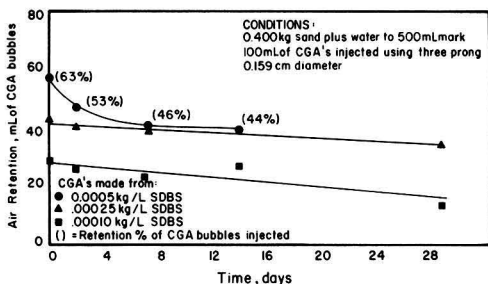


Figure 1. Injection and retention of colloidal gas aprons made with sodium dodecyl benzene sulfonate during laboratory sparging tests.

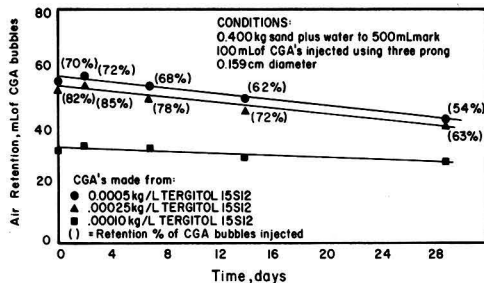


Figure 2. Injection and retention of colloidal gas aprons made with tergitol 15-S-12 nonionic surfactant during laboratory sparging tests.

larger bubbles of coalesced aprons. Some bubbles apparently either slowly dissolved into the water or escaped from the soil matrix and rose to the surface.

Similar tests with direct room air injection into the bed using the same three prong probe yielded retentions of 5 to 6 cc of air at a maximum. While some retention was certainly observed, the weight accuracy is limited by the ability to refill the flask consistently to 500 ml. In any case, the level of retention was small.

Another series of tests was conducted to determine the retention of CGA's on a pea gravel and on oyster shells. Again, some retention was observed and agitation by a spatula demonstrated this. However, the cc of retention was within the precision of refilling the flask to the 500 ml mark. In general, the oyster shells appeared to be more effective at CGA retention. With both materials, the CGA's made with a cationic surfactant (1g/liter) resulted in considerable flotation of the soil fines. The positively charged CGA's apparently bonded or complexed with the negatively charged silt mixed in with these materials.

Samples of both the pea gravel and ground oyster shells were fixed in a plastic mesh bag and placed in the trickling filter of the Tyndall AFB waste treatment plant. An active biological culture developed on the surface. After ten days, the samples were retrieved, hastily weighed, and CGA retention studies completed. Considerable flotation of the microorganisms occurred and 5 to 25 ml of CGA's were retained. The foam froth in the neck above the 500 ml mark made precise measurement of the weight impossible after adding the CGA's.

A final series of tests was completed on standard EPA soil, Clarkburg Borough Soil Pit, Typic Hapludults [22]. This soil is being used for *in situ* treatment studies being conducted by JRB Associates for U.S. EPA, Edison, N.J., Laboratory (Tony Tafuri, Contract Officer). The soil contains low organic carbon, and 8% by weight clay sized particles, although the fines are mostly quartz. When 100 cc of a 69% CGA quality mixture, made from 0.5 g/liter solution of sodium dodecyl benzene sulfonate (SDBS), was injected into 400 g (dry weight) of the saturated soil, covered with water, between 34.3 to 46.7 cc of CGA air bubbles were retained. Similarly, when 100 cc of a 68% CGA quality mixture, made from a 0.5 g/liter solution of Tergitol 15-S-12, was injected, between 18.6 to 23.2 cc of the air bubbles were retained. The pick-up with the SDBS was better, but only 18.6 to 38% of the CGA bubbles injected adhered to the soil. A week later, the CGA bubbles were still very dispersed with little coalescence apparent.

The adhesion and retention was generally not as good as with the golf course sand. However, this "standardized" EPA soil seemed to pack poorly and have a low bulk density. The particle density also seemed low. During the test, the bubbles just expanded the soil matrix and escaped up through the very unconsolidated and rather fluidized soil water mixture.

In summary, CGA's have been shown to adhere to sand and other soil matrices and to be retained for long periods

of time. Thus, the possibility of changing a wet and possibly a dry anaerobic soil environment into an aerobic environment looks most promising.

Phenol Degradation *in Situ*

The adhesion and sustained hold-up of CGA's in various matrices, particularly sand, were most encouraging. The next phase of this study was to demonstrate the feasibility of injecting a combination CGA plus microorganism in a nutrient solution into a contaminated saturated sand matrix and to show subsequent biodegradation.

The specific testing conducted at Virginia Tech involved CGA's made with sodium dodecyl benzene sulfonate plus *Pseudomonas putida* and nutrients and an unconsolidated saturated sand matrix containing phenol. Tests were conducted in a manner similar to the retention studies above except that the water layer just covered the sand. In addition, the saturated matrix was stripped with CO₂ to remove any entrained air prior to injecting CGA's.

A culture broth of *Pseudomonas putida* was cultivated on a media containing 500 mg/liter for approximately 24 hours. This medium was diluted 1 to 10 with surfactant solution prior to CGA generation and injection into locally obtained river sand contaminated with a solution of 300 mg/liter phenol. The test vessels were sealed to prevent any exposure and oxygen transport from the room air. Table I shows the results and Figure 3 a plot of degradation with time. Phenol analyses were determined using a colorimetric assay, based on rapid condensation of phenol with 4-aminoantipyrine, followed by oxidation with potassium ferricyanide. As noted, more than 60% of the phenol in the sand matrix was biodegraded (disappeared) after 24 hours of operation with a single injection of CGA.

Thus, the injection of a combination of CGA's plus appropriate microorganisms and nutrients resulted subsequently in the aerobic biodegradation of organics in a saturated sand environment (normally anaerobic). Increased activity would be expected in the CGA's made with oxygen or an oxygen enriched air. High CGA retention would be expected to change many saturated soils, fine particle, or thickened sludge mixtures from an anaerobic to aerobic matrix. In addition to *in-situ* biodegradation as described, this shift in oxidation/reduction potential might be useful for extended sludge (aerobic) decomposition, chemical reaction or odor control, or for altering or adjusting other chemical or biochemical reaction mechanisms.

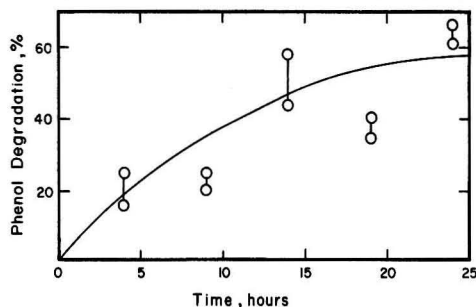


Figure 3. *In-Situ* Degradation of phenol using *Pseudomonas putida* injected with colloidal gas aprons.

CONCLUSIONS

1. Colloidal Gas Aprons have been shown to adhere and be retained as small bubbles in various saturated soil and ground matrices for a prolonged period of time.
2. A combination of CGA's and *Pseudomonas putida* plus nutrients injected into a phenol contaminated sand matrix void of air, successfully degraded over 60% of the phenol present within 24 hours.

ACKNOWLEDGMENTS

The authors are greatly indebted to Captain Terry Stoddart, USAF, for his support and encouragement in carrying out the CGA retention studies. We are also indebted to Brecc Avellar, a senior at Virginia Tech, for his assistance in conducting the *in-situ* phenol degradation studies with support funds from Olin Corporation.

LITERATURE CITED

1. Neely, N. D., Gillespie, F. Schauf, and J. Walsh, "Remedial Actions at Hazardous Waste Sites—Surveys and Case Studies," EPA-430/9-81-05 SW-910 (1981).
2. EPA Environmental News (1981).
3. U.S. Environmental Protection Agency, "Survey and Case Studies of Remedial Actions at Hazardous Waste Sites," U.S. E.P.A.-MERL-CINC (JRB Contractor) (in press).
4. Gross, R., Personal Communications (October 21, 1983).
5. Cummins, M. D., Personal Communications (1982).

TABLE I. *IN SITU* BIODEGRADATION OF PHENOL USING *PSEUDOMONAS PUTIDA* AND CGA'S AS ONLY AIR SOURCE

Sample	1	2	3	4	5	6	7	8	9	10
(1) Initial Liquid (ml)	106	103	100	103	101	110	101	102	101	107
Concentration (mg/l)	300	300	300	300	300	300	300	300	300	300
(2) Liq. Removed (total ml)	80	62	58	60	66	67	68	56	61	71
Concentration (mg/l)	220	235	270	230	190	240	230	260	260	245
(3) Air Retained (ml)	35	33	29	31	27	31	27	27	24	28
O ₂ (m/mole)	0.33	0.31	0.27	0.29	0.25	0.29	0.25	0.25	0.23	0.26
O ₂ (mg)	10.5	9.9	8.7	9.3	8.1	9.3	8.1	8.1	7.2	8.4
(4) Phenol @ t = 0 (mg)	14.2	16.3	14.3	17.1	17.8	16.9	14.7	16.0	15.9	14.7
(5) Time (hr)	4	4	9	9	14	14	19	19	24	24
Phenol Present (mg)	10.65	14.0	11.4	13.7	7.4	9.5	8.9	10.5	5.4	5.5
Phenol Degraded (mg)	3.55	2.3	2.9	3.4	10.4	7.4	5.8	5.5	10.5	9.2
% Degradation	25%	16%	21%	25%	58%	44%	40%	34%	66%	62%
(6) mg Phenol Degraded mg O ₂ present	0.25	0.23	0.33	0.37	1.28	0.80	0.72	0.62	1.46	1.09

6. Harsh, K. M., "In Situ Neutralization of an Acrylonitrile Spill," pp. 187-189, in "Proceedings of 1978 National Conference on Control of Hazardous Material Spills," (April 11-13, 1978). Information Transfer, Inc., Rockville, Md.
7. Winn, B. M. and J. H. Schulte, "Containment and Clean-up of a Phenol Tank Can Spill, May-June 1978, Charleston, SC," pp. 11-14 in 1982 Hazardous Material Spills Conference, Government Institutes (April, 1982).
8. Zitrides, T. G., "More on Microorganism," *Environ. Sci. Technol.*, **16**, 431A-432A (August, 1982).
9. Jhaveri, V. and A. J. Mazzacca, "Bio-Reclamation of Ground and Ground Water," in 4th National Conference on Management of Uncontrolled Hazardous Waste Sites, HMCRI, Silver Spring, Md., November 2, 1983.
10. Texas Research Institute, "Underground Movement of Gasoline on Groundwater and Enhanced Recovery by Surfactants," Submitted to the American Petroleum Institute, September, 1979.
11. Texas Research Institute, "Test Results of Surfactant Enhanced Gasoline Recovery in Large-Scale Model Aquifer," Submitted to the American Petroleum Institute, April, 1982.
12. Kobayashi, H. and B. E. Rittmann, "Microbial Removal of Hazardous Organic Compounds," *Environ. Sci. Technol.*, **16**, 170A-183A (March, 1982).
13. Texas Research Institute, "Enhancing the Microbial Degradation of Underground Gasoline by Increasing Available Oxygen," Final Report to the American Petroleum Institute, February, 1982.
14. Carlson, C., Personal Communications, 1982.
15. Sebba, F. and S. M. Barnett, "Separation Using Colloidal Gas Aphrons," *Proc. 2nd Int. Congress of Chem Eng.*, IV, pp. 27-31 (1981).
16. Barnett, S. M. and S. F. Liu, Proc. Conf. on Seafood Waste Management in the 1980's (1980).
17. Sebba, F. and R. H. Yoon, "The Use of Micron-Sized Bubbles in Mineral Processing," in "Interfacial Phenomena in Mineral Processing," ed. B. Yarar and D. J. Spottiswood, 161 (1982).
18. Auten, W. L. and F. Sebba, Use of Colloidal Gas Aphrons (CGA) for Removal of Slimes from Water by Flocc-Flotation, "Solid and Liquid Separation", ed. John Gregory, Ellis Howard, Chichester, England, 41, (1984).
19. Sebba, Felix, "The Behavior of Minute Oil Droplets Encapsulated in a Water Film," *Colloid and Polymer Sci.*, **257**, 392 (1979).
20. Sebba, Felix, "Investigation of the Modes of Contaminant Capture in CGA (MGD) Foams," Report to O.W.R.T., 14-34-0001-0489, October, 1982.
21. Sebba, Felix, "Preparation and Uses of Polyaphrons," Presented at Colloid and Surface Symposium of ACS, Blacksburg, 1982. Submitted to "Chemistry and Industry."
22. U. S. Department of Agriculture, "Soil Taxonomy: Basic System of Soil Classification for Making and Interpreting Soil Survey," Agriculture Handbook No. 436 (1975).



Donald Michelsen has just recently rejoined the staff of Chemical Engineering as an Assistant Professor. He has served the University as Director of their Engineering Graduate Program in Northern Virginia and spent a year as a consulting engineer with JRB Associates. His current research interest is the area of mass transfer and hazardous waste treatment. He earned his B.S. degree from Penn State, S.M. from M.I.T. and a Ph.D. in Chemical Engineering from Cornell University.



David Wallis is an Assistant Professor in the Chemical Engineering Department at Virginia Tech. He is currently conducting research in the areas of hazardous waste treatment and biotechnology. He earned his B.S. and Ph.D. degrees from Virginia Tech, and his M.S. degree from the University of Virginia.



Felix Sebba is a Visiting Professor in the Department of Chemical Engineering and of Chemistry at Virginia Tech. He took his doctorate at University of Capetown, South Africa, where he served as a Senior Lecturer in Physical Chemistry and then became Professor of Physical and Inorganic Chemistry and Head of the Department of Chemistry in the University of the Witwatersrand, Johannesburg, until his retirement in 1978. He specializes in liquid interfaces and was a pioneer in ion flotation, precipitate flotation, colloidal gas aphrons and polyaphrons, all related to separation processes.

Oil Shale—Potential Environmental Impacts and Control Technologies

Where do we really stand today on the question of fuels from oil shales? Here is an authoritative assessment.

E. R. Bates, W. W. Liberick, and J. Burckle, U.S. EPA, Cincinnati, Ohio 45268

The U.S. Environmental Protection Agency's Industrial Environmental Research Laboratory in Cincinnati, Ohio (IERL-Ci) has performed research related to oil-shale processing and disposal since 1973. This research is in support of the Clean Air Act, the Federal Water Pollution Control Act, the Resource Conservation and Recovery Act, the Safe Drinking Water Act, and the Toxic Substances Control Act. Potential environmental impacts from oil-shale development activities have been identified and potential control technologies are being evaluated through a combination of laboratory and field tests on actual oil-shale waste streams. This paper discusses recent results

from this program. Included are field test results on control of sulfur gases at Occidental Oil Shale's Logan Wash Site and Geokinetic's Kamp Kerogen Site, wastewater treatability studies on retort water and gas condensate at Logan Wash, and results of laboratory and field testing on raw and retorted oil shales.

AIR POLLUTANTS AND CONTROLS

The mining and processing of oil shale to produce a refined shale-oil product has the potential to produce a large variety of air pollutants, many of which have a

significant potential for adverse environmental impact if not properly managed. These pollutants include those given in Table I which are emitted from various operations: fugitive emissions from mining, transportation, and materials handling; process emissions from materials preparation such as sizing for indirect-fired retorting; process emissions from oil upgrading and storage facilities; fugitive emissions from waste handling and disposal; process emissions from utility generation; and process and fugitive emissions from infrastructure development and secondary pollution sources.

Processes for removal of reduced sulfur and carbon dioxide from gases are called acid-gas removal or gas-sweetening processes and involve adsorption and chemical conversion (direct processes), or adsorption and stripping to form a more concentrated stream which is then processed for sulfur conversion and recovery (indirect processes). More than 30 such processes have been commercialized. IT Environcience conducted an in-depth evaluation of a large number of emissions-reduction systems to determine applicability for removal of hydrogen sulfide from retort off-gases (Lovell *et al.* 1982) [1]. The study found that, because gases from direct-fired retorts have a high content of carbon dioxide relative to hydrogen sulfide and contain large amounts of ammonia and unsaturated hydrocarbons, they are significantly different from gases encountered in commercialized applications of desulfurization technologies. Hence, such technologies cannot be simply applied at full-scale through technology transfer: such transfer must be achieved through an application-research program to minimize risk and maximize success.

Since retort off-gases will be produced in very large volumes at near atmospheric pressure, many desulfurization processes cannot be economically applied. The high concentration of CO₂, and CO₂/H₂S ratios, and the presence of oxygen, unsaturated hydrocarbons, or organic sulfur species also make application of a number of desulfurization techniques impractical.

Of the systems studied, the Stretford, EIC, MDEA, (Selectamine and Adip), Benfield, Diamox, and Selexol appear to have the potential for the greatest H₂S selectivity for application to direct-fired retorts. Except for the Diamox process, these systems should be capable of

controlling H₂S to about 10 ppmv, resulting in an H₂S control efficiency of 99+ %. However, organic sulfur compounds, principally COS, are not significantly removed or are only partly removed by the various processes. Therefore, the presence of such compounds may lower the overall reduced-sulfur control efficiency to about 98% (Table 2).

For the purpose of discussing reduction of emissions from oil-shale retorting operations, it is useful to classify the retorting processes as direct-fired (where the combustion occurs within the retort itself) or as indirect-fired (where combustion to produce the heat required for retorting occurs outside of the retort). This distinction is important because it influences the nature of the retort off-gas to be treated (Table 3) and hence poses distinctly different duty requirements which must be considered in the selection of an emissions-reduction technology. The predominate factor in the selection process is the CO₂/H₂S ratio. Direct-fired retorts have CO₂/H₂S ratios that range from 75 to more than 165. Such high ratios require a process that selectively removes H₂S in preference to CO₂ in order to prevent excess consumption of reagent capacity by the CO₂ and the resulting increase in processing costs. Indirect-fired retorts produce off-gases having a CO₂/H₂S ratio in the range of 4.5 to 5, which permits the use of a non-selective process.

Based upon a cost evaluation of a model case, the Stretford process appears to be the most cost-effective approach for direct-fired retorts (Lovell, *et al.* 1982) [1]. Table 4 compares the relative costs for using the Stretford, MDEA selective-absorption followed by Stretford or Claus sulfur-recovery systems, and the Diamox process. The estimated cost for sulfur control using the Stretford process directly is fifty cents per barrel of oil, which is less than half that of the indirect process.

Based upon the results of this study, EPA funded the design and construction of a Stretford pilot unit, which subsequently has been utilized in three series of tests. These three test series were conducted at Occidental's Logan Wash retorts 7 and 8 (OXY-6/17/82 to 7/1/82), Geokinetics, Kamp Kerogen (GKI-9/15/82 to 10/1/82), and the U.S. Bureau of Mines coal-gasification facility at Twin Cities Research Center (TCRC-11/5/82-11/22/82). The results are summarized in Table 5.

TABLE 1. POTENTIAL POLLUTANTS FROM OIL SHALE MINING AND PROCESSING

Criteria Pollutants	Hazardous Pollutants	Other Pollutants
particulate	asbestos	ammonia
sulfur dioxide	arsenic	hydrogen sulfide
nitrogen oxides	beryllium	trace metals
carbon monoxide	mercury	reduced organic
hydrocarbons	polycyclic organics	sulfides
lead	radionuclides	

TABLE 3. CONCENTRATION OF MAJOR SULFUR SPECIES IN RETORTED OFF-GAS

	Direct Fired	Indirect-Fired
	H ₂ S	0.1 - 0.6 percent v
COS	100 - 600 ppmv	100 - 1000 ppmv
CS ₂	100 - 600 ppmv	100 - 1000 ppmv
CH ₃ - SH	50 - 300 ppmv	50 - 500 ppmv

TABLE 2. VARIATION OF PROCESS EFFECTIVENESS WITH AMOUNT OF COS IN RAW GAS*

	H ₂ O Remaining (ppm)	COS Reduction (wt. %)	Total Sulfur		Estimated Overall Emissions				Overall Sulfur Reduction (wt. %)
			Reduction (wt. %)	Remaining (kg/hr)	Total Sulfur		SO ₂ Equivalent		
					(kg/hr)	(tonnes/day)	(kg/hr)	(kg/bbl of oil)	
Stretford	10	Nil	98.0-99.3	19-58	19-58	0.45-1.35	38-115	0.02-0.05	98.0-99.3
MDEA - 1 stage with Stretford	10	60	99.2-99.5	13-29	20-59	0.45-0.90	40-117	0.02-0.05	98.0-99.3
MDEA - 3 stages with Claus/SCOT	10	60	99.2-99.5	13-29	20.4-36	0.45-0.90	41-72	0.02-0.04	98.0-99.3
Diamox with Claus/BSPR	63	Nil	96.3-97.6	70-109	75-114	1.81-2.70	151-228	0.07-0.11	96.1-97.4

* Based on a Paraho plant producing 8,000^b of oil per day with COS ranging from 10 to 50 ppmv in the raw gas. Source: Lovell, *et al.* (1982).

TABLE 4. RELATIVE COSTS OF VARIOUS GAS DESULFURIZATION OPTIONS*

Category	Stretford Direct Process with Purge Stream Disposal	Stretford Direct Process with Purge Stream Recycle	1-Step MDEA Selective Adsorption with Stretford Sulfur Recovery	3-Step MDEA Selective Adsorption with Claus Sulfur Recovery	Diamox Process with Claus Sulfur Recovery
Installed capital cost	1.00	1.11	1.29	1.17	2.46
Utility costs	1.00	1.51	5.90	9.88	16.79
Total operating costs	1.00	1.13	1.88	2.15	3.90
Value of sulfur recovered	0.92	0.95	0.96	1.00	0.98
Net annual cost	1.00	1.15	2.05	2.37	4.47
Cost effectiveness	1.00	1.15	2.04	2.34	4.54

* Based on a plant processing 10.2 million sm^3 of Paraho gas per day. The most effective or least costly option in each category is shown as unity (1.00). The relative costs of the other options are shown as a ratio to the most effective or least costly system. Source: Lovell *et al.* (1982) [1].

During the OXY test series, the H_2S -control efficiency ranged from 20 percent at start-up to approximately 60 percent at the end of the test. A major field modification of the Venturi absorber was made to improve the gas-liquid contacting; almost all of the improvement in performance is attributed to this measure. Analysis of the resulting test data identified gas/liquid contacting and Stretford solution chemistry as the targets for further efforts to improve performance.

In the GKI test series, the H_2S -removal efficiency ranged from about 60 percent to approximately 85 percent, with brief periods in the mid to high 90's. During the first phase of the test, the effectiveness of the gas/liquid contact using the venturi and an in-line static mixer was investigated with no noticeable difference on removal efficiency. During the balance of the test, various experiments were conducted to evaluate solution chemistry. First, an increase in the vanadium content of the Stretford solution improved H_2S removal. Second, it was suspected that the reaction-vessel retention time was too short to permit the completion of the Stretford-solution reactions, thereby permitting recycling of incompletely regenerated Stretford solution to the venturi scrubber. To verify this effect, the liquid in the reaction tank was raised to its maximum level with the observed effect of improved H_2S removal. Additionally, it was noted that a 99+ percent H_2S removal was obtained whenever the unit was restarted after an extended down-time and during periods of low retort off-gas flow through the venturi.

In a subsequent test series, performed on a coal-gasification off-gas unit at the USBM Twin Cities Research Center, improved results for given operating conditions were achieved as predicted from the GKI tests. The only change in operation from the GKI tests was a reduction in the gas flow rate into the pilot unit through the addition of a gas by-pass arrangement. This change allowed operation at lower liquid-flow rates, while maintaining the required L/G ratio at the scrubber, and resulted in the increase in residence time in the reaction tank needed for complete regeneration of the Stretford solution. Through this change, H_2S -removal efficiencies of 75% at the start of the test were increased under controlled experimental

conditions to 99.7%. It still remains to be demonstrated that high removal efficiency under sustained operation is possible on the off-gas from a direct-fired retort.

In a cooperative program with the Department of Energy's Laramie Energy Technology Center (LETC), EPA sponsored tests for the control of oily particulates remaining in the off-gas from LETC's 150-ton simulated *in-situ* retort after oil and heat recovery. In September, 1980, Monsanto Research Corporation conducted the tests using EPA's mobile scrubber pilot unit.

The particle size (weight-basis) measured indicated that about 60% of the particles were less than 15 μm , 50% were less than 5 μm and the distribution was bimodal with approximately 1/3 of the catch reporting to both the greater than 20 μm and to the 1.0 to 2.0 μm fractions. Qualitative observation of the glass-fiber substrates used for particle collection indicated the presence of a straw-colored oil material and a black, dust-like material.

The control efficiency as measured by the front half of the Method 5 Procedure varied from 67% to 94%. No correlation of control efficiency with the liquid-to-gas ratio (L/G) was found within the relatively narrow experimental range.

Analysis of the "back half" of the Method 5 train indicated the presence of considerable condensable material as compared to the "front half" resulting in back-to-front ratios ranging from 2.7 to 5.5 at the scrubber inlet and 3.7 to 22 at the scrubber outlet. The measured control efficiency for these condensable materials ranged from 40% to 83%, much less overall than the front-half materials. These data indicate the need for careful evaluation of the potential impact of such fine particulate emissions upon visibility, since visibility reduction is generally dominated by particles 0.1 to 2 μm in size, which tend to be formed by condensation.

Retort off-gas content of ammonia, hydrogen sulfide, carbon monoxide, and the C_1 - C_6 hydrocarbons were substantial, that is, greater than those measured for particulate emissions. Emissions characterization showed that Venturi scrubbing had no effect on other pollutants contained in the emission except for ammonia.

Surprisingly, some 50 to 75% (mass-basis) of the ammonia was removed, primarily because of the rapid adsorption of the ammonia by the water. This unexpected result led to consideration of ammonia-bearing retort wastewater for H_2S control. A second test was conducted to explore the feasibility of this concept. As expected, H_2S removal was achieved at reasonable efficiencies with operation at appropriate L/G ratios, scrubbing-fluid pH, and $\text{NH}_3/\text{H}_2\text{S}$ molar ratio. Particulate control efficiency was also found to be enhanced by some 2 to 5% by the addition of NH_3 .

TABLE 5. EPA STRETTFORD FIELD TESTS

Site	H_2S Removal Efficiency
Logan Wash, MIS Retorts 7 & 8	20 - 60%
Geokinetics, <i>in Situ</i> Retorts	60 - 90+%
U.S. Bureau of Mines (coal gas)	75 - 99.7%

EPA is currently investigating approaches to increase the ability to test a variety of chemical systems for controlling both oxidized and reduced forms of sulfur emissions from both direct and indirect-fired oil-shale retorts. The mobile scrubber-research unit is currently undergoing modifications to incorporate capabilities for ammonia and caustic scrubbing of the off-gases prior to their use as fuel. EPA is also planning additional tests to better define the efficiency of the Stretford system in removing H₂S from retort off-gas.

WASTEWATER POLLUTANTS AND CONTROLS

Over the past several years, EPA has assessed the potential environmental impact of oil-shale development particularly in the Western Regions of the U.S. (Colorado and Utah). Detailed development plans submitted by the prospective developers indicate that in the semi-arid region in which the major development will take place the industry will be "water consumptive." This means that oil-shale facilities will have to import water to satisfy their process needs and therefore will have no wastewater discharges ("zero discharge"). Because of the scarcity of water, these facilities will have to seek ways to reuse water and will have to be very conscious of optimizing the "partial treatment" of selective wastewater streams for their "next best use." Developers have proposed that any "unusable" waste streams should be mixed with spent shale for moisturizing, and ultimately be disposed of in the solid-waste piles. This concept leads to the question of what should be the wastewater quality requirements for spent-shale moistening. This question cannot be answered at this time. EPA is investigating the wastewaters from various processing technologies (i.e. *in-situ*, modified *in-situ*, direct and indirect surface retorting) and will continue to sample wastewaters to further understand potential treatment problems. To date, EPA's most significant sampling and analytical effort to determine wastewater-treatment efficiency was the field testing at Occidental Logan Wash 7 & 8 burns during the Summer of 1982.

These MIS oil-shale retorts generate gases and an oil/water mixture from shale pyrolysis, combustion of carbonaceous residues, and decomposition of inorganic carbonates. Off-gases generated exit from the retort bottom and are brought to the surface for treatment. The retort oil/water mixture accumulates in the product-collection sump at the retort bottom and is subsequently pumped out and treated to recover the bulk of the shale oil. The separated gas condensate and retort waters are the wastewaters which were studied at the Logan Wash field site.

At Logan Wash, treatability studies were conducted for three weeks on retort water using filter coalescing, flocculation/clarification, and steam-stripping technologies (Figure 1). Also, studies were conducted for 14 weeks on gas-condensate wastewater using filter coalescing, steam-stripping, conventional and powdered activated carbon (PAC) activated-sludge treatments, sand filtration, and granular activated-carbon adsorption technologies (Figure 2).

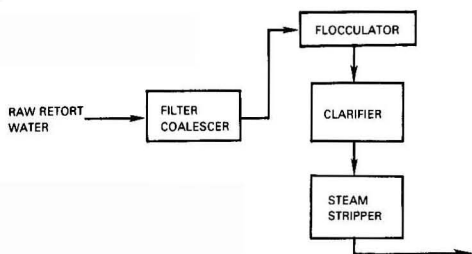


Figure 1. Retort water treatment scheme. Source: Day (1983) [2].

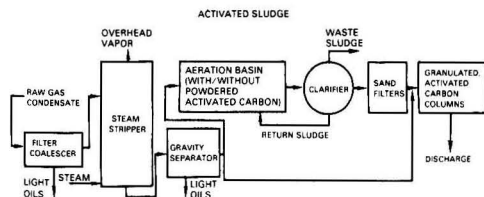


Figure 2. Gas condensate wastewater treatment schemes. Source: Day (1983) [2].

Retort Water

Raw-wastewater characterization data collected over the 16 days of retort water-treatment tests are summarized in Table 6. As expected, the raw retort water contained high concentrations of total dissolved solids (TDS), ammonia, total Kjeldahl nitrogen (TKN), organics, sulfide, alkalinity, phenols, chlorides, and fluorides.

Ammonia and alkalinity were readily stripped from retort water (see Table 7). As expected, removals of these two pollutants increased as the G/L ratio increased. Greater than 97 percent ammonia and 47 percent alkalinity removals were achieved with G/L ratios equal to or greater than 0.18 kg of steam per liter of feed water (1.5 lb/gal.) TKN removals resembling ammonia removals (>99 percent) at G/L ratios as low as 27 to 54 percent were also achieved and the removals appear to depend on G/L ratio and feed-phenol concentration. Using the G/L ratios between 0.07 kg/L (0.6 lb/gal) and 0.30 kg/L (2.5 lb/gal), incidental removals of organics ranged from 0 to 25 percent for dissolved organic carbon (DOC) 5 to 11 percent for soluble BOD₅, and 16 percent for COD.

Retort water was treated primarily to remove oil and grease, suspended solids, ammonia, and alkalinity. The filter coalescer, flocculator/clarifier, and steam stripper in series were used to remove these pollutants. The overall treatment scheme was very effective for ammonia and alkalinity removal. Relatively high sulfide, TKN, and phenols removals were also achieved. Due to low levels of oil and grease, and suspended solids, the scheme was not effective in removing these pollutants, nor was it critical that these low levels be reduced further prior to going to the next series of treatments.

Gas Condensate

Raw gas-condensate wastewater was analyzed for conventional pollutants during 14 weeks of gas-condensate trials. The results of these analyses are summarized in Table 8. As expected, the raw-gas condensate contained high concentrations of ammonia, TKN, organics, alkalinity, phenols, and sulfide. Analytical results for GC/MS organic compounds, metals, and DOC fractionation are presented in Reference [2].

Filter coalescing, steam stripping, conventional activated-sludge treatment, and filtration, and GAC adsorption comprised the overall treatment scheme for the gas condensate. The scheme was very effective in removing ammonia, organics, sulfide, alkalinity, and solids from the gas condensate (Table 9).

The other treatment scheme utilized coalescing, steam stripping, and GAC adsorption. The scheme was effective in removing ammonia, organics, sulfide, alkalinity, and solids from the gas condensate. However, the performance of granular activated-carbon adsorption was relatively poor, and this scheme appeared less effective in removing pollutants than the one with an activated-sludge system included.

In summary, pilot-scale field-treatability studies on real-time oil-shale wastewaters from Occidental *in-situ* MIS retorts demonstrated that retort water had high con-

TABLE 6. RAW RETORT WASTEWATER CHARACTERISTICS

Parameter	Number of analyses performed	Concentration, mg/L	
		Range	Average
Total COD	4	3,400-6,000	4,700
Soluble COD	4	3,100-5,400	4,100
Total BOD ₅	4	2,200-4,000	3,200
Soluble BOD ₅	4	1,900-2,200	2,000
Dissolved organic carbon (DOC)	5	1,400-2,300	1,700
Oil and grease	(5) ^a	(50-170)	(110)
NH ₃ -N	6(5)	1,600-3,900 (1,700-3,700)	2,200 (2,200)
TKN	6(2)	1,700-3,000 (2,100-2,200)	2,100 (2,100)
NO ₃ -N	5	3.0-4.8	4.3
Alkalinity as CaCO ₃ to pH 4.5	6(4)	12,000-17,000 (13,000-16,000)	14,000 (14,000)
Sulfide	3	50-130	90
Phosphorus	4	0.8-2.1	1.5
Cyanide	(4)	(<0.02-0.08)	(0.05)
Phenols	(5)	(47-70)	(56)
Fluorides	7	36-63	45
Chlorides	6	500-1,000	800
TSS	8	27-93	59
VSS	6	23-78	54
TDS	6(1)	10,000-15,500 (15,000)	14,000 (15,000)
pH ^b	(10)	(8.6-9.4)	(8.8)
Temperature ^c	(10)	(21-46)	(35)

^a Data reported in parentheses are from grab samples. The rest of the data are from composite samples.

^b pH is reported in standard pH units.

^c Temperature is reported in °C.

Source: Day (1983) [2].

centrations of ammonia, TKN, alkalinity, dissolved organics, phenols, sulfide, and TDS, and gas condensate had high concentrations of ammonia, TKN, dissolved organics, alkalinity, phenols, and sulfide. Steam stripping was effective in removing ammonia and alkalinity from the retort water. Steam stripping, activated-sludge treatment (both conventional and PAC), sand filtration, and GAC adsorption were effective in removing ammonia, alkalinity, TKN, nitrate, soluble COD, soluble BOD₅, DOC, phenols, sulfide, and TSS from the gas condensate. Pollutant-removal efficiencies across individual treatment units for retort-water and gas-condensate treatment schemes are presented in Tables 7 and 9, respectively.

SOLID WASTE IMPACTS AND CONTROL

Analysis of solid-waste impacts and controls for an oil-shale facility presents unique problems due to the very large volume of waste produced. A typical 50,000 bbl/day (7,949 m³/day) facility fed by 30 gal/ton (103 L/10³ kg) shale

TABLE 7. POLLUTANT REMOVAL EFFICIENCIES ACROSS INDIVIDUAL UNITS FOR RETORT WATER TREATMENT SCHEME^{a,b}

Parameter	Filter coalescer	Flocculation/clarification ^c	Steam stripper ^d
Oil and grease	6		
Ammonia			97
TKN			88
Soluble BOD ₅			5
DOC			4
Phenols			32
TSS	21	0	
VSS	20		
Alkalinity as CaCO ₃ to pH 4.5			47
Fluorides		7	
Chlorides		11	

^a Average removal efficiencies are reported.

^b Blanks indicate data not collected.

^c Lime dosage at 90 mg/L.

^d G/L = 0.18 kg/L (1.5 lb/gal).

Source: Day (1983) [2].

will produce 22-26 million tons/year (20-24 · 10⁹ kg/yr) of spent shale alone, which, over an operating life of 30 years, would cover an area of 3.5 square miles (9 km²) to a depth of 150 feet (45.7 m) (Bates and Thoen, 1980) [3]. Hence, even though this waste may not be hazardous, it will require special handling and control to prevent significant impact upon the environment. Potential impacts or problems include:

- Degradation of surface-water quality by runoff.
- Degradation of air quality by release of vapors or dust.
- Siltation of surface streams by erosion.
- Degradation of air quality from auto ignition.
- Aesthetic impact.
- Mass failure of disposal piles threatening life or property.
- Degradation of surface and groundwater quality by leachates.

Technologies to prevent or control most of these problems already exist in other mining industries or have been developed and demonstrated on a small scale for oil shale. Runoff can be collected and treated, infiltrated or evaporated, and, if the disposal site is top-soiled and revegetated, will be of a quality equivalent to runoff from undisturbed areas. Emission of vapors can be prevented by removing volatiles from wastewater disposed with the shale and by cooling the shale prior to disposal. Fugitive dust can be controlled with water sprays or chemical binders during placement and by vegetation after reclamation. Technology to revegetate spent shale, through the use of top-soil covers, irrigation, water-harvesting techniques, fertilization and use of selected plant species has been demonstrated through small-scale field studies. Good reclamation techniques will substantially improve the appearance of the disposal sites as well as control erosion and prevent generation of wind-blown fugitive dust. Studies are presently in progress by EPA to assess the auto-ignition potential of carbonaceous retorted shales and fine-grained raw-shale wastes. Although the work will not be completed for another year, the preliminary indications

TABLE 8. RAW GAS CONDENSATE WASTEWATER CHARACTERISTICS

Parameter	Number of analyses performed	Concentration mg/L	
		Range	Average
Total COD	2	2,000-4,100	3,100
Soluble COD	37 (13) ^a	1,400-4,100 (2,000-4,200)	2,700 (2,800)
Soluble BOD ₅	8	600-1,000	800
DOC	33	500-1,400	890
Oil and grease	(13)	(1.8-76)	(18.6)
NH ₃ -N	40 (33)	6,100-14,000 4,800-11,000	9,000 (8,200)
TKN	21	1,300-9,700	6,800
NO ₃ -N	16	0.3-3.0	1.1
Alkalinity as CaCO ₃ to pH 4.5	27 (19)	1,000-37,000 (22,000-40,000)	31,000 (31,000)
Sulfide	17	18-190	72
Phosphorus	6	<0.01-1.3	0.26
Cyanide	(4)	(<0.02-0.11)	(0.04)
Phenols	(21)	(70-150)	(120)
Fluorides	9	0.07-1.05	0.43
TSS	8	<5-14	7
VSS	8	<5-6	5
TDS	6	48-140	98
pH ^b	(~560)	(8.3-8.7)	(8.5)
Temperature ^c	(~560)	(26-45)	(34)

^a Data reported in parentheses are from grab samples. The rest of the data are from composite samples.

^b pH is reported in standard pH units.

^c Temperature is reported in °C.

Source: Day (1983) [2].

are that these materials appear to have the same or less potential for auto ignition than bituminous coals. Mass failure of the disposal piles can be prevented through good engineering design similar to that used for earth-filled dams, so long as moisture movement within the pile can be controlled. It is this last area, moisture movement with the spent-shale disposal pile, which remains unknown and the subject of much controversy.

When precipitation falls on a disposal site, some runs off, some evaporates, some infiltrates. Of the moisture which infiltrates, most, and perhaps all, will be transpired by plants on the reclaimed disposal site. However, any moisture which infiltrates too deeply to be transpired will become net infiltration into the retorted shale. The quantity of this net infiltration into the disposal pile, in conjunction with the hydraulic properties of the retorted shale, are particularly significant as they determine the quantity of leachate produced and the potential for a portion of the disposal pile to become saturated and fail. Care must also be taken in spent-shale pile location and design to prevent

groundwater, springs, and streams from infiltrating the pile.

In cooperation with the oil-shale industry, EPA is currently sponsoring laboratory studies at Colorado State University to determine the hydraulic properties of spent-oil shales and soon will initiate study of co-disposal of wastewaters with retorted shale and field determinations of the quantity of net infiltration for Western Colorado disposal sites. Current laboratory studies, under the direction of Dr. David McWhorter, are focused on determining the nature of leachate which may be produced from various retorted and raw shales and the permeability and water-holding capacity of retorted shales for various compactive efforts and loading conditions.

Retorted oil shales will be placed in disposal sites at relatively low moisture contents, generally between 5 and 20 percent, as required for dust control and to achieve desired compaction. As water penetrates into the pile from initial irrigation or seasonal precipitation, a portion of the water will be in storage behind the wetting front. The water thus

TABLE 9. POLLUTANT REMOVAL EFFICIENCIES ACROSS INDIVIDUAL UNITS FOR GAS CONDENSATE TREATMENT SCHEME^{a,b}

Parameters	Filter coalescer	Steam stripper ^c	Activated sludge treatment ^d	Sand filter	GAC Adsorption column ^e
Oil and grease	28				
Ammonia		99	6		
TKN		96			
Soluble COD		56	59		95
Soluble BOD ₅		60	91		70
DOC		29	52		89
Phenols		97	93		99.5
Sulfide					
TSS				70	
Alkalinity as CaCO ₃ to pH 4.5		99			

^a Average removal efficiencies are reported.

^b Blanks indicate data not collected.

^c G/L = 0.19 kg/L (1.6 lb/gal) average.

^d Hydraulic retention time = 16 hours, sludge age = 32 days.

^e Contact time = 19 minutes.

Source: Day (1983) [2].

held in storage is not available to extend the wetting front deeper into the pile. Given the huge size of proposed spent-shale disposal piles and the relatively low precipitation in Western Colorado and Utah, this water-holding capacity will be a significant factor influencing moisture movement in the shale pile. Table 10 shows water-holding capacities for three retorted shales. Water-holding capacities are quite large, but are inversely related to initial compaction and to loading pressures. These values are important, not only as a measure of sorptive capacities for net infiltration, but also as an indication of whether the bottom of a disposal pile will saturate from loading pressures given an initial moisture content and compactive effort.

In addition to waterholding capacity, the hydraulic conductivity or permeability is obviously important in assessing potential moisture migration in a retorted shale pile. An apparatus for measuring hydraulic conductivity for various compactive efforts and loading pressures is illustrated in Figure 3. Table 11 presents permeability values for several given initial moisture contents and compactive efforts as these samples were subjected to increasing loading pressures. Generally, the hydraulic conductivity decreases sharply with increased initial compaction but decreases only slightly with increased loading pressures. This indicates that the desired permeability values should be achieved by initial compaction at the time of placement rather than depending upon secondary compaction through loading.

As discussed, net infiltration, water-holding capacity,

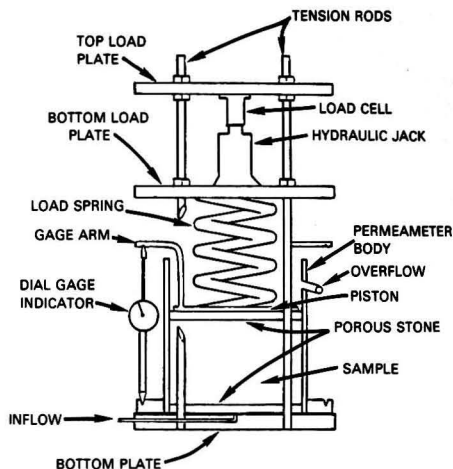


Figure 3. Schematic of permeameter. Source: McWhorter (1982) [4].

and permeability are influenced by engineering design and will be important in determining the quantity of leachate that may be produced. Also of interest is obtaining an estimate of quality of leachate from either raw-shale storage piles or retorted-shale disposal sites. Standardized tests such as the RCRA EP (acetic acid) or ASTM (water) shaker tests as well as various column leaching

TABLE 10. WATER HOLDING CAPACITY OF RETORTED SHALES (EXPRESSED AS WEIGHT % WATER/DRY SOLID)

Sample	14.7 psi 0.10 MPa	44.1 psi 0.30 MPa	73.5 psi 0.51 MPa	147 psi 1.01 MPa	200 psi 1.38 MPa
LURGI					
No Compaction (Ash)	73.6	62.0	64.5	63.1	59.5
No Compaction	27.5	27.6	26.9	25.3	15.5
1.30 g/cc (Ash)	62.4	62.3	62.2	62.0	61.7
1.45 g/cc (Ash)	60.2	58.7	56.6	55.5	55.2
1.60 g/cc (Ash)	47.2	46.3	45.8	44.4	43.7
1.60 g/cc	20.7	20.2	19.8	19.8	19.0
TOSCO II					
No Compaction	48.0	45.8	45.9	43.8	44.7
1.30 g/cc	42.2	42.0	41.9	41.6	41.4
1.45 g/cc	36.0	33.8	32.9	32.1	30.5
1.60 g/cc	34.6	33.5	32.1	30.8	30.5
HYTORT					
1.30 g/cc	35.2	33.7	32.6	31.8	31.0
1.45 g/cc	31.0	27.6	25.3	23.8	23.2
1.60 g/cc	30.5	30.3	28.9	25.4	24.6

Source: McWhorter (1982) [4].

TABLE 11. SUMMARY OF HYDRAULIC CONDUCTIVITY MEASUREMENTS (CONSTANT HEAD)

Material	Water %	Density g/cm ³	Permeability cm/s		
			50 psi 0.34 MPa	100 psi 0.69 MPa	200 psi 1.38 MPa
TOSCO II	20.8	1.56	6.8 × 10 ⁻⁶	6.2 × 10 ⁻⁶	5.6 × 10 ⁻⁶
	11.0	1.39	5.6 × 10 ⁻⁵	4.6 × 10 ⁻⁵	3.9 × 10 ⁻⁵
	11.4	1.29	6.7 × 10 ⁻⁵	4.0 × 10 ⁻⁵	2.5 × 10 ⁻⁵
LURGI-RG-I	26.6	1.41	1.0 × 10 ⁻⁶	6.5 × 10 ⁻⁷	6.5 × 10 ⁻⁷
	10.4	1.33	3.0 × 10 ⁻⁵	1.9 × 10 ⁻⁵	2.0 × 10 ⁻⁵
*LURGI-ULG-I	dry	1.81	8.3 × 10 ⁻⁵		
*LURGI-RB	dry	1.22	1.2 × 10 ⁻⁵		
PARAHO	20.0	1.67	4.7 × 10 ⁻⁷	4.2 × 10 ⁻⁷	4.5 × 10 ⁻⁷
	10.0	1.36	9.7 × 10 ⁻⁴	7.1 × 10 ⁻⁴	2.5 × 10 ⁻⁴
*PARAHO	dry	1.09	4.6 × 10 ⁻⁴		
*TOSCO II	dry	1.46	2.8 × 10 ⁻⁵		

* Leaching Columns (Constant Rate Injection)
Source: McWhorter (1982) [4].

TABLE 12. RAW SHALE LEACHATES BY LEACHING METHOD (MG/L)

Parameter	C-b			C-a			Field(mean)
	RCRA	ASTM	Field(mean)	ASTM	Column*	Column	
Pore Volume					Initial	.73 PV	
pH	7.67	8.57	7.7	8.22	8.17	8.08	7.5
EC (μ S/cm at 25°C)	4350	850	7000	2500	39,000	5800	20,000
HCO ₃	2461	141	177	150	183	86.9	384
CO ₃	4.9	2.2	-	1.1	1.16	0.45	-
TDS	5884	710	6450	2430	-	-	30,080
Cl	1.9	2.8	14.2	84.5	2433	16	163
SO ₄	154	315	3680	1480	25,224	4110	20,500
F	-	2.4	7.8	1.5	18.5	5.8	10.4
Mg	252	38	218	173	6465	680	4,490
Na	36	76	1045	117	4660	236	880
Ca	1092	50	451	350	430	472	633
K	3.5	14	7.8	7.0	53	4.0	7.8

* Column leaching by constant rate injection method, initial values and after 0.73 pore volumes. Source: McWhorter (1982) [5].

tests have been used for this purpose. Tables 12 and 13 present major ion concentration in raw shale, retorted shale, and when available, field lysimeters. The apparatus for producing leachate by constant-rate injection into a dry packed column is illustrated in Figure 4. Column leachate data varies depending upon the quantity (pore volume) of water that has passed through the material. Data presented

is for initial leachate produced and for leachate produced after approximately one pore volume (PV) has passed through the material. (Note that the material has been contacted by one more pore volume than shown since the column must be wetted with one complete pore volume before any leachate is eluted).

Examination of the data in Tables 12 and 13 reveals that

TABLE 13. RETORTED SHALE LEACHATES BY LEACHING METHOD (MG/L)

Shale/Parameter		Field	RCRA	ASTM	Column Initial	Column 0.918
Paraho	Pore Volume					
	pH	9.57	9.27	12.05	11.55	12.35
	Ec (μ S/cm at 25°C)	21,100	4600	2800	9230	6250
	HCO ₃	-	2723	5	15.3	4.8
	CO ₃	-	217	236	232	463
	SO ₄	12,350	226	536	3840	2045
	Cl	526	29	7	49	14
	F	11.9	-	13.5	21	11.4
	Mg	7.7	484	0.5	1.6	1.7
	Na	5591	37	145	1500	285
	Ca	421	724	266	610	670
	K	834	6.5	31	140	38
	TOSCO II	Pore Volume				Initial
pH		8-9	7.72	8.69	9.24	9.21
Ec (μ S/cm at 25°C)		10,000	5710	2650	35,080	5180
HCO ₃		-	3325	191	619	188
CO ₃		-	-	-	46	13
SO ₄		30,270	229	1130	25,000	2470
Cl		-	22	10	178	13
F		13	-	20.2	27	29.5
Mg		156	81	35	628	60
Na		10,270	131	545	10,095	945
Ca		463	1872	31	545	83
K		110	3.9	8	89	11
LURGI*		Pore Volume	Field	RCRA	ASTM	Column Initial
	pH	-	8.67	11.85	12.24	11.93
	EC	-	5650	4270	59,500	4250
	HCO	-	2940	6.9	10.5	7
	CO ₃	-	59	210	775	203
	SO ₄	-	880	2290	34,000	2070
	Cl	-	19	17	2250	15
	F	-	-	6.3	26.4	7.6
	Mg	-	430	0.4	3.5	0.3
	Na	-	55	275	18,770	325
	Ca	-	1479	713	535	575
	K	-	11	64	1464	150

* Several Lurgi shales have been tested and results differ slightly. Example provided is Lurgi shale provided by Rio Blanco Oil Shales. Source: McWhorter (1982) [4], for laboratory data. Bates & Thoem (1980) [3], for Paraho field data; Metcalf & Eddy Engineers (1975) [6] for TOSCO field data.

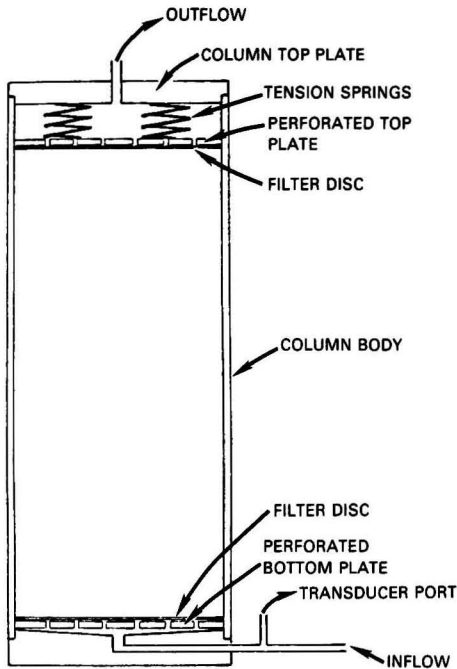


Figure 4. Schematic of leaching column—constant rate injection tests. Source: McWhorter (1982) [4].

none of the laboratory methods provides an especially good indication of what happened under field conditions. Generally, the ASTM and RCRA shaker tests seem to correlate more closely with the column-produced leachate after one or more pore volumes while the initial column-produced leachate correlates more closely with the field data. Logically, this might be expected, since the RCRA and ASTM tests contact the shale with much more water than occurs under field conditions. Generally, all the laboratory methods are indicative of what will be leached, but do not provide a good indication of the concentration of species in solution. Hence, the results of laboratory leaching tests on raw or retorted oil shales should be interpreted with caution, because results from actual disposal may be significantly different. Presently, column tests are being conducted with the material being packed into the columns in a pre-wetted state rather than dry, as it is felt this may better reflect field conditions. Results from this procedure will be reported in subsequent papers.

LITERATURE CITED

1. Lovell, R. J., S. W. Dylewski, and C. A. Peterson, IT Environscience, "Control of Sulfur Emissions from Oil Shale Retorts," EPA 600/7-82-016, U.S. EPA, Cincinnati, Ohio (1982).

2. Day, R. Duane, Bharat O. Desai, and Walter W. Liberick, "The Treatability of Wastewaters Produced During Oil Shale Retorting," 16th Oil Shale Symposium Proceedings, Colorado School of Mines Press, Golden, Colorado (August, 1983), pages 512-533.
3. Bates, E. R. and T. L. Thoen, Editors, "Environmental Perspective on the Emerging Oil Shale Industry," EPA 600/2-80-205a, U.S. EPA, Cincinnati, Ohio, page 85 (1980).
4. McWhorter, D. B., "Leaching and Hydraulic Properties of Retorted Oil Shales," unpublished report, USEPA, Cincinnati, Ohio (1982).
5. McWhorter, D. B., "Quality and Quantity of Leachate from Raw Mined Colorado Oil Shale-Interim" unpublished report, U.S. EPA, Cincinnati, Ohio (1982).
6. Metcalf & Eddy Engineers, "Water Pollution Potential from Surface Disposal of Processed Oil Shale from the TOSCO II Process," A Report to Colony Development Operation at Atlantic Richfield Company, Operator, Volume I, page A4-6, mean valves for twelve samples (1975).



Edward R. Bates, a Senior physical scientist for the USEPA, earned his B.S. and M.S. degrees in Geology from Michigan State University. Since joining the USEPA in 1977, he has specialized in environmental research related to oil shale development and presently is manager for the oil shale program at the Industrial Environmental Research Laboratory in Cincinnati.



Walter W. Liberick, Jr., Acting Chief, Oil Shale and Energy Mining Branch, Energy Pollution Control Division, Industrial Environmental Research Laboratory, Cincinnati, earned his B.S. in Civil Engineering at Marquette University and a M.S. in Sanitary Engineering at the Georgia Institute of Technology. Since joining the federal government in 1961 he has worked in several areas of environmental engineering including water distribution and wastewater collection and treatment, radiological health, and solid waste management and disposal. Presently he has responsibility for a pollution control research program for synthetic fuel production processes, specifically oil shale, tar sands, geothermal and advanced oil and gas recovery.



John O. Burekle, a senior research engineer for the USEPA Office of Research and Development, earned his BChE and MChE degrees at the University of Louisville. From 1963 through 1967, he worked in industry in process design and pilot plant development. Since joining the federal government in 1967, he has specialized in environmental research for air pollution and solid/hazardous waste protection technology.

A Methodology for Predicting Fugitive Emissions for Incinerator Facilities*

The ability to predict the possible range of fugitive emissions is an important step toward an increased understanding of controlling processes.

G. A. Holton and C. C. Travis, Oak Ridge National Laboratory, Oak Ridge, Tenn. 37830

Research is being conducted to determine public exposure to atmospheric pollutant concentrations from stack and fugitive volatile organic compound (VOC) emissions of hazardous waste incineration facilities. VOC fugitive emissions are defined herein as those caused by leaky pump fittings, sampling connections, flanges, storage tanks, and other non-stack equipment. The relative importance of stack versus fugitive emissions has been studied using measured (Staley *et al.*, 1983 [8]) and predicted (Harrington *et al.*, 1983 [4]) estimates. These studies show that atmospheric pollutant concentrations and population exposures at close-in locations are understandably more affected by fugitive releases because of emission characteristics (low temperature, near ground-level).

Another characteristic of fugitive emissions is their apparent wide variability. Some pieces of equipment operate with little or no measurable releases, whereas others of the same type, under the same conditions, leak liquids in sufficient quantity to cause puddles. This variability makes standard setting, enforcement, measurement, and assessment of effects caused by fugitive emissions particularly difficult activities. To determine a range of possible fugitive emission rates, a prediction methodology which incorporates error analysis and Monte Carlo modeling was developed (Holton *et al.*, 1982 [5]). An important result of this initial work was the clear need to resolve differences between measured values and predicted fugitive emission estimates. Both the improvement in parameter quantification employed in the prediction methodology and the development of a broader fugitive emissions measurement data base was recommended. The U.S. Environmental Protection Agency (USEPA) has recognized the shortcomings of the measurements and has gathered additional data at a number of incinerator facilities. Presented herein are improvements in parameter quantification and their subsequent effect on emission predictions.

APPROACH

The goal in creating the methodology was to determine the variability which could exist in fugitive emission estimates. Compilation of individual equipment emission rate and facility operation equations into a model to estimate incinerator facility fugitive emission rates has been performed and reported elsewhere (Holton *et al.*, 1982 [5]).

The steps taken in this initial work (Steps 1 through 3 below) were straightforward. However, to employ these equations in a fugitive emission prediction methodology required additional, detailed work. Each parameter in the emission and facility operation equations had to be analyzed to determine its inherent variability, using available data in literature and/or engineering judgement to define upper and lower estimates. Monte Carlo sampling and emission rate computation procedures then had to be devised. The steps incorporated into the complete prediction methodology are summarized below.

1. Determine design, equipment, waste burned, and operating practice for a typical incinerator facility.
2. Construct emission rate equations for each piece of equipment employed in the facility design.
3. Construct facility throughput and operating time equations based on fuel oil and waste physicochemical properties.
4. Assign distributions of variability to each parameter in the emission rate and facility operation equations.
5. Estimate fugitive emission rates and variability for the site by location and equipment type using Monte Carlo sampling techniques.

Assumptions employed to formulate emission rate equations, choose parameter variability, and design the Monte Carlo sampling procedures are detailed below.

EMISSION RATE EQUATIONS AND PARAMETER VARIATION PROCEDURES

Table 1 contains equations developed by the authors to estimate facility operation (Equations 1-3) and fugitive emissions (Equations 4-10). Equations 1 and 2 calculate waste and fuel oil throughput. These equations are valid when the heat of combustion of fuel oil (a typical condition) and the densities of the waste and fuel oil are approximately equal. Time and throughput were determined to be the most important facility operation characteristics that had to be computed before fugitive emissions could be estimated. Values for the heat of combustion of the waste, supplemented with No. 2 fuel oil, waste and oil liquid densities, and incinerator capacity were used in these equations. Tank emissions were calculated from Equation 4, a combination (with slight modification) to two equations for breathing and working losses from fixed-roof tanks (USEPA, 1980 [10]). Factors were included to convert from gallons to pounds, to calculate emissions from an area containing more than one tank, and to allow application of pollution control. Equations 5 through 10 were used to calculate fugitive emissions for six other major types of equipment. These equations incorporate source emissions

*Although the research described in this article has been funded wholly or in part by the United States Environmental Protection Agency (EPA) through Interagency Agreement DOE 40-1174-81 and EPA AD-89-F-1-768-0 to Oak Ridge National Laboratory under Union Carbide Corporation Contract W-7405-eng-26 with the United States Department of Energy, it has not been subjected to EPA review and therefore does not necessarily reflect the views of EPA and no official endorsement should be inferred.

TABLE 1. EMISSION EQUATIONS

Number	Parameter	Symbol	Units
1	Waste throughput	TP_w	gal/y $TP_w = 7200 \left[\frac{1000 C_F}{10 \times 10^6} (\Delta H_c)_{fo} - C_F \right] / (\rho_{tw} [(\Delta H_c)_{fo} - (\Delta H_c)_w])$
2	Fuel oil throughput	TP_{fo}	gal/y $TP_{fo} = 7200 \left[C_F - \frac{1000 C_F}{10 \times 10^6} (\Delta H_c)_w \right] / (\rho_{fo} [(\Delta H_c)_{fo} - (\Delta H_c)_w])$
3	Operating time	OT	h/y $OT_w = TP / 60(FR)$
4	Tank emissions	L_T	lb/y $L_T = \Sigma [9.15(P_w/(14.7 - P_w))^{0.68} D^{1.73} H^{0.51} \Delta T^{0.5} F_p C + 0.0109 P_w (TP_w)] / 0.0022 M_w N_T (1 - EFF_T)$
5	Pump emissions	L_P	lb/y $L_P = E_P (\Sigma N_P OT) (1 - EFF_P)$
6	In-line valve emissions	L_{ILV}	lb/y $L_{ILV} = E_{ILV} (\Sigma N_P OT) R_{ILV} (1 - EFF_{ILV})$
7	Open-ended valve emissions	L_{OEV}	lb/y $L_{OEV} = E_{OEV} (\Sigma N_P OT) R_{OEV} (1 - EFF_{OEV})$
8	Flange emissions	L_F	lb/y $L_F = E_F (\Sigma N_P OT) R_F (1 - EFF_F)$
9	Instrument connection emissions	L_{IC}	lb/y $L_{IC} = E_{IC} (\Sigma N_P OT) R_{IC} (1 - EFF_{IC})$
10	Sampling connection emissions	L_{SC}	lb/y $L_{SC} = 7200 E_{SC} N_T (1 - EFF_{SC})$

factors, control factors, and various ratios. Explicit representation of emissions and control factors facilitates updating and application of improved estimates. Ratios are used to relate quantities of particular types of equipment to the number of pumps in the facility. For example,

sampling connections were assumed to be related to the number of tanks by a 1:1 ratio (except auxiliary fuel tanks, which were assumed not to require sampling).

Defined in Table 2 are the various parameters found in Equations 1-10 of Table 1. Listed also are expected values

TABLE 2. EQUATION PARAMETERS — DEFINITION AND VARIABILITY

Symbol	Parameter	Units	Lower Bound	Expected Value	Upper Bound
$(\Delta H_c)_w$	Heat of combustion — waste	Btu/lb	1500 ^a	3000 ^b	6000 ^a
M_w	Vapor molecular weight — waste	lb/mol	75 ^a	150 ^b	300 ^a
P_w	Vapor pressure — waste	psia	0.05 ^a	0.10 ^b	0.20 ^a
ρ_{tw}	Liquid density — waste	lb/gal	7 ^a	14 ^b	28 ^a
$(\Delta H_c)_{fo}$	Heat of combustion — fuel oil (#2)	Btu/lb	18,500 ^c	19,000 ^b	19,500 ^c
M_{fo}	Vapor molecular weight — fuel oil (#2)	lb/mol	128.7 ^c	130.0 ^b	131.3 ^c
P_{fo}	Vapor pressure — fuel oil (#2)	psia	0.0057 ^c	0.0058 ^b	0.0059 ^c
ρ_{fo}	Liquid density — fuel oil (#2)	lb/gal	7.1 ^c	7.2 ^b	7.3 ^c
C	Diameter-adjustment factor	—	-14% ^d	See Table 3	+34% ^d
C_F	Incinerator capacity	Btu/h	No error ^e	139,000,000	No error ^e
D	Tank diameter	ft	-17% ^f	See Table 3	+53% ^f
E_P	Pump-emission factor ^g	lb/h	0.024	0.11	0.49
E_{ILV}	In-line valve-emission factor ^g	lb/h	0.0051	0.016	0.036
E_{OEV}	Open-ended valve-emission factor ^g	lb/h	0.0013	0.0038	0.036
E_F	Flange-emission factor ^g	lb/h	0.00076	0.0018	0.0038
E_{IC}	Instrument-connection emission factor ^g	lb/h	0.00024	0.00066	0.0029
E_{SC}	Sampling-connection emission factor ^g	lb/h	0.011	0.033	0.11
EFF_T	Tank-control efficiency	—	0 ^h	0.96	0.98 ⁱ
EFF_P	Pump-control efficiency	—	0 ^h	0.80	1.00 ⁱ
EFF_{ILV}	In-line valve-control efficiency	—	0 ^h	0.77	1.00 ⁱ
EFF_{OEV}	Open-ended valve-control efficiency	—	0 ^h	0.89	1.00 ⁱ
EFF_F	Flange-control efficiency	—	0 ^h	0.70	1.00 ⁱ
EFF_{IC}	Instrument-connection control efficiency	—	0 ^h	0.70	1.00 ⁱ
EFF_{SC}	Sampling-connection control efficiency	—	0 ^h	0.89	1.00 ⁱ
F_p	Paint factor	—	1.00 ^j	1.29	1.58 ^j
FR	Flow rate for pumps	gal/min	No error ^e	See Table 4	No error ^e
H	Average vapor-space height	ft	-19% ^d	See Table 3	+27% ^d
R_{ILV}	In-line valve: pump ratio	—	11 ^a	13	15 ^a
R_{OEV}	Open-ended valves: pump ratio	—	1 ^a	2	3 ^a
R_F	Flanges: pump ratio	—	21 ^a	24	27 ^a
R_{IC}	Instrument connections: pump ratio	—	3 ^a	4	5 ^a
ΔT	Average diurnal temperature change	°F	15 ^a	20	30 ^a

^aFactor-of-two variation assumed.

^bDean (1973)[3], Perry and Chilton (1973) [6], Reid *et al.* (1977) [7], and Thibodeaux (1979) [9].

^cEngineering judgement.

^dDerived from error in explicitly related parameter.

^eParameters obtained from flowsheets are assigned "no error."

^fBuffalo Tank-Division (1981) [1].

^gUSEPA (1982) [13].

^hNo control assumed.

ⁱState-of-the-art control assumed.

^jUSEPA (1980) [10].

for each parameter, along with their estimated upper and lower bounds. Methods used to estimate each entry are noted by superscripts in the table and described below. Waste properties (vapor pressure, density, molecular weight, and heat of combustion) were determined from Weast (1973 [14]) and by calculation procedures of Dean (1973 [3]), Perry and Chilton (1973 [6]), Reid *et al.*, (1977 [7]), the Thibodeaux (1979 [9]), using chemical analysis information as much as possible. Because of variability in waste samples, a factor-of-two error bound was applied. Previous work (Holton *et al.*, 1982 [5]) assumed an unrealistic error bound of $\pm 1\%$. Engineering judgement was used to set error bounds in several cases where no data were available in the literature. For example, the various equipment ratios were assigned a simple $\pm 10\%$ error bound. Numbers of pumps, pump capacities, numbers of tanks, and tank volumes were assigned no error value, however, because these values were specified on facility flowsheets. The method used to estimate error bounds for fuel oil material properties (density, vapor pressure, etc.) involved assessing either the accuracy of literature values or the particular approximation method used (since in several instances, properties had to be estimated using other known substance characteristics). Several parameters were also functionally related to each other. Therefore, the choice of error bounds for one was directly dependent upon the choice of bounds for another. The specific parameters involved were D (tank diameter), H (average vapor space height: half the tank height), and C (diameter-adjustment factor). D was chosen as the independent variable, although assuming H to be independent would not have influenced the results. Thus, by determining bounds for D , bounds for H and C were calculated. The criterion used to determine upper and lower bounds for D (where h is the tank height) was

$$0.25 h < D < h, \text{ with } h \leq 10.7 \text{ m (35 ft).}$$

These criteria were based on tank vendor literature (Buffalo Tank Division—1981 [1]) and the premise that a commercial facility would desire to keep the tank farm area to a minimum. Using these limitations, upper and lower values for tank diameters (and thus H and C) were calculated (Table 3).

Expected values and error bounds for different source emission factors were originally based on 95% confidence

levels presented in a study of fugitive emissions from refinery operations (USEPA, 1981a [11]). Results (USEPA, 1982 [10]) of recent emission sampling show that there are substantial differences between fugitive emission rates from synthetic organic chemical manufacturing (SOCM) and the refining industry. Consequently, both SOCM and refining emission factors are used and differences in predictions caused by these factors are quantified. (Because of similarities in equipment and maintenance procedures, synthetic organic chemical manufacturing emission factors may be more similar to hazardous waste incinerators than refining operations emission factors). Expected values and error bounds for SOCM emission factors required some conversion, however, to insure that employed values were consistent with the chemicals being incinerated. Furthermore, only light liquid emission factors are presented (Table 2) because of the nature of the waste.

All control efficiency values were assigned lower bounds of 0, which represents the case of uncontrolled emissions. Upper bounds were determined from literature (USEPA, 1980 [10] and 1981b [12]) to be 1.0 for all equipment except tanks. Tank control efficiency was set at 0.98 because small leaks will inevitably occur unless pressure vessels are used (a highly impractical alternative—USEPA, 1980 [10]).

MONTE CARLO SAMPLING PROCEDURE

The Monte Carlo sampling methodology is embodied in a computer program called MONTE (an adaptation of the program SEAP, written by Carney *et al.*, 1981 [2]) that determines emission estimates under conditions of potentially wide variability. These emission estimates, which depend on variables such as waste and fuel oil heats of combustion, are described by a set of parameterized equations described previously. Triangular distributions of each parameter were assumed, based on estimated minimum, maximum, and expected values. The program then randomly sampled from these parameter distributions and computed solutions for each emission equation. Throughput (TP) and operating time (OT) were intermediate solutions for total emissions equations from tanks (L_T), pumps (L_P), in-line valves (L_{ILV}), open-ended valves (L_{OEV}), flanges (L_F), instrument connections (L_{IC}), and sampling connections (L_{SC}).

TABLE 3. TANK PARAMETERS

Area	NT	D(ft)			H(ft)			C(ft)		
		Lower bound	Expected value	Upper bound	Lower bound	Expected value	Upper bound	Lower bound	Expected value	Upper value
Receiving	6	8.72	10.5	16.1	6.34	7.83	9.94	0.458	0.533	0.714
Storage	4	22.5	27.1	41.4	14.2	17.5	22.2	0.860	1.00	1.34
Feed	1	20.1	24.2	37.0	14.2	17.5	22.2	0.835	0.971	1.30

TABLE 4. PUMP PARAMETERS

Area	Pump type	NP	Expected throughput (TP) [gal/y/pump]	Expected flow rate (FR) [gal/min]	Expected operating time (OT) [h/y/pump]
Receiving	Unloading	3	1,427,325	20	118.9
	Receiving	1	4,281,975	200	356.8
Storage	Circulating	2	2,140,187	5	7200.0
	Storage	1	4,281,975	20	356.8
Feed	Feed	1	4,281,975	10	7200.0

To demonstrate the Monte Carlo sampling methodology, details for obtaining pump emission estimates are presented. Pumps are employed to handle waste in three areas of the incinerator facility; unloading and receiving, storage, and feed. The pump emissions equation (Number 5 of Table 1) was thus applied three different times to get results that could be totalled for the entire facility.

Application of the pump emissions equations requires using error bounds for four different parameters: pump emission factors (E_p), number of pumps (NP), operating time (OT), and pump control efficiency (EFF_p). For each area (unloading and receiving, storage, and feed), the light liquid emission factor was used. The number of pumps, based on facility design, is assumed to have no error (one pair in unloading and receiving, three pair in storage, and one pair in the feed area). Pairs of pumps were treated as single pumps, since only one of a pair would be operated at one time. The operating time (Table 1) was calculated from Equation 3. Calculating error bounds for operating time, however requires knowledge of the variability of throughput and error bounds for several more parameters. These parameters, such as those related to material properties, are given in Table 2. The variability for pump control efficiency can also be read directly for Table 2.

Once equations and parameter variability were established, emissions from pumps could be estimated. Expected parameter values and error bounds were employed to create assumed triangular distributions. These distributions were then randomly sampled individually to obtain a value for each parameter required in the pump emission equation. Computation of this equation for one location completed one iteration.

Emission estimates for each tank, flange, etc., were similarly obtained concurrently. These emission estimates for one iteration were summed to yield ETOTAL, the total emissions for the site. An initial solution was computed using the expected values for all parameters, and all succeeding solutions were computed from random values. This sampling and computation were performed in an iterative manner (1000 times) to develop distribution of emission rate estimates that were subsequently analyzed to prepare statistical, tabular, and graphical results. Total facility emission rates were compiled by summing individual equipment types within each process area. Individual chemical emission rates were then calculated from the total hydrocarbon emission rate prediction using vapor pressures and Raoult's Law under simple gas liquid equilibrium assumptions.

RESULTS

Effect of Waste-Characterization Error Bounds

To determine the effect of waste characterization error bounds on emission predictions, release rates for three fugitive emissions areas (receiving, storage, and feed) of an incinerator facility were calculated using the prediction methodology of this paper. Two principal organic hazardous constituents (POHC's), chloroform and hexachloroethane, high- and low-volatile compounds, were chosen for analysis.

The fugitive emission methodology contains four explicit waste properties (i.e. heat of combustion, vapor molecular weight, vapor pressure, and liquid density) to characterize wastes. When available, it is recommended that chemical analysis information be used as far as possible to quantify these properties. Such information is not always gathered, however. In the absence of such data, an important question to ask is whether these waste properties are important to predict fugitive emissions. To determine the effect of potential variability in waste samples, a factor of two error bound was applied and compared to results where an error bound of $\pm 1\%$ was used. Results of this comparison are given in Table 5.

As expected, increasing the variability of waste parameters increases the variability of emission predictions. For each emission area studied, both 95% confidence limits expand, meaning that the cumulative 2.5% emission prediction point decreases while the 97.5% point increases. The amount of change is small (i.e., up to 14% for the lower point and up to 33% for the upper), however. This small change suggest that heat of combustion, vapor molecular weight, vapor pressure, and liquid density are not important contributors to emission variability.

Expanding the waste property error bounds also increases the mean. This result was also expected because a factor of two variation produces a 50% decrease in lower bound property values (which leads to lower emission estimates) but a 100% increase in upper bound values (which leads to higher emission estimates). This skewing of property bounds causes a higher prevalence of increased predictions, thus increasing the mean.

One potential source of variability in waste properties, the concentration of chloroform and hexachloroethane, was assumed to be constant. Because simple gas liquid equilibrium assumptions were employed where the concentration of the pollutant in the vapor is directly related to its concentration in the liquid waste (with an activity

TABLE 5. SUMMARY OF MEASURED AND PREDICTED EMISSION RATES FOR THE CINCINNATI MDS INCINERATOR

Pollutant case	Emission rate, g/s			
	Receiving	Feed	Storage	Total
Chloroform				
Measured	8.3E-4	1.0E-3	2.3E-3	4.1E-3
Expected ^a	4.0E-2	3.6E-2	7.6E-2	1.5E-1
Predicted 95% limits ^a	1.4E-2 to 1.2E-1	1.8E-2 to 7.2E-2	3.7E-2 to 1.5E-1	6.9E-2 to 3.4E-1
Expected ^b	4.4E-2	3.9E-2	8.2E-2	1.7E-1
Predicted 95% limits ^b	1.2E-2 to 1.6E-1	1.8E-2 to 8.8E-2	3.7E-2 to 1.8E-1	6.7E-2 to 4.3E-1
Expected ^c	4.3E-2	3.4E-2	7.1E-2	1.5E-1
Predicted range ^c	1.1E-2 to 1.6E-1	1.4E-2 to 8.5E-2	2.9E-2 to 1.8E-1	5.4E-2 to 4.3E-1
Hexachloroethane				
Measured	2.5E-7	3.0E-7	7.1E-7	1.3E-6
Expected ^a	1.2E-5	1.1E-5	2.3E-5	4.6E-5
Predicted range ^a	4.1E-6 to 3.6E-5	5.6E-6 to 2.2E-5	1.1E-5 to 4.6E-5	2.1E-5 to 1.0E-4
Expected ^b	1.3E-5	1.2E-5	2.5E-5	5.0E-5
Predicted range ^b	3.7E-6 to 4.8E-5	5.3E-6 to 2.7E-5	1.1E-5 to 5.6E-5	2.0E-5 to 1.3E-4
Expected ^c	1.3E-5	1.0E-5	2.2E-5	4.5E-5
Predicted range ^c	3.5E-6 to 4.9E-5	4.1E-6 to 2.6E-5	8.7E-6 to 5.4E-5	1.6E-5 to 1.3E-4

^aEmission estimates using narrow ($\pm 1\%$) waste-parameter error bounds and refining-industry emission factors.

^bEmission estimates using wide (factor of two) waste-parameter error bounds and refining-industry emission factors.

^cEmission estimates using wide (factor of two) waste-parameter error bounds and SOCM industry emission factors.

coefficient of one), any change in chemical concentration in the waste would result in a proportional change in the predicted vapor concentration. This potential variability was not included in the methodology because emission measurements of each chemical were obtained similarly, i.e., total hydrocarbon calibrated to methane was measured, and individual chloroform or hexachloroethane release rates were then estimated based on concentrations in the waste.

Effect of SOCM Versus Refining Emission Factors

To determine the effect of using SOCM versus refining industry emission factors on emission predictions, release rates for the same three facility areas and POHC's were calculated (Table 5). Results show that both the mean and the lower 95% confidence limit are reduced for each area when SOCM emission factors are employed. This reduction is small (less than 20%) however, implying that emission factors alone are not the cause of measurement-prediction discrepancies.

Comparison of Measured to Predicted Emission Rates

Measured fugitive emission rates by area for an incinerator located in Cincinnati (Staley *et al.*, 1983 [8]) are outside the 95% confidence bounds of all predicted values (Table 5). Earlier work (Holton *et al.*, 1982 [5]) suggested that measurement-prediction differences were due to inappropriate emission factors. Table 5 shows however, that, although some difference occurs between use of SOCM versus refining industry emission factors, predictions do not agree with measured values. In fact, using the SOCM emission prediction distributions, measured values lie seven standard deviations from the mean. A possible reason for this difference is that the Cincinnati incinerator is new, well operated, and maintained. Consequently, emission factors developed for an entire industry may not be appropriate for this facility. However, measurement data reflect only a few days of operation (not annual operation). Thus, conclusions based on these data must be made cautiously, as they can not be tested until further data are available. USEPA has recognized this shortcoming and is currently gathering additional data.

CONCLUSION

The ability to predict the possible range of fugitive VOC emissions is an important step to increase understanding of controlling processes. Quantification of emissions as a function of physicochemical variables could prioritize future research and/or explain existing facility emission phenomena.

Several conclusions can be drawn from the results. Analyses which summarize fugitive emissions by both area and equipment type provide useful information. Area emission summaries provide information for sampling, modeling, and analysis. Equipment emission summaries show where the largest potential benefit from future research could occur.

Estimates of expected fugitive emissions have a large effect on predictions of the most exposed, close-in portion of the populations. This means that resolving differences between measurements and prediction methodologies is particularly necessary. This analysis showed that additional research to improve error bounds and distributions of waste parameters may not be necessary, for they contribute little to the overall variation in prediction; only an adequate analysis to determine mean waste properties is suggested. Error bounds of individual chemical concentrations can not be ignored, however.

Estimates of fugitive emissions are also relatively insensitive to choice of emission factors. Use of SOCM emission factors and error bounds reduced emission estimates about

10% from those obtained using refining values. Non-agreement with measured values was little improved using SOCM estimates.

Application of error and Monte Carlo analyses revealed a potentially wide variability in fugitive emissions; each area exhibited over a ten-fold difference between 95% confidence limit predictions and a potential hundred-fold difference in specific sources (equipment). This means that some averaging for each area is occurring within the methodology. For a given simulation, some valves or pumps within an area may be predicted to be leaking large amounts, but these leak rates are offset and averaged-out by other pieces of equipment leaking very little. Consequently, measurements taken over a short period of time may not reflect any dominating, large emission sources (which was the case at the Cincinnati incinerator). This implies the need for a more extensive measurement data base over longer periods of time to adequately test the emissions prediction methodology.

LITERATURE CITED

1. Buffalo Tank Division, Bethlehem Steel Corporation, *Vendor Tank Information, Booklet 33-21c*, Towson, Maryland (1981).
2. Carney, J. H., R. H. Gardner, J. B. Mankin, and R. V. O'Neill, "SEAP: A Computer Program for the Error Analysis of a Stream Model, Monte Carlo Methodology and Program Documentation," ORNL/TM-7654, Oak Ridge National Laboratory, Oak Ridge, Tennessee (1981).
3. Dean, J. A., Ed., *Langes Handbook of Chemistry*, Eleventh Edition, McGraw-Hill Inc., New York, New York (1973).
4. Harrington, E. S., G. A. Holton, and F. R. O'Donnell, "An Initial Emission Assessment of Hazardous Waste Incineration Facilities," *Proceedings, 1982 UCC-ND and GAT Environmental Protection Seminar*, Gatlinburg, Tennessee, CONF-820418 (1983).
5. Holton, G. A., F. R. O'Donnell, C. C. Travis, and L. J. Staley, "Impact of Fugitive Volatile Organic Compound Emissions from a Municipal Hazardous Waste Incinerator on the Surrounding Community," *Proceedings on Fugitive Emissions: Measurement and Control*, Charleston, South Carolina (1982—in press).
6. Perry, R. H. and C. H. Chilton, *Chemical Engineer's Handbook*, Fifth Edition, McGraw-Hill Inc., New York, New York (1973).
7. Reid, R. C., J. M. Prausnitz, and T. K. Sherwood, *The Properties of Gases and Liquids*, Third Edition, McGraw-Hill Inc., New York, New York, (1977).
8. Staley, L. J., G. A. Holton, F. R. O'Donnell, and C. A. Little, "An Assessment of Emissions from a Hazardous Waste Incineration Facility," *Incineration and Treatment of Hazardous Waste: Proceedings of the Eighth Annual Research Symposium*, Ft. Mitchell, Kentucky, March 8-10, 1982, EPA-600/9-83-003, U.S. Environmental Protection Agency, Cincinnati, Ohio (1983).
9. Thibodeaux, L. J., *Chemodynamics*, John Wiley & Sons Inc., New York, New York (1979).
10. U. S. Environmental Protection Agency, *Organic Chemical Manufacturing, Volume 3: Storage, Fugitive, and Secondary Sources*, EPA-450/3-80-015, Office of Air Quality Planning and Standards, Research Triangle Park, North Carolina (1980).
11. U. S. Environmental Protection Agency, *Project Summary—Assessment of Atmospheric Emissions from Petroleum Refining*, EPA-600/S2-80-075, Office of Environmental Engineering and Technology, Research Triangle Park, North Carolina (1981a).
12. U. S. Environmental Protection Agency, *VOC Fugitive Emissions in Petroleum Refining Industry—Background Information for Proposed Standards*, EPA-450/3-81-015a, Office of Air Quality Planning and Standards, Research Triangle Park, North Carolina (1981b).
13. U. S. Environmental Protection Agency, *Fugitive Emission Sources of Organic Compounds—Additional Information on Emissions, Emission Reductions, and Costs*, EPA-450/3-82-010, Research Triangle Park, North Carolina (1982).
14. Weast, C. C. (Ed.), *Handbook of Chemistry and Physics*, 54th Edition, CRC Press, Cleveland, Ohio (1973)



Gregory Holton is Manager and Senior Scientist of the Hazardous Waste Program in the Environmental Technology and Waste Management Division of The MAXIMA Corp. He obtained a B.S. from the United States Military Academy in 1970 and was a commissioned officer on active duty in the U.S. Army for five years. From 1977 through 1980, he was a consultant to Research Triangle Institute in North Carolina and to the Environmental Resources Group in Virginia. He most recently was a Research Associate with the Health and Safety Research Division of Oak Ridge National Laboratory, from 1980 through 1983, prior to accepting his current position with MAXIMA. A major in the U.S. Army Reserve, he received an M.S. (1977) and a Ph.D. (1981) in environmental engineering from the University of North Carolina. His principal research interest involves the study and design of innovative technologies to process recyclable or hazardous materials. He is a member of the American Chemical Society and the Air Pollution Control Association.



Curtis C. Travis is an applied mathematician, is in the Office of Risk Analysis of the Health and Safety Research Division of Oak Ridge National Laboratory. He received his Ph.D. degree in applied mathematics from the University of California, Davis, in 1971. From 1971 to 1976 he held academic positions at Vanderbilt University and the University of Tennessee. His principal research interest involves the development and evaluation of mathematical models to estimate human health effects of energy technologies. He has also studied the health effects of a large coal liquefaction facility and of hazardous chemical incineration; the health and safety aspect of wood-burning stoves; and the environmental transport, dosimetry, and health effects of tritium and cadmium.

The Environmental Representative Program

Establishment of a group of environmentally trained plant personnel is aimed at preventing fines, citations, and negative publicity.

Bruce P. McLeod, Monsanto Company, Inc., Pensacola, Fla. 32575

It is believed that an Environmental Representative Program would improve the regulatory compliance status of any large plant. Given the normal situation, when the plant environmental staff is not large enough to physically inspect the entire facility daily, they must rely on operations personnel to achieve compliance. Therefore, a good deal of the daily compliance assurance depends on the actions of people with no formal environmental training.

The need for environmentally knowledgeable plant personnel is becoming increasingly more important. Miscommunications between the environmental staff and plant operations personnel is a danger as new regulations are created and existing regulations are made more complex. A miscommunication could result in fines, citations, or negative publicity. The Environmental Representative Program is one solution to this concern.

Unlike typical quality or safety programs which must endeavor to reach every plant employee, relatively few plant personnel directly affect environmental compliance status. This is fortunate in that a much smaller awareness training program can be used with plantwide effects.

The keys to maintaining a plantwide state of ongoing compliance is a daily knowledge of individual emission source status and input into operation decisions affecting compliance security. It is fairly obvious that the environmental staff could never match the effectiveness of the operations and process engineering groups in these areas. Those groups possess real time knowledge and an ability to directly influence environmental compliance which cannot be surpassed. Therefore, the solution to this situation, to be effective, must involve the operations and process engineering groups. This is precisely what the Environmental Representative Program is designed to do.

The Environmental Representative Program can be divided into two segments as follows:

A. PROGRAM INITIATION

1. General Considerations

2. Representative Selection
3. Authorization by Management
- B. PROGRAM IMPLEMENTATION
 1. Requirements Training
 2. Responsibilities Development
 3. Incorporation into Annual Goals
 4. Program Maintenance

Goal and Desired Result

The goal of the program is on-going daily compliance assurance. This goal is selected to achieve a result of no fines, citations, or negative publicity because of out-of-compliance situations.

Following is a discussion of how each part of the program is accomplished.

PROGRAM INITIATION

General Considerations

The initiation segment is by far the most important and challenging part in the establishment of an Environmental Representative Program. Let's examine three reasons why this is so.

First, the plant personnel have very little knowledge of environmental matters in general. An "environmental program" may appear to be unnecessary work for them.

Second, the program is plantwide in scope, crossing many operating area boundaries. Environmental concerns and department organization will differ between departments.

Third, a substantial amount of communication, both formal and informal, will be necessary with plant supervisory personnel at all levels. This is needed to allow them to knowledgeably support the program.

The program goal and desired result must be kept clearly in focus. The Program Coordinator should be just

as concerned about keeping the responsibilities assigned to the representatives within the intent of the goal statement as he or she is in making sure that goal is adequately addressed. If the Coordinator desires to increase representative involvement, a more comprehensive goal should be selected. Plant support for the program will be reduced if responsibilities are given to the representatives that are outside the scope of the program.

A good first step by the Program Coordinator is to discuss the program informally with the plant area supervision. The primary purpose of these discussions should be to solicit their opinion concerning environmental compliance assurance needs. This meeting should also be used to increase the supervisors' awareness of the environmental requirements in their area and to describe the Environmental Representative Program concepts.

During the same period in which the Program Coordinator is contacting area supervisors, the coordinator's supervision should be informally briefing upper management about the program concepts. This will anticipate and prevent misinformation from reaching the plant superintendents from their supervisors.

Once the suggestions of the supervisors are incorporated into the program, planning for representative selection and management authorization can be completed. The discussions with the supervisors will promote their support and will provide them with an understanding of the program. This is necessary for effective completion of the representative selection step. Additionally, incorporation of the supervisor's suggestions will be a selling point to management. Before the superintendents are likely to fully endorse the program they will want to know what their supervisors think about it. Being able to make the statement that many plant supervisors support the program will prevent unnecessary resistance.

Representative Selection

A general organization chart will be an important tool in deciding how many representatives are needed. Here the coordinator can influence the number and size of areas represented, to reflect his or her personal experience. This can be done by depicting the organization by significant environmental areas rather than by function or personnel factors.

Some important considerations are the frequency of environmental concerns in an area, the interplant communication limitations, and specific area items that need closest surveillance. These concerns can be addressed in the development of the organizational chart.

Generally, it will be necessary to have at least one representative in each operating area. The reason is that communications within an area are well developed, while there may be no routine communications between areas. Since the Environmental Representative Program is primarily an information transmittal network, designing the program to avoid communication obstacles is critical.

Management will respond to the need for representation according to the information presented in the organization chart. At this point, selection of specific representatives and the exact number is best left up to the plant supervisors and superintendents to decide. Many factors, such as current staffing levels, personnel experience, individual representative interest in the program will affect the selection process. This is one area in the program initiation segment where the efforts of the plant organization cannot be surpassed by the Program Coordinator or the environmental staff.

Representative selection is done by plant management at the superintendent level. Transmittal of the names of the people designated to be representatives should be done in writing from the superintendents to the Program Coordinator with copies to the representative and all intermediate supervision. This will insure that all levels of

management, as well as the representatives themselves, know that the commitment of time and talent has been authorized.

Authorization by Management

Attainment of two goals is sought in this segment:

1. Authorization of the program by the plant manager.
2. This authorization clearly indicated to all plant superintendents.

The Environmental Representative Program is likely to be perceived as an additional assignment to the plant manufacturing and technical groups. The overall effect of the program results in about the same level of area environmental involvement, but now that effort is focused. Heretofore the interaction of the plant environmental staff with the plant was diffuse and random, depending on the problem at hand. The result is better effectiveness for both the environmental staff and the plant personnel.

A recommended method for obtaining authorization for the program by the plant manager is to prepare a formal presentation to the plant manager and staff. The organizational chart discussed above is used. Four areas should be covered:

1. The reason why an Environmental Representative Program is needed.
2. The plant departments to be included in the program.
3. A description of how the program will be implemented.
4. The specific task of the superintendents upon leaving the staff meeting (i.e., to select the representatives for their areas and transmit those names in writing to the Program Coordinator).

PROGRAM IMPLEMENTATION

Requirements Training

This is a time intensive step for the Program Coordinator and his or her secretarial support. Each representative will receive copies of all the pertinent environmental information relevant to his or her area. These materials are likely to be:

- Applicable air pollution permits
- Plant waste disposal procedures
- The Spill Prevention Control and Countermeasures Plan (SPCC)
- Other "spill" or emergency response procedures
- The plant Effluent Permits

Binders should be prepared to contain these materials even if they are available separately in existing plant procedures manuals. The author has used printed notebooks with the title "ENVIRONMENTAL REPRESENTATIVE RESOURCE BOOK." This "book" quickly becomes an invaluable receptacle for other important environmental memos and documents. The benefit of the "Resource Book" is that it remains in the operating area permanently, thereby preserving important environmental information for the area. This information is undisturbed by operations or environmental staff personnel movements.

The Environmental Representative is given the resource book after receiving a thorough review of the information. The representative will then need to study the information and develop a general understanding of it.

At this point the representative will be responsible for completion of the responsibilities development items.

Responsibilities Development

With a general understanding of the environmental permits and procedures, the first task of the representative is to summarize the environmental requirements of his or her area. These requirements, once reviewed by the Program Coordinator, become the first addition to the Environmental Representative Resource Book.

Once the area requirements are defined, the represent-

ative must develop the responsibilities that he or she will assume to achieve the program goal of "daily compliance assurance." These responsibilities will vary depending on the area and therefore the level of responsibility will be different for each representative. These responsibilities will be reviewed by the Program Coordinator for adequacy in meeting the program objectives. The Coordinator will modify the responsibilities, with the input of the representative, as needed.

Since the goal of daily compliance assurance is rather all encompassing, another way to assess the adequacy of the responsibilities is by measurement against the best case result, that being "receive no fines, citations, or negative publicity because of out-of-compliance situations."

It is recommended that the representative be requested to issue the requirement and responsibility summaries formally, with the distribution to include the Program Coordinator, the representative's supervisor, and personnel up to the superintendent level. This accomplishes two things. First, it informs the representative's supervisor of the time commitment being made to compliance assurance. Secondly, it provides feedback to upper management of the progress of the program.

Responsibilities development is another time consuming phase for the Program Coordinator. Two meetings, probably three, will be required with each representative individually. One-on-one review meetings are recommended rather than group meetings. This task will be an unfamiliar one for the representatives and will require the environmental knowledge and experience of the Coordinator on an individual basis. It is believed that the commitment of the Program Coordinator to the program goals and their timely completion is critical at this step.

At the completion of the resource book review session, the timetable for requirements and responsibilities completion should be set. Two weeks per task is probably adequate. Follow up meetings with each representative specifying the date and time should be set at the resource book review session. These sessions should be held regardless of the degree of completion of the representative assignments. Additional meetings at two week intervals can be added as needed until the requirement and responsibility documents are acceptably completed.

Incorporation Into Annual Goals

With the above items completed, full implementation of a continuing representative program is accomplished by incorporation of a compliance assurance goal into the annual goal planning document of each representative. That statement can be as simple as "Perform the responsibilities of the area Environmental Representative."

Program Maintenance

A very favorable aspect of the Environmental Representative Program is its self-renewing design and the small amount of continuing environmental staff time needed to keep the program ever green. One reason for this is because improvements in compliance assurance by the rep-

resentatives is influenced by the degree of knowledge and experience that they possess. As the representatives grow in ability and expertise in their jobs, they are at the same time improving their ability to assure daily environmental compliance.

Some level of continuing involvement by the Program Coordinator or environmental staff is very necessary. Several activities are very useful in maintaining contact with and an information flow of current environmental concerns to the representatives. All of these take very little additional time:

1. Send a copy of the Environmental Staff Monthly Report to each representative.
2. Develop a standard form for use by the environmental staff to inform the representatives of scheduled agency visits and important environmental developments.
3. Place the representatives on distribution for spill or environmental incident reports that occur in their area.

An annual or biannual meeting of the representatives and environmental staff members should be held. This will provide an opportunity to give special recognition of good representative performance and restatement and reemphasis of program goals. An evaluation and feedback of the past compliance results and areas of improvement is in order. Feedback from the representatives should be solicited.

Daily interface with the representatives and plant operating personnel should build up the status of the representative. Policing of the representatives is unnecessary as they will be held accountable for compliance status the same as the environmental staff.

To promote and facilitate the expert status of the representatives, they should receive copies of all environmentally related correspondence relevant to their area. The areas should be encouraged to interface directly with the representatives. Where appropriate, the representative may serve as a liaison between the environmental staff and the plant.

Conclusions

With an Environmental Representative Program in place, compliance assurance will be enhanced. This occurs because of a leveraging of environmental staff manpower. Environmental activities will be more effectively conducted due to involvement of plant personnel and a focused interaction between the environmental staff and operations.



Bruce P. McLeod is an environmental specialist in the permitting and compliance group at Monsanto's Pensacola plant. This plant is considered to be the largest unified nylon 6,6 production facility in the world. He holds a B.S. Chemical Engineering degree from the University of Wisconsin. He is a registered professional engineer in Florida. His experience consists of five years as a process engineer in nylon chemical intermediates and most recently five years in environmental regulatory affairs activities. He is a member of the AICHE.

Recovery Process for Complexed Copper-Bearing Rinse Waters

A state-of-the-art review of the advantages and disadvantages of currently available technologies.

R. M. Spearot and J. V. Peck, OMI International Corp., Warren, Mich. 48089

The presence of complexing agents in waste solutions increases the difficulty of removing heavy metals, such as copper. This fact is of vital importance to the metal finishing industry because of the growth in the use of printed circuit boards for consumer products and telecommunications equipment, and to the growing utilization of plated plastics for shielding electronic enclosures such as office equipment and personal computers. These growth markets require electroless copper which means that the waste solutions will contain significant levels of an organic complexing agent such as EDTA or Quadrol. One consequence of these developments is that it is becoming increasingly difficult for many manufacturers to meet existing and proposed requirements for the amount of copper discharged to publicly owned treatment works (POTW) or to receiving surface waters.

The EPA regulations for the Metal Finishing Industry, which were finalized July 15, 1983, set the copper pretreatment standards for new and existing metal finishing sources at a maximum for any one day of less than 3.38 milligrams per liter (mg/liter) copper and a average monthly, which shall not exceed 2.07 mg/liter copper.

For existing job shop electroplaters and printed circuit job shops, the pretreatment standard is 4.5 mg/liter maximum for any one day and 2.7 mg/liter for the average of 4 consecutive monitoring days. However, many POTW's and receiving streams have required limits for copper much more stringent than EPA Guidelines, and values of <0.1 mg/liter copper occasionally must be met.

Treatment methods for electroless copper rinse waters depend greatly on the particular copper complexing agent used in the electroless copper process. Treatment methods to be discussed are grouped into three categories, chemical, physical, and electrochemical. The chemical methods include substitution, reduction of the metal ion, oxidation of the complexor, and ion exchange. The physical methods are evaporators and reverse osmosis. The electrochemical methods are electrolytic plate out, electrowinning and electrochemical displacement.

BACKGROUND

The advantages of using electroplated plastics over their metal counterparts include more freedom in part design, reduced weight, lower raw material costs, and the elimination of costly surface preparation operations such as polishing and buffing.

Although many plastics can be plated, adhesion varies widely. Only those which provide the best adhesion are used for electroplating applications. The basic electroplating cycle for plastics is divided into two stages. The first stage is called the preplate cycle. The purpose of this

cycle is to provide an adherent, conductive metallic film on the surface of the plastic part so that the second stage, electroplating the decorative or functional finish, can be added by conventional electroplating technology.

The last step of the preplate cycle is to cover the surface with a thin layer of nickel or copper. This layer is deposited autocatalytically from an electroless solution, which contains the nickel or copper salt, a reducing agent, a complexing agent, a stabilizer, and a pH buffering system. The chemistry of this electroless solution is such that the copper or nickel is reduced spontaneously as the catalyzed plastic surface contacts the solution, and a very thin uniform metallic coating is then formed. In many applications, a copper deposit is preferred to a nickel deposit due to its superior adhesion, ductility, corrosion performance under both wet and dry conditions, and its electrical properties.

The nature of the electroless copper plating solution is such that the copper ion is held in solution by the complexing agent until a catalyst initiates the action of the reducing agent. Hence, any solution going to waste treatment that is pulled out of the bath through surface tension, or lost due to spills or bath dumps, will contain the metal ion tightly held in solution by the complexing agent. The complexing agent is used in molar excess to ensure that the metal ion is not reduced, and thus precipitate out of solution under normal operating parameters.

The two principal complexing agents predominantly used in electroless copper solutions are EDTA (ethylenediaminetetraacetic acid) or Quadrol (N,N,N',N'-tetrakis (2-hydroxypropyl)-ethylenediamine) as shown in Figures 1 and 2.

The complexing agent, because of its nature, will complex with cations in other effluent streams. Thus, it is obligatory that the electroless copper effluent stream be segregated from other plant wastes and treated separately to remove the copper. The concentration of the copper in the stream is usually too high to be suitable for direct discharge. Restrictions usually do not apply regarding the discharge of organic complexing agents, since these organic compounds are biodegradable in the presence of light.

CHEMICAL TREATMENT METHODS

Chemical treatment methods for electroless copper, which are traditionally used in industry to remove the copper, generate voluminous amounts of sludge, require costly capital expenditure, and are labor-intensive. The treatment of electroless copper-containing rinse wastes of either EDTA or Quadrol have been thoroughly discussed by Wing [1].

Wing *et al.* found that these complexes can be treated

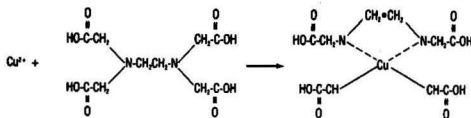


Figure 1. EDTA-Cu complexing-reaction mechanism.

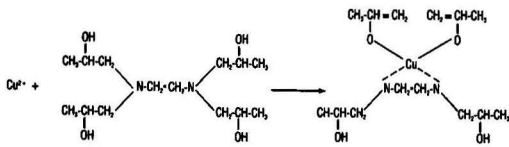


Figure 2. Quadrol-Cu complexing-reaction mechanism.

with calcium hydroxide, calcium oxide, calcium chloride, or calcium sulfate at a pH of 11.6 to 12.5. However, to effectively reduce copper to a concentration of less than 1 mg/liter from an original concentration of 50 mg/liter, a large excess of calcium is required (up to 15X stoichiometric excess). This is because the equilibrium constant, k , for the equation was found to lie between 5.6 and 14.0 (with a mean of 10), thus providing a rough measure of the amount of calcium required for adequate copper displacement.

This calcium treatment is not effective for Quadrol-copper complexes. The copper displaced from the complex precipitates from the solution as copper hydroxide.

Another effective method of displacing the copper from the EDTA or Quadrol complex is to lower the pH to between 2.7 and 5.0 and add ferrous sulfate or ferric chloride. The reduction in pH weakens the copper complex bond and facilitates the substitution of the copper for iron. Approximately one gram of ferrous sulfate or ferric chloride was added per 50 mg of copper present, indicating a 7X stoichiometric excess of iron is necessary to displace the copper. The pH was then raised to 9.0, using lime or caustic, and the precipitated copper hydroxide filtered from the solution.

The high pH, calcium substitution treatment procedure and the iron substitution procedure reduce the copper concentration to an acceptable level for discharge. However, large amounts of sludge which require disposal are generated.

The copper has also been removed from the complex by using strong reducing agents such as sodium hydrosulfite, Kamperman [2], or sodium borohydride, Jula [3]. Sulfide precipitation of the copper is also discussed by Scott [4] and Anderson and Weiss [5]. All these processes, however, generate a sludge that has to be disposed of in an environmentally acceptable manner.

Further work carried out (shown in Table 1) indicates that these methods produced only partially acceptable re-

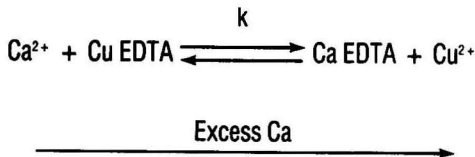


Figure 3. Equilibrium equation for EDTA-Cu-Ca.

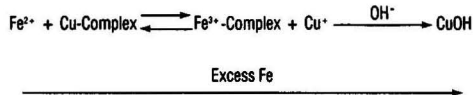


Figure 4. Equilibrium equation for copper removal using iron.

TABLE 1. COPPER REMOVAL FROM EDTA OR QUADROL COMPLEX USING SODIUM HYDROSULFITE AND SODIUM BOROHYDRIDE

Technology	EDTA* mg/liter	QUADROL* mg/liter
Sodium hydrosulfite	7.2	0.46
Sodium borohydride	14.0	2.4

* Initial copper concentration 50 mg/liter.

sults for copper removal from solutions containing initially 50 mg/liter of copper.

If the organic complex is destroyed by oxidation techniques, the copper-containing stream may then be mixed with other plant effluent streams for conventional treatment. Cullivan [6] has investigated the economics of using either chlorine or ozone to oxidize large quantities of organic containing effluents. However, this survey was for large quantities of organic containing wastes. For electroless copper containing wastes it would prove uneconomical. Work carried out in our laboratory, using sodium hypochlorite to oxidize the EDTA or Quadrol, prior to copper precipitation using lime, yielded less than 60% removal of the copper from an initial concentration of 50 mg/liter copper to 22.4 mg/liter for the EDTA and 16.7 mg/liter for the Quadrol based solutions, respectively.

The addition of UV activation to the ozone oxidation process has been investigated by Prengle and Mauk [7], who found that promising oxidation of the organics occurred. Macure *et al.* [8], further discussed the ozone/UV destruction of EDTA. This method is currently in commercial use. However, it is important, during the ozone/UV process, to remove the copper as it is released from the complex. If this is not done, the released copper will selectively initiate the ozone degradation, and thus no oxidation of the EDTA will occur. In general, oxidation of the organic complex is not a practical method of treating an electroless copper waste stream.

Ion exchange can be used as a method to remove copper from a complexed solution, thus rendering the solution depleted in copper and able to be discharged directly. Development of suitable ion exchange techniques has been delayed because the specialty resins required to remove the copper have only recently been available for industrial use.

The resin used to remove the copper has to be a powerful complexing agent which will selectively remove the complexed copper from the copper complex compound in the electroless copper effluent. A process has been recently developed by Courduvelis *et al.* [9], and Whalen [10], using a resin with an iminodiacetic acid functional group.

This resin has been found to remove copper from a variety of complexing agents such as carboxylic acid and alkanolamine type compounds.

However, no separation of copper takes place in the presence of ethylenediaminetetracetic acid (EDTA), and other amino acid type complexing agents.

This result appears to agree with the expectation based on the respective complex equilibrium constants [10], shown in Table 2.

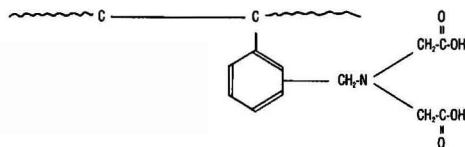


Figure 5. Polystyrene-bearing iminodiacetic-acid functional groups [10].

TABLE 2. RELATIVE STRENGTH OF EQUILIBRIUM CONSTANTS FOR COPPER WITH VARIOUS COMPLEXING AGENTS [10].

Complexing Agent	Equilibrium Constant k
EDTA	$10^{18.8}$
Iminodiacetic acid	$10^{10.55}$
Tartaric Acid	$10^{9.9}$

The efficiency for copper separation from Quadrol is greater in an acidic solution, pH = 2.7-7.0, than it is in an alkaline solution. When the resin is exhausted, it is regenerated with dilute sulfuric acid, which redissolves the copper retained on the resin. Thus, copper bearing acid solution can then be treated by conventional hydroxide precipitation, or the copper can be plated out and the acid recycled to be used in the next regeneration sequence. As with most ion exchange procedures, copper removal is extremely sensitive to process variables such as pH, flow rate, copper loading, and temperature.

Starch-based products, such as Insoluble Starch Xanthate (ISX) have been developed by Wing [1] and are presently commercially available. ISX acts as an ion exchange material, removing the copper ions from the stream by exchanging them for sodium and magnesium ions. ISX can be used in the solid form for batch operations and as a slurry or filter precoat for continuous operation. Since a pre-coated filter is required to remove the solid following the batch operation or the slurry during continuous operation as sludge is generated. This sludge must be disposed of in an environmentally acceptable manner. Application of ISX is most effective as a polishing or secondary treatment, where the initial copper concentration is approximately 10 mg/liter. Plant operations have yielded copper reductions to as low as 0.02 mg/liter.

Currently, only one technology exists which can successfully recycle the copper complex to the bath. This process is detailed by Zeblicky [11], and is only applicable for alkanolamine and copper-alkanolamine type complexes such as (ethylenedinitro)-tetra-2-propanol, triethanolamine, ethylenedinitrotetraethanol, nitrilotri-2-propanol, etc., which can protonate and therefore have a net positive charge. At high pH values, these complexes will deprotonate and become species with no electrical charge, as shown in Figure 6.

The free ligand also reacts in a similar way. Therefore, the complex copper and ligand in an alkanolamine type electroless copper bath such as (ethylenedinitro)-tetra-2-propanol can be removed and recovered from waste electroless copper solutions using a cationic exchange system. The pH of the waste electroless copper bath is lowered to form the cationic copper-complexor species. The copper-complexor is retained on a cationic exchange resin and then reclaimed from the resin, either by using standard resin regenerating techniques or by raising the pH of the resin bed with hydroxide. Raising the pH of the resin bed reclaims the copper complex by converting the complex to a zero charged species and releasing it from the ion exchange resin in a form suitable for additions to an electroless copper bath. This process is shown schematically in Figure 7.

An alternative method of regenerating the Cu-Quadrol complex is to pass sulfuric acid over the loaded resin, and

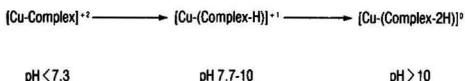


FIGURE 6. Effect of pH on Copper Complex Charge

Figure 6. Effect of pH on copper-complex charge.

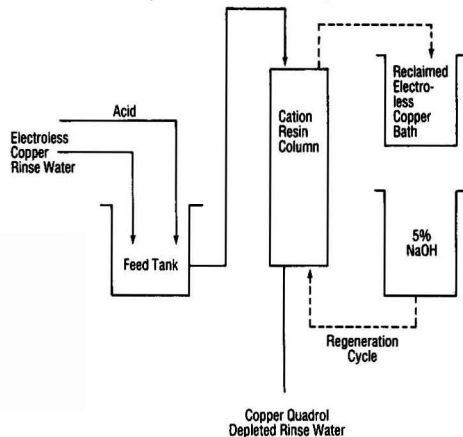


Figure 7. Schematic for copper-Quadrol recovery [11]

then wash the copper complex from the resin, using water. The process is used mainly to reclaim Cu-Quadrol from concentrated solutions and not from rinse water. The Cu-EDTA-type complex does not protonate on pH change; thus, this process is not applicable. If the pH of an EDTA-Cu bath is lowered to a pH of 2.5, the EDTA-Cu complex dissociates and the EDTA separates to form a lower layer. The EDTA can be thus recovered and reused to replenish the bath EDTA concentration. The resulting supernate is an acidic solution containing large amounts of copper and small amounts of EDTA. Depending upon the degree of copper removal required, the solution should be segregated from other plant effluents so that it can be treated, using techniques discussed previously.

PHYSICAL TREATMENT METHODS

Physical treatment techniques, such as evaporation or reverse osmosis, cannot be used to concentrate the dilute electroless copper effluent stream to give a concentrate which can be returned to the electroless copper bath. This is because changes in bath chemistry can be anticipated on reconcentration, which could initiate copper deposition, thus rendering the recovery equipment inoperative. Also, the electroless copper bath is extremely sensitive to contaminant build-up. The return of recovered concentrate back into the bath will be accompanied by the return of recovered contaminants, and operation of the bath will become increasingly difficult.

ELECTROCHEMICAL TREATMENT METHODS

A variety of electrochemical processes have been developed to remove the copper. These are either by electrolytically plating out the copper as a copper sheet by Stewart *et al.* [12], or by electrowinning by DasGupta *et al.* [13] and Toller [14]. However, the effluent, as a result of these processes, normally has a copper concentration of between 10-50 mg/liter. We have developed a method by which the copper is selectively removed from a solution containing copper in a complexed form by electrochemical displacement, Arcilesi *et al.* [15]. The mechanism of the removal is shown in Figure 8. The process is shown schematically in Figure 9.

The electroless copper containing rinse water flows into a feed tank in which the pH is adjusted by the addition of acid to the optimal level for selective electrochemical displacement. The residence time allowed in the feed tank permits adequate blending. The pH-adjusted rinse water

TABLE 3. SUMMARY OF FIELD RESULTS

Time in Service	8 Hours	40 Hours
Canister #1	0.5 mg/liter	1.5 mg/liter
Canister #2	0.05 mg/liter	0.05 mg/liter

is then pumped through a pair of filter media-containing canisters in which the copper is selectively removed from the solution and replaced by a metal complex. The use of the canisters in series is alternated to optimize the removal media use. The majority of the copper is removed in the first canister and the stream is polished in the second canister. Removal rates of greater than 90% are achieved in each canister.

Field results to date indicate that copper is removed to a level of less than 1 mg/liter from an initial level of 100 mg/liter from solutions such as EDTA copper, Quadrol copper, Tartrate copper, pyrophosphate copper, ammonium persulfate etch, and peroxide sulfuric copper etch.

The results are summarized in Table 3.

The results were achieved on a solution of electroless copper rinse water* with an initial copper concentration of 58 mg/liter at a flow rate of 5 GPM, at a pH of 4, and an ambient temperature. Six pounds of copper was removed in the forty-hour period. When the copper concentration exiting the lead canister exceeds 4 mg/liter, its media is replaced and the flow through the canisters is alternated to make this the second canister in the series. The copper plated base metal is classified as non-hazardous and the media can be either sold or disposed of as scrap metal.

The effluent from this process still contains complexor and must be segregated from other plant waste streams until they have been treated prior to discharge.

The equipment** for this process is shown in Figure 10. The unit is skid mounted, prepiped, and prewired for easy

* UDIQUE® 820.
** CUPRATROLLER™

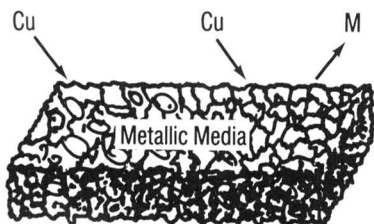


Figure 8. Selective electrochemical-displacement mechanism.

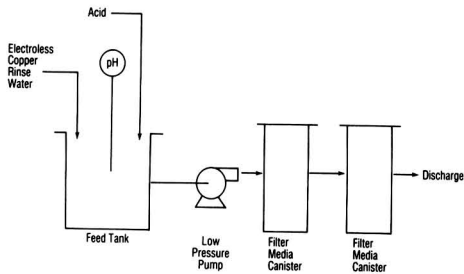


Figure 9. Schematic of copper-removal process.

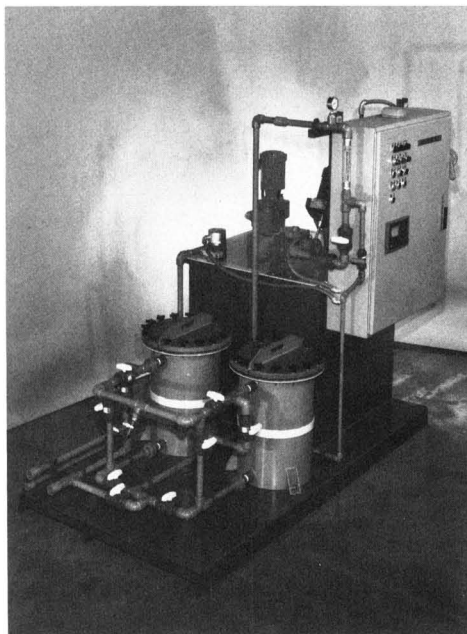


Figure 10. Apparatus to remove copper from copper-containing complexed solutions [15].

installation. The only hook-ups that have to be made are electroless copper waste waters, city water for intermittent flushing of the canisters, and a line to take away the effluent from the equipment; also required is an electrical hook-up to the panel of 440 volt, 3 phase power.

DISCUSSION

The main disadvantages of current waste treatment methods for copper removal are the following:

- Calcium or iron displacement produces large amounts of hazardous sludge which must be disposed of in classified landfills. The costs for hazardous landfill are increasing daily, and even though the calcium or iron displacement methods are very effective on treating certain electroless copper waste streams, it can be seen that, in the future, processes which produce large amounts of sludge will actually become a liability to the companies using them.
- Sodium borohydride and sodium hydrosulfite, when used to effect copper removal, both prove to be costly from the chemical and process viewpoint, as well as producing a sludge which has to be disposed of in an environmentally acceptable manner.
- Destruction of the complexing agent is not economical for small quantities of rinse, and it is not effective on all copper complexes.
- Removal of the copper by ion exchange is not an effective method on all electroless copper streams and the regenerant still requires further processing to remove the copper.
- ISX is an effective copper removal method, but only becomes cost effective as compared to other known methods for final polish water containing less than 10 mg/liter of copper.
- The recycle of the copper complex using ion exchange is presently only applicable to copper Quadrol solutions; it is not effective on dilute streams, and has an extremely high operating cost

due to the complexity of the process and the equipment that has been developed.

- Recycle of the copper using evaporation or reverse osmosis is ineffective because it cannot be used on dilute streams and upsets the bath chemistry by returning recovered contaminants.
- Removal of the copper by most electrochemical techniques requires equipment that has a high capital cost. Also, the efficiency of these processes is very low at very low concentrations of copper.

The advantages of copper removal using selective electrochemical displacement are:

- Selective electrochemical displacement is effective on any copper containing stream.
- It is a simple direct copper removal method.
- The copper plated onto the base metal can be classified as non-hazardous for disposal purposes and may be sold or reclaimed.
- Equipment has been developed that offers low maintenance, and low capital and operating costs.

SUMMARY

Conventional chemical treatment methods of removing the copper from metal finishing waste streams prior to discharge generate large quantities of hazardous sludge with associated disposal problems. Newer technologies recently introduced provide economical recovery of the copper, which may be used for other purposes, but not for reuse in the bath. The resulting copper-depleted rinse solutions can then be discharged with other treated metal finishing wastes to POTW or receiving waters as required. Of these newer technologies, selective electrochemical displacement appears to be the best approach in terms of operational efficiency and cost.

LITERATURE CITED

1. Wing, R. and D. McFeeters, "Insoluble Starch Xanthate (ISX) Dissolved Heavy Metal Removal Case History Reports." Paper presented at the First AES Federal/State/Municipal/Industrial Waste Management and Control Conference

- for the Surface Finishing Industry, Orlando, January 10-11, 1983.
2. Kamperman, D. R., "Treatment of Electroless Process and Stripping Solutions." U.S. Patent 3,770,630 (November 6, 1973).
3. Jula, T., "Heavy Metal Recovery with Sodium Borohydride." Lecture presented at the Institute of Printed Circuits Meeting, Chicago, September 25-29, 1977.
4. Scott, M. C., "Sulfex™—A New Process Technology for Removal of Heavy Metals from Waste Steams." Paper presented at the 32nd Industrial Waste Conference, Purdue, 1977.
5. Anderson, J. R. and C. O. Weiss, "Method for Precipitation of Heavy Metal Sulfides." U.S. Patent 3,740,331 (June 19, 1973).
6. Cullivan, B. M., "Industrial Toxics Oxidation—An Ozone—Chlorine Comparison." Paper presented at the 33rd Annual Industrial Waste Conference, Purdue, 1978.
7. Prengle, H. W. and C. W. Mauk, "Ozone/UV Chemical Oxidation Waste Water Process for Metal Complexes, Organic Species and Disinfection." Paper presented at the 83rd National AIChE Meeting, Houston, March 20-24, 1977.
8. G. J. Macur, W. A. Alpangh, and J. E. Sharkness, "Oxidation of Organic Compounds in Concentrated Industrial Wastewater with Ozone and Ultraviolet Light." Paper presented at the 35th Annual Industrial Waste Conference, Purdue, 1980.
9. Courduvelis, C. I. and G. C. Gallager, "Selective Removal of Copper or Nickel from Complexing Agents in Aqueous Solution." U.S. Patent 4,303,704 (December 1, 1981).
10. Whalen, B. A., "New Developments for the Treatment of Waste Water Containing Metal Complexes." Paper presented at the Fourth EPA/AES Conference (January 20, 1982).
11. Zeblysky, R. J., "Treatment of Liquids Containing Complexed Heavy Metals and Complexing Agents." U.S. Patent 4,076,618 (February 28, 1978).
12. Stewart, F. A. and J. H. Weet, "Electrolytic Cell." U.S. Patent 4,139,429 (February 13, 1979).
13. DasGupta, S., J. K. Jacobs, and S. Mohanta, "Apparatus for Waste Treatment Equipment." U.S. Patent 4,308,122 (December 19, 1981).
14. Toller, W. H., "Electrowinning of Electroplating Wastes." Paper Presented at the IPC 25th Annual Meeting, Boston Park Plaza Hotel, Massachusetts, April, 1982.
15. Arcilesi, D. A., J. V. Peck, and R. M. Spearot, "Apparatus and Method for Copper Recovery." Patent applied for.

* Registered Trademark of OMI International Corporation
™ Trademark of OMI International Corporation



Rebecca Spearot is currently a Senior Process Engineer for Environmental Services of OMI International Corporation. She joined the Company in 1980 and is responsible for the design and development for waste treatment and recovery processes in the Udylite and Sel-Rex businesses. Prior to joining OMI, she was an Assistant Professor of Chemical Engineering at the University of Detroit, specializing in kinetics and catalysis.

A Chemical Engineer by training, she received her PhD in 1973. She is currently a member of the AES Research Board, AIChE Student Chapters Committee, and a Registered Professional Engineer in the State of Michigan.



John V. Peck is currently a Product Supervisor for Environmental Services of OMI International Corporation. He joined the company in 1974 and is responsible for the design and development of waste treatment and recovery processes in the Udylite and Sel-Rex businesses. Prior to joining OMI, he held a variety of Mechanical Engineering positions.

A Mechanical Engineer by training, he received his BME in 1959. He is currently a member of the MFEA Environmental Committee and is a Registered Professional Engineer in several states including Michigan.

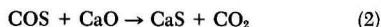
Surface Area of Calcium Oxide and Kinetics of Calcium Sulfide Formation

Details of a new limestone injection multistage burner aimed at reducing harmful emissions from existing power plants.

Robert H. Borgwardt, Industrial Environmental Research Laboratory, U.S. Environmental Protection Agency, Research Triangle Park, N. C. 27711 and Nancy F. Roache and Kevin R. Bruce, Northrop Environmental Services, Inc. Research Triangle Park, N. C. 27709

Recent studies [1] suggest that a 50 percent reduction in emissions of SO_2 and NO_x may be necessary to avoid environmental damage by acid deposition. The U.S. Environmental Protection Agency is developing the limestone injection multistage burner (LIMB) as an economical and practical method of achieving this degree of reduction in emissions from existing power plants. The process involves injection of pulverized limestone into coal burners that are designed to minimize NO_x formation by staged combustion [2]. It is well known that limestone can capture sulfur with modest efficiency in boilers equipped with conventional burners by reaction of CaO with SO_2 following combustion, and this reaction is also the principal mechanism of sulfur capture so far identified in the LIMB process. A lower flame temperature and a more favorable time/temperature profile resulting from staged combustion are expected to enhance prospects for sulfur capture compared to conventional burners where deadburning of the CaO was a potential limitation. The reducing conditions which prevail in the first stage of LIMB may afford additional sulfur capture if limestone can react with the reduced sulfur species, predominantly H_2S and COS , that are released there during coal pyrolysis. Since the residence time of the limestone particles in the reducing zone is short, the feasibility of improving the overall sulfur capture by CaS formation will depend, in large part, on reaction kinetics.

Measurements of the rate of H_2S reaction with CaCO_3 by direct displacement [3] show favorable low temperature kinetics for micrometer-size limestone particles, but strong inhibition by hydrogen. Studies of the calcination kinetics of those particles [4] have shown that the rate and activation energy are greater for calcination than for the reaction of CaCO_3 with H_2S . If CaS formation is to contribute to the performance of LIMB, it must therefore occur through reactions with CaO :



Reaction (1) has been investigated by Pell [5] and by Kamath and Petrie [6] using calcined dolomite. It has also been studied by Keairns, *et al.* [7], using calcined limestones, and by Attar and Dupuis [8] with CaO prepared from calcite. The reported value of the activation energy, which is the critical parameter for extrapolating those data to combustion temperatures, ranges from 3.6 to 37 kcal/mol. Only the latter value could yield significant sulfur capture in LIMB by this mechanism. Reaction (2), studied by Yang and Chen [9] using reagent grade CaO , is re-

ported to have an activation energy of 4.3 kcal/mol. In most cases, the available data was obtained with particles too large to be appropriate to the LIMB process, or to ensure that the measurements were not dominated by intraparticle pore diffusion. Nor have the experimental methods used in prior work been capable of operating with sufficient particle dispersion to eliminate the interparticle diffusion resistance that generally dominates rate measurements with powdered solids due to agglomeration of the sample in the reactor. The lower values of activation energy reported for Reactions (1) and (2) are typical of gas diffusion control and suggest that those data do not reflect true chemical kinetics. Although most experiments have included a test for gas-side diffusion resistance by varying the gas velocity, the result is valid only if the particles are individually exposed to the full gas flow. Most importantly, no prior study has included the surface area of CaO as an experimental variable in spite of its importance to the reaction kinetics of porous solids [10]. It is known that the specific surface area of CaO produced by calcination of small limestone particles at maximum rate is an order of magnitude greater than the surface areas produced at the slower calcination rates that are characteristic of large or non-dispersed particles [4]. The relationship between surface area and reaction rate must therefore be understood if maximum performance of LIMB is to be obtained by any mechanism.

Calcination, Porosity, and Surface Area

When limestone particles are calcined at temperatures below 1000°C , their decomposition to CaO generally occurs without change in particle dimensions. This experimental fact, together with the difference between the densities of CaCO_3 (2.71 g/cm^3) and CaO (3.32 g/cm^3), requires that the total volume of the CaO grains within the CaO particle will occupy only 45 percent of the volume of the original CaCO_3 particle. The total volume of the intergrain voids within the CaO particle (i.e., the porosity) will thus be 55 percent of the volume of the particle, plus whatever percentage porosity was present in the original limestone. The density of CaS (2.61 g/cm^3) is such that complete conversion of the CaO grains to CaS will reduce the porosity from 55 to 25 percent, but the fully expanded grains will not fill the intergrain void space within the particle. This ability to achieve 100 percent conversion is an important feature of Reactions (1) and (2), since the available intraparticle void space can be a limiting factor for other reactions, such as CaSO_4 formation.

The size of the CaO grains formed within a particle (and, therefore, the number of grains and their total surface) is

related to the calcination kinetics [4]. Low temperatures (600°C) and maximum calcination rate yield surface areas as large as 90 m²/g, corresponding to a grain radius, r_g , of 100 Å as defined for spherical grains by:

$$r_g = \frac{3}{S_g \rho_{CaO}} \quad (3)$$

where S_g is the specific surface area determined by the B. E. T. (Brunauer-Emmett-Teller) method [11] and ρ_{CaO} is the true (helium) density of CaO. As calcination temperature increases, the rate of grain growth accelerates and the specific surface area drops accordingly. Nevertheless, limestone particles smaller than 90 μm calcine rapidly enough in a dispersed system to yield B. E. T. surface areas of 50 to 60 m²/g at temperatures up to 1075°C [4], corresponding to a grain radius of 150 Å. Since sintering rate is independent of particle size, maximum surface area is attained when particles of minimum size are calcined at minimum temperature and maximum rate; i.e., without CO₂ equilibrium or mass transfer limitations.

Surface Area and Reaction Rate

The rate of reaction of a gas with a porous solid particle is related by grain theory to the size of the non-porous grains (in this case CaO) which comprise the interior matrix of the particle. It assumes that H₂S or COS diffuses through the CaS product layer surrounding the individual grains and reacts at the interface between the product layer and the unreacted core. The CaO within the unreacted core of a grain is assumed to be static physically and chemically. Within these assumptions, and the further condition that the particle size is sufficiently small that gas diffusion through the intergrain voids is an insignificant resistance, the overall rate can be limited by the chemical reaction at the interface, by diffusion through the product layer, or by a combination of the two. In the first case, the conversion (X) vs. time (t) response is given for irreversible first order reactions by:

$$t = \frac{\rho_{CaO}}{kC} r_g \left[1 - (1 - X)^{1/3} \right] \quad (4)$$

and for the second case by:

$$t = \frac{\rho_{CaO}}{6D_r C} r_g^2 \left[1 - 3(1 - X)^{2/3} + 2(1 - X) \right] \quad (5)$$

where k is the reaction rate constant, C is the gas phase concentration of H₂S or COS, and D_r is the effective diffusivity through the product layer.

The effect of surface area on reactivity predicted by Equations (3) to (5) is thus quite pronounced: the time required to reach a given conversion should be inversely proportional to the B. E. T. surface area for chemical reaction control and inversely proportional to the square of the surface area for product layer diffusion control. Given the fact that micrometer size limestone particles can yield specific surface areas as large as 50 to 60 m²/g when "flash-calcined" in a dispersed system such as LIMB, this variable can clearly be the most important—if not determining—factor for sulfur capture in such a system. In any case, no reliable prediction can be made for the efficiency of sulfur capture without a knowledge of the quantitative relationship between surface area and CaO reactivity. The purpose of this experimental study is to evaluate that relationship. Measurements are made within a range of temperatures where reaction rates can be accurately determined as a function of surface area, including those surface areas representative of the maximum values anticipated for small particles calcined in dispersed systems. On the basis of these measurements, extrapolations to the combustion temperatures of LIMB will be made to estimate potential sulfur capture efficiencies.

EXPERIMENTAL

Materials

The CaO was prepared from the same limestone, Fredonia White (BCR 2061), used in the prior study of the H₂S/CaCO₃ reaction [3]. The limestone contained 95 percent CaCO₃ and 1.3 percent MgCO₃, has a porosity of 8 percent, and a grain size of 2 μm. The pulverized stone was fractionated into samples of narrow particle size distribution with a Donaldson Accucut Classifier. A size fraction of 1 to 3 μm, having a B. E. T. surface area of 2.2 m²/g, was used for calcination. All reagent gases were blended from compressed gas or liquid-N₂ cylinders.

Apparatus

Limestone calcination and reaction of the CaO with H₂S or COS were carried out in a differential reactor fabricated of quartz glass as illustrated in Figures 1 and 2. The feed gas entered the bottom of the reactor, passed upward through a 3.0-cm I. D. × 95-cm outer shell and downward through an annular 2.0-cm I. D. × 77-cm reactor tube. The limestone (or CaO) sample was positioned at the center of the reactor tube in a 1.4-cm I. D. removable holder which was sealed by a ground glass joint to the gas exhaust tube. The particles were dispersed in a quartz wool substrate (Thermal American Fused Quartz Co.) through which the entire gas flow passed. The sample holder/exhaust tube assembly was inserted at the bottom of the reactor through a ball joint which sealed it into the gas preheat section formed by the annular space between the two larger reac-

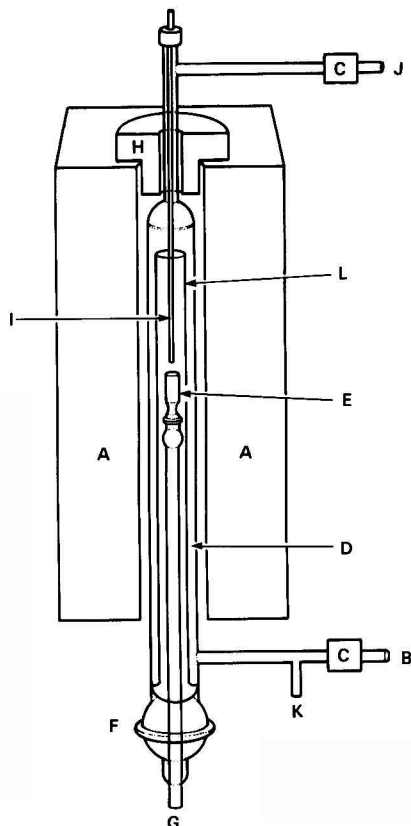


Figure 1. Differential reactor: (A) electric furnace, (B) gas inlet, (C) solenoid valve, (D) gas preheat zone, (E) limestone sample holder, (F) ball joint, (G) gas exhaust, (H) ceramic plug, (I) thermocouple, (J) CO₂ gas inlet, (K) monometer connection, (L) reactor tube.

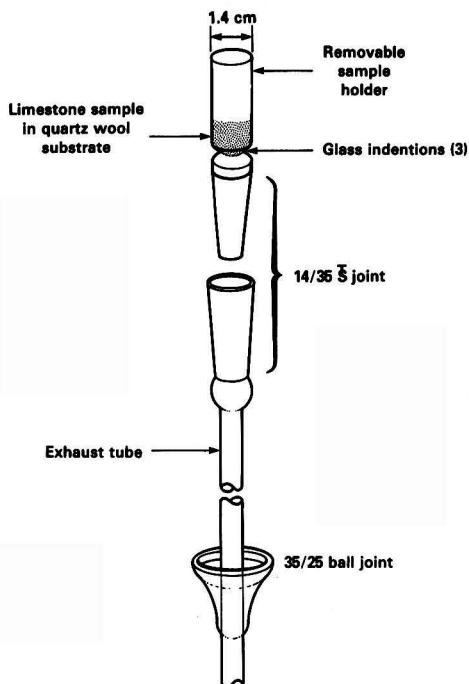


Figure 2. Differential reactor: detail of limestone sample holder/exhaust tube assembly.

tor tubes. The upper 60 cm of the reactor was heated by an electric furnace to temperatures that were varied from 600° to 900°C.

The surface areas of the solids were determined by nitrogen adsorption at -195°C using a Micromeritics Mod. 2100E analyzer and the B. E. T. method. Comparisons of the surface area measurements against calibration standards (Duke Scientific Co.) of 3, 24, and 81 m²/g showed average agreement of ± 3.2 percent, reproducible to ± 1.3 percent.

Calcination

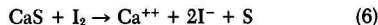
To prepare CaO of high surface area, the sample holder was charged with 15 mg of 2- μ m limestone particles and inserted into the reactor flushed with pure CO₂. After equilibration of the sample to reactor temperature, the calcination reaction was begun by feeding CO₂-free N₂ to the reactor at a rate of 23 standard liters per minute (SLPM). At 700°C, the conversion to CaO was complete in 90 sec. B. E. T. measurements on composites of multiple samples calcined in this manner showed a surface area of 79 m²/g. The calcined sample was either exposed to reactive gases immediately following its preparation or was retained in the reactor (without gas flow) for varying periods to reduce its surface area by sintering prior to exposure. At 700°C, a sintering period of 20 min reduced the surface to 40 m²/g and 60 min reduced it to 32 m²/g. Further reduction of the surface was obtained by calcining and sintering at higher temperatures. For example, 30 min sintering at 850° and 950°C yield 27 and 6 m²/g, respectively. When samples were calcined at one temperature for reaction at a different temperature, the CaO was stored in glass vials sealed with wax. Tests showed the surface areas to be stable over periods of a least 6 weeks storage at room temperature.

CaO Reaction

The CaO, calcined and sintered *in-situ* (or 8.4 mg of precalcined CaO of known surface area, dispersed into the quartz wool of the sample holder and heated to reactor

temperature), was exposed to the reactive gas at a total flow rate of 23 SLPM. In the case of H₂S, the reactive gas consisted of 5000 ppm H₂S, 45 percent H₂, and the balance N₂, except where otherwise noted. In the case of COS feed, it consisted of 5000 ppm COS, 20 percent CO, and the balance N₂. The H₂ and CO were added to ensure that equilibrium did not favor dissociation of the reactants at the higher temperatures. Each CaO sample was exposed to the reactive gas for varying times in a series of runs that defined the conversion vs. time response from 10 to 90 percent conversion to CaS.

After exposure of the CaO for the desired reaction period, the gas flow was terminated and the sample withdrawn from the reactor. The sample holder was removed at the ground glass joint, and the reacted CaO (with the quartz wool substrate) was ejected into 100 ml of 0.005 M buffered iodine solution for analysis of sulfide. The iodine was magnetically stirred in a sealed glass container for 45 min, then titrated with 0.005 M arsenite to determine the amount of iodine unconsumed by the reaction:



When the sulfide analysis was completed, calcium was determined in the same solution by adding NaOH and titrating with 0.5 percent EDTA to a murexide endpoint. The percent conversion of CaO to CaS was calculated from the mol ratio of sulfur/calcium thus established. Agreement between the calcium recovery indicated by the titrations and the calcium charged to the reactor showed that the loss due to entrainment with the reactor exhaust gases was negligible for 2 μ m particles. X-ray fluorescence analyses of total sulfur in selected samples showed good agreement with the iodometric analyses, showing that no product other than CaS was present and that no oxidation occurred during the brief air exposure.

RESULTS

The reaction rate of CaO with H₂S is shown as a function of the specific surface area of the calcine in Figure 3. In each case, the reaction was carried out at a temperature of 700°C and H₂S concentration of 5000 ppm. The effect of CaO surface area on its rate of reaction with COS is shown in Figure 4 at the same reaction conditions. Included in Figure 4 are data for the reaction rates of CaO prepared from three different particle sizes of limestone: 1, 5.7 and 9.4 μ m.

To determine the effect of temperature on the reaction rate, the surface area of the CaO must be held constant. Since the rate of dissipation of surface area by sintering, (i.e., by grain coalescence and growth) is also affected by temperature [12, 4], the CaO was pre-sintered at a temperature higher than those at which the reaction rates were measured. For this purpose, a batch of calcine was prepared (950°C, 30 min) having a B. E. T. surface area of 5.8 m²/g, and 8 mg samples were used for each reactor exposure. The results of exposures to 5000 ppm H₂S are shown in Figure 5 as a function of time and reactor temperature. Figure 6 shows similar runs made with a reactor feed gas containing 4300 ppm COS.

The effect of hydrogen on Reaction (1) is shown in Figure 7. Comparisons were made at 700°C for three values of CaO surface area when the feed gas contained 0, 10, or 45 percent H₂, 5000 ppm H₂S, with the balance nitrogen.

DISCUSSION OF RESULTS

Figures 3 and 4 show that the reaction rate of CaO with either H₂S or COS is strongly influenced by its specific surface area. The time required to reach a given conversion to CaS is plotted logarithmically vs. the B. E. T. surface area of the calcines in Figure 8. Within the validity of the assumptions implicit in Equations (4) and (5), the slope

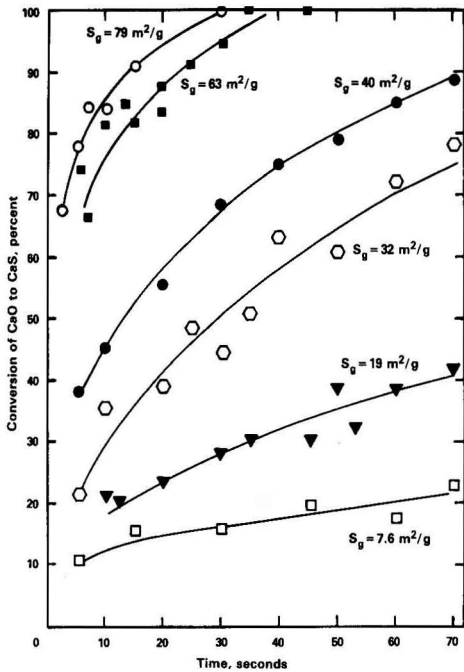


Figure 3. Reaction of 2 μm CaO particles with 5000 ppm H_2S at 700°C, as a function of the B. E. T. surface area (S_g) of the calcine. H_2 in feed gas = 45 percent.

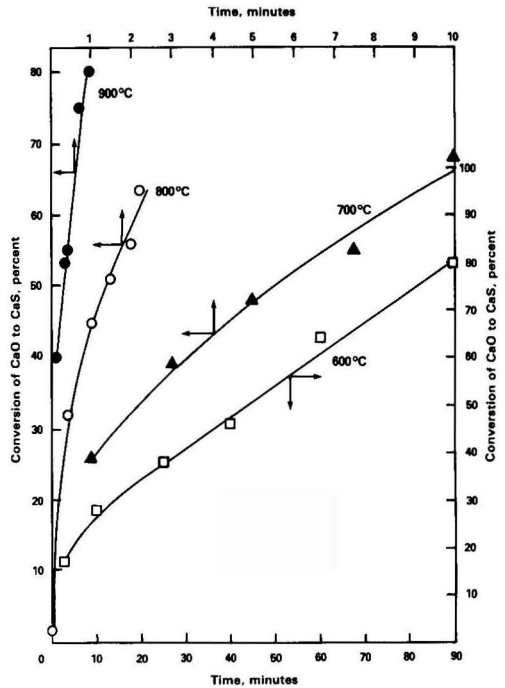


Figure 5. Reaction of CaO particles with 5000 ppm H_2S as a function of temperature. $S_g = 5.8 \text{ m}^2/\text{g}$; H_2 in feed gas = 45 percent.

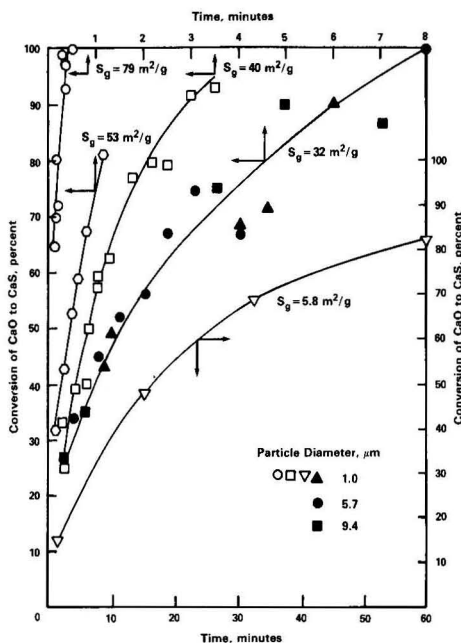


Figure 4. Reaction of CaO particles with 5000 ppm COS at 700°C as a function of the B. E. T. surface area (S_g) and particle size of the calcine.

of such plots should be -1 for chemical reaction control by the shrinking grain core mechanism or -2 for product layer diffusion control. Figure 8 yields slopes of about -2.3 for both Reactions (1) and (2). The results thus indicate that the reactivity of CaO is even more sensitive to sur-

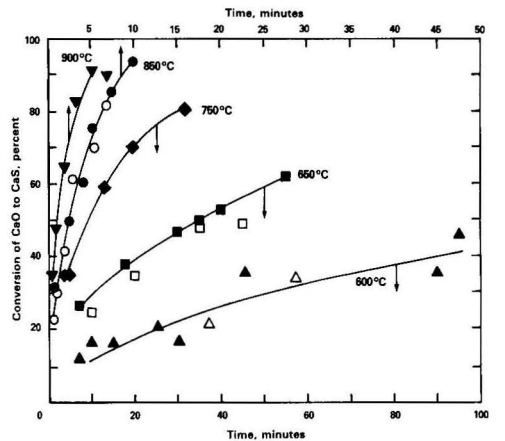


Figure 6. Reaction of CaO particles with 4300 ppm COS as a function of temperature. $S_g = 5.8 \text{ m}^2/\text{g}$ (closed symbols); open symbols = replicate calcine, $5.6 \text{ m}^2/\text{g}$.

face area than predicted by the grain model for pure diffusion control. Logarithmic plots of the reaction rates, evaluated at a given conversion as the slope of the curves in Figures 3, 4 and 7, likewise indicate an exponential dependence on surface area.

The effect of temperature on the overall reaction rate can be correlated by the Arrhenius relationship over the full range of this study (600° to 900°C) as shown in Figure 9. The reaction rates plotted in Figure 9 were evaluated directly from Figures 5 and 6 as the slopes of the curves at 50 and 40 percent conversion, respectively. The apparent activation energies indicated by the slopes of the straight lines of Figure 9 are 31.0 kcal/mol for both Reactions (1) and (2). This value compares favorably with the 37

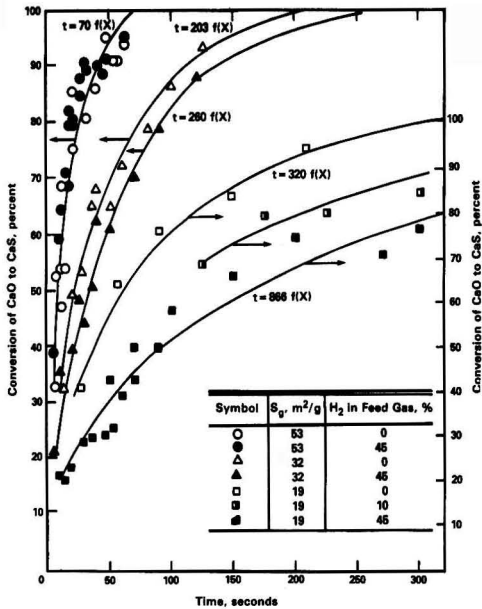


Figure 7. Effect of hydrogen on the reaction of CaO with 5000 ppm H₂S at 700°C; $f(X) = [1 - 3(1 - X)^{2/3} + 2(1 - X)]$.

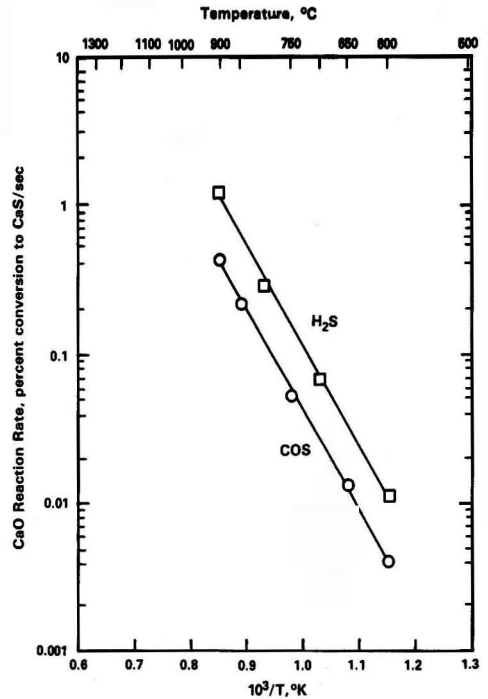


Figure 9. Arrhenius plots of the reaction rate of CaO particles ($S_g = 5.8 m^2/g$) with □ 5000 ppm H₂S, and ○ 4300 COS.

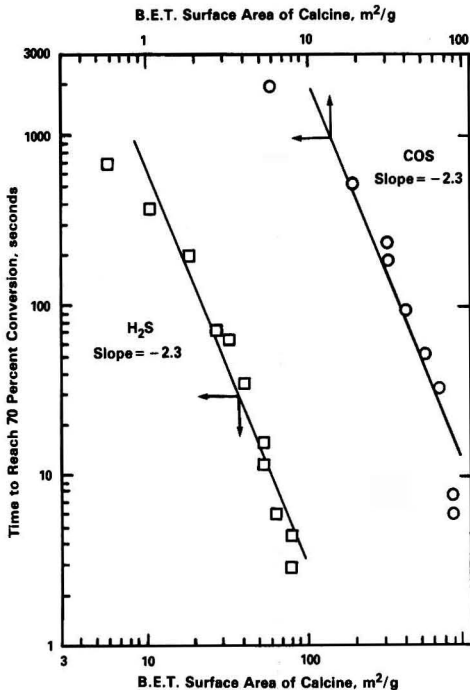


Figure 8. Test of Equations (4) and (5) to determine rate limiting mechanism.

kcal/mol reported for Reaction (1) by Attar and Dupuis [8] in the temperature range 560° to 670°C. Although the conversion vs. time responses are most consistent with product layer diffusion control, the activation energy is an order of magnitude greater than that which would correspond to diffusion of H₂S or COS through a porous or cracked CaS layer (reflecting the 1.5-power dependence

of D_p on temperature). This problem of interpretation also occurs with the application of grain theory to the CaO/SO₂ reaction, in which case it has been explained as a manifestation of solid state diffusion [13, 14]. If this is also the case for Reactions (1) and (2), the similarity of their activation energies would suggest that the diffusing species are the same for both reactions.

On the basis of the temperature dependence of the reaction rates, obtained from Figure 9, and the effect of the surface area, obtained from Figures 3 and 4, the data can be extrapolated for the purpose of estimating sulfur capture at the higher temperatures appropriate to LIMB. Table 1 summarizes the results of such extrapolations to a temperature of 1250°C using the measured reaction rates with CaO having a surface area of 40 m²/g.

TABLE 1. PROJECTED SULFUR CAPTURES

Reactant (5000 ppm)	Time to 40% Conversion, sec
	H ₂ S
COS	0.12

At temperatures that can reasonably be expected in the first stage of LIMB, Table 1 indicates that high sulfur captures should be attainable through the CaS mechanism if the intrinsic solid reactivity is the only resistance. Forty percent conversion corresponds to 80 percent sulfur capture at twice the stoichiometric limestone injection rate if no sulfur is lost during CaS oxidation in later stages of combustion.

The data of Figure 4 show that the reaction rate is not affected by increasing the particle size by a factor of 9 under the conditions studied. This result is interpreted as verification that the reaction occurs equally throughout the surface of the grain matrix within the particles; i.e., pore diffusion resistance is insignificant at 700°C.

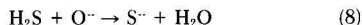
Mechanism

The strong influence of surface area on the reactions shown by Figure 8 implies that the rate is most probably limited by a diffusion process in the product layer surrounding the individual CaO grains. This conclusion is supported by the close fit of the conversion *vs.* time data to the response curve of Equation (5) as shown in Figure 7 for a range of constant grain sizes. The results are thus consistent with the conclusion of Pigford and Sliger [15] regarding the reaction of SO₂ with small CaO particles.

Results similar to this study are reported by Bhatia and Perlmutter [16] for the reaction



which is also dominated by product layer diffusion while showing a high activation energy. They conclude that the diffusing species for Reaction (7) are the ions CO₃²⁻ and O²⁻. For the same reasons, the results discussed here are best explained if an analogous solid-state process limits Reactions (1) and (2): diffusion of S²⁻ toward the product layer/CaO interface and counterdiffusion of O²⁻ to the product layer/gas surface as illustrated in Figure 10. The surface reactions are thus postulated as:



The effect of hydrogen shown in Figure 7 is consistent with earlier studies [4] which showed the reaction of H₂S with CaCO₃ to be inhibited by H₂ to a degree that is H₂-concentration and particle size dependent. For example, with 45 percent H₂ in the feed gas, the maximum (20 min) conversion of limestone particles to CaS increased as shown in Table 2.

TABLE 2. REACTION OF CaCO₃ WITH H₂S

Particle Diameter, μm	Specific Surface, m^2/g	Maximum Conversion, %
5	1.2	4
2.8	1.9	10
1.6	4.5	25
<1	7.0	60

This effect is greater than would be expected if H₂ were inhibiting the chemical reaction rate and was interpreted as evidence that H₂ affects diffusion through the product layer. In terms of the solid-state mechanism of diffusion, this might be explained by the entry of molecular hydro-

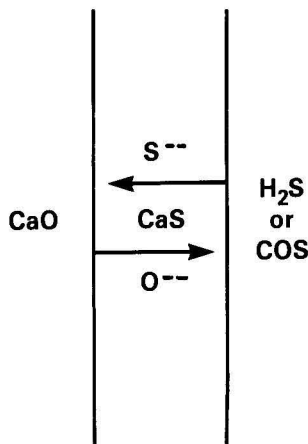


Figure 10. Probable mechanism of CaS formation by ionic diffusion through the product layer.

gen into the CaS lattice, occupying vacancies and thereby blocking the mobility of CO₃²⁻ and S²⁻.

As shown in Figure 7, the effect of H₂ on the reaction of H₂S with CaO is also grain size dependent: calcines with large grains (low surface areas) are inhibited to the greatest degree, while calcines with grains smaller than ~600Å (32 m²/g) were not detectably affected by H₂. As indicated in Figure 7, the responses fit Equation (5) whether H₂ is present or not. Thus, removal of H₂ increases D_e—by a factor of 2.7 when the surface area is 19 m²/g—but does not appear to eliminate diffusion as the rate limiting resistance. This conclusion is supported by the data of Figure 8 which show no reduction in slope as the grain size is reduced to a minimum. A reduced slope would be expected if chemical reaction became controlling, in accordance with Equation (4).

In the region of surface areas greater than 30 m²/g, the data of Figure 8 show a slope approaching 3. When the reactions are viewed as a solid-state process, this apparent excessive (>2.0 exponential) sensitivity to surface area can be explained by a dependence of D_e on the solid phase concentration or the crystalline disorder. In the latter case, the rate would be expected to increase not only with specific surface, reflecting the effect of product layer thickness at a given conversion, but also with the concentration of defects within the CaO crystal lattice. Maximum defects will exist immediately after CaO formation by calcination; consequently, the smallest grains would also have the highest defect concentration. When the grain size is increased by sintering, not only does the specific surface decrease, but also a more perfect CaO lattice is formed by the annealing process. Thus, a lower solid-state diffusion coefficient may reasonably be associated with larger grain size.

The dependence of D_e on grain size is further illustrated in Figure 11, which shows a nearly linear relationship between the surface areas of the calcines and their conversions in a given reaction time (30 sec). The response pre-

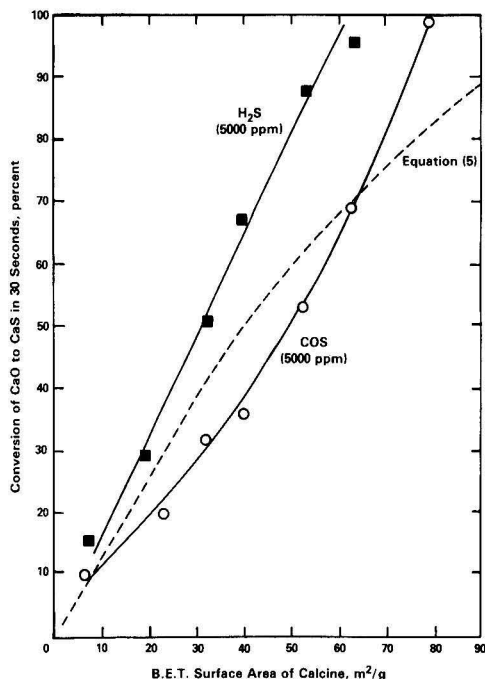


Figure 11. Comparison of CaO reactivity with the response predicted by Equation (5) for constant diffusivity in the product layer. Temperature = 700°C.

dicted by Equation (5) for a constant D_e , shown as the dashed curve in Figure 11, is significantly lower than the conversions attained by the high-surface calcines. The assumption of constant D_e is thus valid for any given grain size (as shown by Figure 7), but is not valid when grain size is changed by sintering.

CONCLUSIONS

- The rate of CaS formation increases exponentially with the specific surface area of CaO in micrometer size particles.
- The effect of surface area on reactivity is at least as great as that expected for pure diffusion control.
- The activation energy of CaO reaction with H_2S or COS is 31 kcal/mol for the limestone studied.
- On the basis of the activation energy measured between 600° and 900°C, and the reaction rates measured for CaO of 40 m^2/g surface area, efficient sulfur capture would be predicted at 1250°C in a dispersed-particle system if the kinetics of CaS formation is the only limitation.
- The results are consistent with the assumption that the rate of CaS formation is limited by solid-state diffusion in the CaO grains of micrometer size particles.

NOMENCLATURE

- D_e = Diffusion coefficient of the product layer, cm^2/sec
 C = Gas phase concentration of H_2S or COS, ppm
 k = Rate constant for chemical reaction, cm/sec
 r_g = Radius of CaO grains in calcine particle, cm
 S_g = Specific (B. E. T.) surface area of calcine, cm^2/g
 t = Time, sec
 X = Conversion of CaO to CaS, mol percent
 ρ_{CaO} = True (helium) density of CaO, g/cm^3

LITERATURE CITED

1. Calvert, J. G., "Acid Deposition: Atmospheric Processes in Eastern North America," Committee on Atmospheric Transport and Chemical Transformation, Environmental Sciences Board, National Academy of Sciences Press, ISBN 0-309-03389-9 (1983).
2. Drehmel, D. C., G. B. Martin, and J. H. Abbott, "SO₂ Control with Limestone in Low NO_x Systems: Development Status," in Proceedings: Symposium on Flue Gas Desulfurization, Vol. 2, EPRI CS-2897, 689-712 (March, 1983).
3. Borgwardt, R. H. and N. F. Roache, "Reaction of H₂S and Sulfur with Limestone Particles," *Ind. Eng. Chem., Process Des. Dev.*, in press.
4. Borgwardt, R. H., "Calcination Kinetics and Surface Area of Dispersed Limestone Particles," *AIChE J.*, in press.
5. Pell, M., "Reaction of Hydrogen Sulfide with Fully Calcined Dolomite," PhD Thesis, City University of N. Y. (1971).
6. Kamath, V. S. and T. W. Petrie, "Rate of Reaction of Hydrogen Sulfide-Carbonyl Sulfide Mixtures with Fully Calcined Dolomite," *Environ. Sci. Technol.*, **15**, 966-8 (1981).
7. Keairns, D. L., D. H. Archer, R. A. Newby, E. P. O'Neill, and E. J. Vidt, "Evaluation of the Fluidized-Bed Combustion Process, Vol. IV, Fluidized-Bed Oil Gasification/ Desulfurization," EPA-650/2-73-048d, (NTIS PB 233-101) 1973.

8. Attar, A. and F. Dupuis, "The Rate and the Fundamental Mechanisms of the Reaction of Hydrogen Sulfide with the Basic Minerals in Coal," *Ind. Eng. Chem., Process Des. Dev.*, **18**, 607-18 (1979).
9. Yang, R. T. and J. M. Chen, "Kinetics of Desulfurization of Hot Fuel Gases with Calcium Oxide. Reaction between Carbonyl Sulfide and Calcium Oxide," *Environ. Sci. Technol.*, **13**, 549-53 (1979).
10. Szekeley, J., J. W. Evans, and H. Y. Sohn, "Gas-Solid Reactions", Academic Press, New York (1976).
11. Brunauer, S., P. H. Emmett, and E. Teller, *J. Am. Chem. Soc.* **60**, 309 (1938).
12. Glasson, D. R., "Reactivity of Lime and Related Oxides, VIII Crystal Size Variation in Calcium Oxide Prepared from Limestone," *J. Appl. Chem.* **11**, 201-6 (1961).
13. Hartman, M. and O. Trnka, "Influence of Temperature on the Reactivity of Limestone Particles with Sulfur Dioxide," *Chem. Eng. Sci.* **35**, 1189-94 (1980).
14. Bhatia, S. K. and D. D. Perlmutter, "The Effect of Pore Structure on Fluid-Solid Reactions: Application to the SO₂-Lime Reaction," *AIChE J.* **27**, 226-34 (1981).
15. Pigford, R. L. and G. Sliger, "Rate of Diffusion Controlled Reaction between a Gas and a Porous Solid Sphere," *Ind. Eng. Chem. Process Des. Dev.*, **12**, 85 (1973).
16. Bhatia, S. K. and D. D. Perlmutter, "Effect of the Product Layer on the Kinetics of the CO₂-Lime Reaction," *AIChE J.* **29**, 79-86 (1983).



Robert H. Borgwardt is a Chemical Engineer with EPA's Office of Research and Development where he has responsibilities for in-house evaluation of processes for controlling sulfur emissions from coal combustion. In addition to basic research, he was extensively involved in pilot scale development of the limestone wet scrubbing process. He received his B. S. degree from M.I.T.



Nancy Roache is a Senior Scientist with Northrop Services, Inc., working on the EPA IERL in-house research for LIMB sulfur capture. She is a graduate of Winthrop College in Chemistry.



Kevin R. Bruce earned his B.S. in Chemistry from the University of North Carolina at Chapel Hill in 1982. He is currently employed as an Associate Scientist with Northrop Services, Inc.

Mineral Processing Water Treatment Using Magnesium Oxide

Comparative tests show magnesium oxide to be superior to silica sand and garnet sand for the filtration of several different particulates and to lime for the precipitation of heavy metals.

Joseph E. Schiller, Daniel N. Tallman, and Sanaa E. Khalafalla*, Twin Cities Research Center, Bureau of Mines, U.S. Dept. of the Interior, Minneapolis, Minn. 55817

Removal of Suspended Solids

"This paper describes two applications where magnesium oxide (MgO) can be used to purify process water in two ways; (1) to filter out suspended solids and (2) to precipitate dissolved heavy metals. Granular MgO (periclase mineral) out-performs sand in deep bed filters, since an MgO filter system operates with cycles up to twice as long and gives a cleaner filtrate than a comparable sand filter. To precipitate heavy metals, powdered MgO (magnesia chemical) is used instead of lime or caustic soda. The MgO-formed sludge cements into a solid mass on standing and occupies only about 20 to 30 pct of the volume as the precipitates produced by more soluble bases."

Media used in deep-bed filters are commonly silica sand and, more recently, a combination of anthracite coal, silica sand, and garnet sand [1, 2]. Suspended solids are retained in the filter by a combination of mechanisms which include 1) short-range London-van der Waal's attractive forces between the filtering medium and the suspended particles, 2) chemical bridging caused by flocculation, 3) chemical bonding, and 4) interstitial straining. MgO filters introduce an electrokinetic attractive force which aids particle attachment to the filter grains. Most mineral surfaces are negatively charged in water because their cations have a higher hydration energy than do the anions. Consequently, more cations leave the solid surface, and the surface acquires an excess of negative charges. The surface of MgO is positively charged in water at pH values below 11 [3]. Therefore, an electrokinetic attractive force between the unlike charges assists particle attachment to MgO filters. Negatively charged filter materials can be chemically modified to become positively charged and thereby improve their efficiency. Cationic polyelectrolytes and alum ($KAl(SO_4)_2$) have been successfully used to treat diatomite [4, 5]. The increased efficiency of a positively charged medium has also been demonstrated for membrane filters [6], and commercial products are available which are based on this concept (Zetapor Membranes manufactured by AMF Cuno Division, Meriden, Conn.).**

Granular MgO (periclase) has distinctive properties that make it an excellent filter medium. In addition to its positive electrokinetic charge at neutral pH values, MgO is rel-

atively inexpensive and is nontoxic. Its density of 3.6 g/cm^3 is close to that of garnet sand. Crushed crystalline MgO is irregular in shape, resulting in filter beds with large pore size and high capacity.

Removal of Heavy Metals

Chemical precipitation of metal hydroxides is the most common way to remove dissolved metals from water. In general practice, sufficient lime or caustic soda is added to raise the pH above 8 or 9, forming a fluffy, suspended hydroxide precipitate. After adequate settling, the metal sludge is disposed of or reclaimed. Care is required to prevent dissolution of the sludge by acidic water or resuspension by agitation. Lime is almost always used because of its low cost, and coagulants are generally added to improve the settling process. The most common coagulants for hydroxide precipitates are water-soluble organic polymers. These polymers attach to particles and cause small ones to collect together to make larger aggregates that settle more rapidly.

Chemical precipitation of metals as carbonates with soda ash (sodium carbonate) or sulfides using sodium sulfide are also used where insoluble compounds result [7]. More specific chemicals are sometimes employed for particular metals. Starch zanthate is precipitant with functional groups that form several insoluble metal salts [8]. Reverse osmosis, ion exchange, activated-carbon adsorption, cementation, and extraction are other processes applied for metals removal.

The solubility, basicity, and surface charge of MgO allow it to form compact precipitates. Although MgO is quite insoluble in water (the solubility is 5 mg/liter), it is a strong base, giving saturated solutions a pH of 10.5. When MgO is added to a solution containing hydrated heavy metal ions, it readily reacts to form metal hydroxides. However, the precipitation reaction apparently occurs at the MgO surface, giving much less occluded water than when a soluble base is used. Usually 5 to 15 minutes are required for MgO to raise the pH, and this gradual increase may lead to larger hydroxide crystals and a more compact precipitate. Another factor that may contribute to the compactness of the sludge is the positive surface charge on MgO and the negative surface charge on most heavy metal hydroxides [3]. The resulting mutual attraction may cause water to be expelled from the spaces between the particles giving a denser solid.

*Author to whom correspondence should be made.

** Reference to specific trade names or manufacturers does not imply endorsement by the Bureau of Mines.

EXPERIMENTAL WORK

Filtration Research

Laboratory-scale filtrations were performed using either a three-stage, 2.5-cm-diameter filter system or a one-stage, 20-cm-diameter filter. Since 2,000 to 5,000 liters were required for each 20-cm-diameter filter run, the suspension to be filtered was continuously made up as it was used. Tap water (Minneapolis city water, pH 7.4 to 7.8) was passed through a 0.2- μ m cartridge filter into the 100-liter stirred reservoir, and a pump added a concentrated suspension of fine quartz or clay to the reservoir to maintain a fixed concentration of suspended solids. An auxiliary pump added alum to the reservoir at a rate sufficient to give a concentration of 5 to 15 ppm. The added solids and alum lowered the pH of water to be filtered to 7.0 to 7.5. A larger capacity pump transferred turbid water from the reservoir to the filter at a rate of 8.7 liter/min (4.6 mm/sec). The pressure across the column was determined with a gauge, and filtrate turbidity was measured every 15 minutes using a Hach Model 2100A turbidimeter. The gauges read 0 to 15 psi with 0.5-psi graduations (0 to 103 KPa with 3.4-KPa graduations). At the beginning of the filter runs, concentrated suspension and alum were added to the reservoir to produce the desired concentrations, and pumps maintained this concentration throughout the several hours of the run.

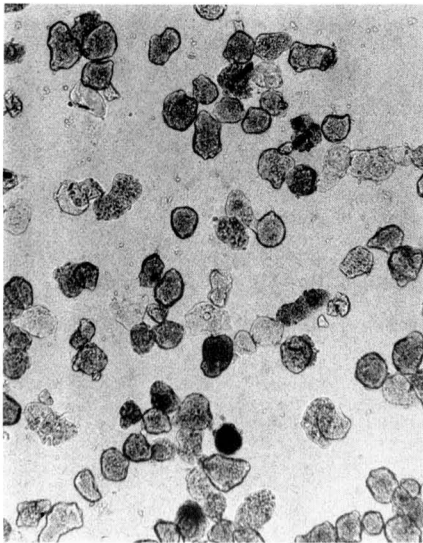
A three-stage filter allowed use of different materials or different mesh sizes in series to simulate mixed-media filters. Being able to measure the pressure drop across each column made it possible to determine where pressure buildup was taking place. Water containing suspended particulates was prepared and stirred in a 20-liter reservoir and pumped through the filter at 100 to 120 ml/min (0.21 to 0.25 m/min). The flocculant and suspension were brought together by a two-channel pump and allowed to mix for 8 to 10 minutes before they entered the first filter column. The pressure at the head of each column was monitored using a gauge, and the filtrate turbidity was measured every 15 minutes during a run. Filtrate turbidities and pressure increases were essentially the same when a given suspension was filtered through the same media in either the 2.5- or the 20-cm-diameter filter.

Synthetic suspensions of solids were prepared from finely ground quartz, kaolin, and bentonite. Kaolin and bentonite were purchased from Baker Chemical Co. Ordinary quartz sand was ground in a Beuhler mill to make fine material from which suspensions were prepared. The water used was filtered Minneapolis City tap water containing about 40 ppm Ca and 15 ppm Mg; it had a pH of 7.4 to 7.8 and a turbidity of about 0.1 nephelometric turbidity unit (NTU). MgO and sand media were also used to filter for an iron ore processing plant water using the 2.5-cm-diameter system. Media depth was 45 cm of 20/30 mesh sand or MgO, the flow rate was 100 ml/min, and the alum dosage was 15 ppm.

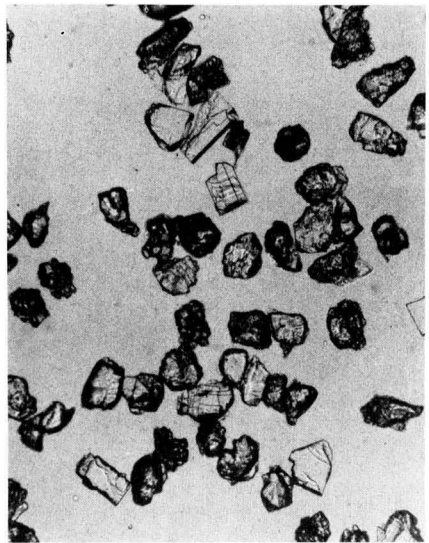
"Figure 1 shows photomicrographs (x120) of the two forms of MgO; (A) powdered magnesite used for precipitation research (vide infra), and (B) granular periclase used for filtration research. Conventional filter sand is more spherical than the periclase shown in Figure 1B." The periclase used in this work was obtained from two sources: Basic, Inc., Cleveland, Ohio, and Kaiser Refractories, Oakland, Calif. Both materials performed equally as filter media, and each was 97 to 98 percent pure. Impurities, in decreasing order of concentration, were the oxides of calcium, silicon, iron, and aluminum. The MgO from Basic, Inc., was a "minus 18 mesh" product from which 20/30 mesh and 30/50 mesh fractions were separated by sieving. The Kaiser Refractories material was their "K-grade periclase" which is pelletized into nominally 0.5- by 1-cm pillows. This product was crushed and sieved to give the size fractions used as filter media. Garnet sand and "flint" (silica) sand were purchased from Neptune Microfloc, Inc., Corvallis, Ore., and sieved prior to use.

Metals Precipitation Research

To perform metals removal tests, 250 to 1,000 ml of solution was placed in a beaker. A weighed quantity of powdered MgO (Magox HR 98, a product of Basic Chemicals) was added all at once, and the pH was monitored with a pH meter and recorder as the solution was stirred magnetically. After 20 to 30 minutes reaction time, a 0.05-percent solution of Separan AP-30 (an anionic polyacrylamide) was added, followed by another 5 to 10 minutes of stirring.



A



B

Figure 1. Photomicrographs of powdered MgO (A) and crushed periclase (B).

Quantities of MgO and Separan AP-30 solution were 0.1 to 1.0 g/liter and 1.0 ml/liter, respectively. After flocculation, the suspension was either filtered through Whatman #5 paper or poured into a cone to settle. The filtrate or supernatant solution was analyzed by atomic absorption spectroscopy for residual dissolved metals, and the volume of the settled sludge was measured. When a lime slurry was used in parallel tests, the procedure was the same, except that the base was added dropwise until the pH reached 8 to 9. Separan AP-30 solution was used at 1.0 ml/liter. A sodium hydroxide solution was tested on two solutions, but since it gave sludge volumes and metal removals similar to lime, it was not studied further. Adding a weighed quantity of solid lime all at once gave sludge volumes and metals removal equal to those using a lime slurry. Using a threefold to fourfold excess of lime gave pH values of 10.5 to 11.5. Sludge volumes and metals removal were the same as at pH 9, except for Mn and Cd, which were more insoluble at the higher pH values. MgO and lime were used to treat two ore beneficiation waste waters, one mine drainage water, and three prepared solutions.

RESULTS AND DISCUSSION

Comparison of Filter Media

Parallel tests where MgO was compared with silica sand show the enhanced performance of the former. Results using the 20-cm-diameter filter are summarized in Table 1. During runs of 7 hours with kaolin and fine quartz, MgO allowed about half as much particulate to pass through as did sand; even so, the pressure increase was only 2 KPa compared to about 7 to 10 KPa for sand. Figure 2 shows turbidity as a function of time for filtering a 7-ppm quartz suspension using 2.5 ppm alum. In filtrations of kaolin suspensions, filtrate turbidities were very much like that of quartz. Filtrate turbidities for bentonite showed little difference between sand and MgO. However, as with the other particulates tested, pressure increase while using MgO was 2 KPa compared with 11 KPa for the sand. The ability of MgO to retain solids with a lower rate of pressure buildup is due to the loose packing of MgO particles in the filter bed. Sand has about 40% of its bulk volume as voids, while the void volume of MgO is about 55%. Sand of the same nominal grain size would be expected to have a higher straining efficiency, but the positive electrokinetic charge on MgO makes it more effective overall. Figure 3 presents results for iron ore (taconite) processing water in the 2.5-cm-diameter filter, and these follow the results in filtrations of other solids. The filtration rate is 0.20 m/min (5 gpm/ft²). The suspended materials in this water are mainly iron oxide minerals and quartz, but again, MgO operated at least twice as long as sand before breakthrough. An on-site test using a 30-cm-diameter pilot system gave results virtually identical with Figure 3.

Table 2 presents results from comparison of 30/50 mesh MgO with 30/50 mesh garnet sand in a 2.5-cm-diameter dual-media filter. The filter consisted of 15 cm of 20/30

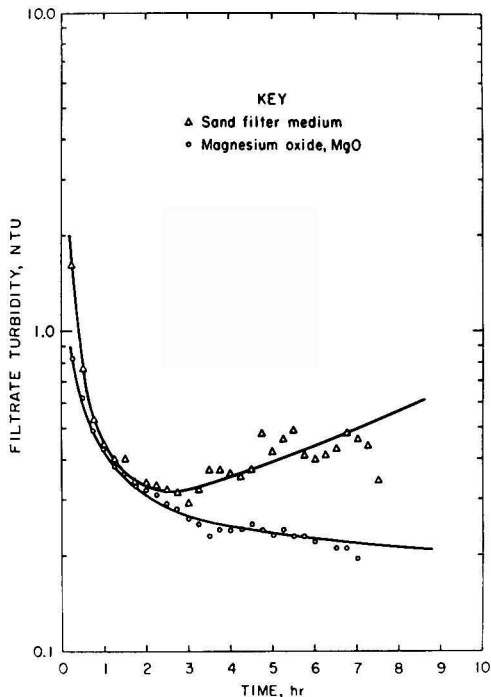


Figure 2. Filtrate turbidity versus time for the filtration of 7 ppm fine quartz with 2.5 ppm alum through MgO and silica sand at a flow velocity of 0.28 m/min.

mesh silica sand followed by 30 cm of 30/50 mesh garnet sand or 30/50 mesh MgO. As with the 20-cm-diameter filter, MgO gave a filtrate of lower turbidity and a lower head loss rate than the garnet sand. For both kaolin and quartz, filtrate turbidities during the first 2 hours were essentially the same for both filters. When kaolin was filtered through garnet sand, the filtrate turbidity began to increase and reached about 1 NTU after 6 hours. In MgO filtration of kaolin, the filtrate turbidity remained very low and increased to only 0.25 NTU in 6 hours. For filtration of the quartz suspension, a breakdown of performance of the garnet sand filter occurred after about 3 hours (see Table 2). MgO removed over 97% of the suspended solids even after 5 hours. The quartz suspension contained over four times as much solids as the kaolin suspension, causing the filters to become saturated and lose effectiveness much more rapidly.

MgO filters were cleaned between filter runs by methods similar to conventional backwashing techniques. Water and air were pumped upward through the 20-cm-diameter filter for 1 to 2 hours to give a 10- to 20-percent bed expansion. This was sufficient to restore the filter to

TABLE 1. SUMMARY OF FILTRATION RUNS USING THE 20-CM-DIAMETER FILTER AT A FLOW VELOCITY OF 0.28 M/MIN.

Suspended solid ^a	Solids concentration, ppm	Alum dosage, ppm	Run duration, hr	Filter medium, 20/30 mesh	Original turbidity, NTU	Filtrate turbidity at 1 hour, NTU	Filtrate turbidity end of run, NTU	Initial pressure drop, KPa	Initial pressure drop, KPa
Kaolin	5.0	5.0	7	Sand	3.1	0.19	0.47	8	15
Kaolin	5.0	5.0	8	MgO	3.3	.18	.15	6	8
Quartz	7.0	2.5	7	Sand	4.5	.44	.46	8	17
Quartz	7.0	2.5	7	MgO	4.8	.43	.20	5	7
Bentonite	5.0	5.0	7	Sand	1.3	.32	.50	10	21
Bentonite	5.0	5.0	7	MgO	1.2	.23	.50	7	9

^a Suspended solids were added to filtered Minneapolis tap water.

TABLE 2. SUMMARY OF FILTRATION RUNS USING THE 2.5-CM-DIAMETER, THREE-COLUMN FILTER SYSTEM AT A FLOW VELOCITY OF 0.24 M/MIN

Suspended solid ^a	Solids concentration, ppm	Alum dosage, ppm	Run duration, hr	Filter medium	Original turbidity, NTU	Filtration Turbidities (NTU) at various times during the runs (hr)						Initial pressure drop, KPa	Final pressure drop, KPa
						1	2	3	4	5	6		
Kaolin	25	10	6	15.2-cm 20/30 mesh sand 30.5-cm 30/50 mesh garnet sand	23	0.31	0.21	0.17	0.40	1.0	0.96	5	15
Kaolin	25	10	6	15.2-cm 20/30 mesh sand 30.5-cm 30/50 mesh MgO	23	.27	.19	.18	.19	0.22	.25	5	11
Quartz	110	15	5	15.2-cm 20/30 mesh sand 30.5-cm 30/50 mesh garnet sand	75	.17	.54	7.5	10.1	10.7	—	7	18
Quartz	110	15	5	15.2-cm 20/30 mesh sand 30.5-cm 30/50 mesh MgO	77	.23	.38	.47	.84	.91	—	7	15

^a Suspended solids were added to filtered Minneapolis tap water.

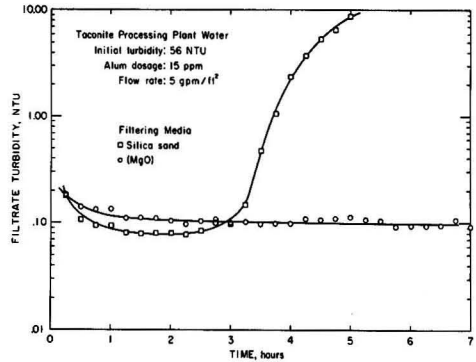


Figure 3. Filtrate turbidity for MgO and sand filtration of taconite processing water.

its original performance. Because of the small size, the 2.5-cm filter could not be cleaned by backwashing. The media was emptied into a beaker, stirred, and rinsed. To determine the long-term stability of MgO filters, the same filter media was used for 50 cycles of filtering a 25-ppm quartz suspension with only air-water backflushing between runs. The testing was spread over one year, and filtrate turbidities and head loss rates were the same for the last runs as for the first ones. No increase in MgO fines was noted from repeated backwashing. Although no loss of performance or media was observed for filtering neutral suspensions, MgO is a basic material so it would dissolve if used to filter acidic solutions.

Unbuffered water initially at pH 6 to 7 has the pH raised to about 8.0 to 8.5 when it is filtered through MgO. The dissolved Mg^{+2} concentration generally increases during filtration by 1 ppm or less.

Metal Concentrations

Table 3 presents the pH and compositions of the waters that were treated. It also compares final metal concentrations when MgO and lime are used to treat them. When equal pH values are attained, MgO leaves less dissolved metal and less metal hydroxide suspended if the solids are separated by sedimentation. The more complete sedimentation of the MgO-metal hydroxide precipitate, compared with the lime precipitate, is due to the low bulk density of the latter.

MgO can remove any metal that is precipitated as the hydroxide. The solubilities of the metal hydroxides determine the required pH, and it is adjusted by varying the quantity of MgO. For example, manganese requires a higher pH than zinc or copper, which in turn requires a higher value than iron. Table 3 also shows the final pH at different MgO dosages for several process water samples. Generally, a threefold to fourfold stoichiometric excess of MgO is required to reach adequate pH values, which are commonly 8 to 9.

Characteristics of Sludge

A principal reason for using MgO instead of lime is the lower volume of hydroxide sludge. Table 4 presents data showing that the lime precipitate occupies about three to five times as much volume. In most cases sludge has to be dewatered or handled in some way, and the more compact material from MgO is clearly advantageous. On standing for about a day or longer, this sludge self-cements into a stable material. The two cones in the photograph (Figure 4) had sediment collected in the bottom, and the cones were tipped to a horizontal position after about 24 hours so the water poured out. The photographs were then taken from above. The sludge on the left was precipitated with

TABLE 3. RESULTS FROM TREATING WATER WITH MgO AND LIME

	pH	Chemical Analysis, ppm							
		Fe	Cu	Zn	Ni	Mn	Co	Cd	Pb
Beneficiation process waste-CM;									
Untreated water	5.4	5.7	0.63	0.55	ND ^b	9.9	ND	ND	ND
Treated with:									
0.1 g/liter ^a MgO, filtered	8.6	<0.2	0.1	<0.1	ND	7.1	ND	ND	ND
0.2 g/liter MgO, filtered	9.2	<.2	.1	<.1	ND	3.4	ND	ND	ND
0.35 g/liter MgO, filtered	9.4	<.2	<.1	<.1	ND	1.3	ND	ND	ND
Beneficiation process waste-BM;									
Untreated water	6.4	<.2	<.1	12.7	<0.2	17.5	ND	ND	ND
Treated with:									
0.16 g/liter MgO, filtered	8.3	ND	ND	<.2	ND	8.3	ND	ND	ND
0.21 g/liter MgO, filtered	8.7	ND	ND	<.2	ND	5.7	ND	ND	ND
0.31 g/liter MgO, filtered	8.9	ND	ND	<.2	ND	1.9	ND	ND	ND
Mine drainage;									
Untreated water	2.7	40	ND	39	ND	41	ND	ND	ND
Treated with 0.5 g/liter MgO, filtered	8.9	.2	ND	.1	ND	15	ND	ND	ND
Prepared solution #1;									
Untreated water	4.2	ND	8.7	ND	12.0	ND	11.1	ND	ND
Treated with:									
0.4 g/liter MgO, filtered	8.9	ND	<.1	ND	<.2	ND	<.2	ND	ND
0.4 g/liter MgO, settled	8.9	ND	.5	ND	.2	ND	.2	ND	ND
0.1 g/liter lime, ^c settled	9.4	ND	.7	ND	1.2	ND	1.6	ND	ND
Prepared solution #2;									
Untreated water	5.4	5.0	.21	2.7	ND	4.4	ND	ND	ND
Treated with:									
0.125 g/liter MgO, filtered	8.9	<.2	<.1	<.1	ND	<.2	ND	ND	ND
0.04 g/liter lime, ^c filtered	8.9	<.2	<.1	.2	ND	2.2	ND	ND	ND
Prepared solution #3;									
Untreated water	4.0	ND	ND	4.2	ND	ND	ND	5.2	4.7
Treated with:									
0.2 g/liter Mg, settled	9.0	ND	ND	<.1	ND	ND	ND	.31	<.5
0.05 g/liter lime, ^c settled	9.0	ND	ND	.8	ND	ND	ND	1.4	1.6

^a The unit g/liter is the grams of MgO used per liter of water treated.

^b ND = not determined, since initial concentrations were below the analysis limit of atomic absorption.

^c Weight of lime is for CaO, not Ca(OH)₂.

MgO, while that on the right was not; the greater stability of the MgO sludge is obvious.

Reaction Times and MgO Dosages

Figure 5 shows a plot of pH vs. reaction time for a range of MgO dosages used to treat process water BM. This water is a mixture of tailings pond overflow and mine water from a Western lead-silver operation. The greater the quantity of MgO used, the more rapidly the pH reached its maximum value. For example, addition of 0.35 g/liter gave essentially the final pH in 5 minutes, but at 0.21 g/liter, the pH is still increasing slowly after 12 minutes. For applying MgO to a full-scale process, a compromise would have to be made between minimum chemical usage on the one hand and sufficiently high pH and minimum reaction time on the other.

For an ideal reaction, the required amount of solid MgO must be added all at once. This permits the slow solid-liquid reaction that is required for a compact precipitate. In one experiment, MgO and water containing metals were continuously added to a stirred beaker. The pH remained at about 9, so the metals reacted with hydroxide in solution rather than with solid MgO. The overflow was collected and allowed to settle, but the precipitate resembled the lime precipitate since it was voluminous and did not cement on standing. In another experiment, a 10-percent slurry of MgO was made and applied in the proper amounts to precipitate dissolved metals. When this slurry was used immediately, results were the same as with solid MgO. However, if the slurry had been prepared for more than 1 to 2 hours before use, the increase in pH was much slower. The sludge was compact, but it did not self-cement.

Disadvantages of MgO in Metals Precipitation

The major disadvantage of MgO is that it costs more than some other basic materials. However, when the total metals content is low, chemical reagents account for only a small fraction of the treatment cost. The savings from easier sludge dewatering, compactness, and stability may more than make up for added reagent costs. If the metal concentration is below 25 to 50 mg/liter, MgO usage will be about 0.25 g/liter (2 pounds per thousand gallons). MgO costing \$330/ton used at this rate would result in chemical expenses of about \$0.08 per m³ (\$0.31 per 1,000 gallons) of water treated. Lime would cost about one eighth as much.

Operation of a continuous process based on MgO is not as straightforward as one where lime or NaOH is used. Since the metals must react directly with solid MgO, a plug-flow or parallel batch reactor system is required to give continuous operation and ensure a compact sludge. Solid reagent is generally not so convenient as a slurry or solution.

TABLE 4. SLUDGE VOLUMES FOR TREATMENT OF PROCESS WATERS WITH MgO AND LIME

	Sludge volume, % ^a	
	Lime, 0.14 g/liter	MgO, 0.55 g/liter
Abandoned metal mine drainage	2.4	0.6
	Lime, 0.025 g/liter	MgO, 0.1 g/liter
Beneficiation process waste-BM	0.9	0.2

^a Volume of sludge per 100 volumes of untreated water.

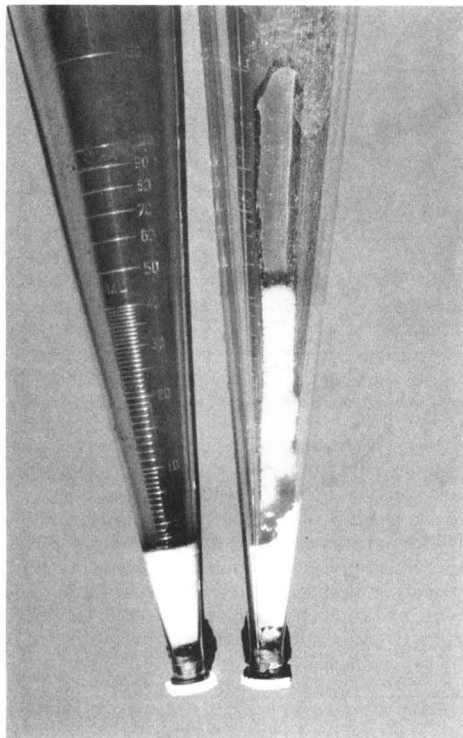


Figure 4. Photograph showing cemented MgO sludge (left cone) compared with normal lime sludge after slight agitation of the sludge.

CONCLUSIONS

The comparative tests described in this paper show MgO (periclase) to be superior to silica sand or garnet sand for filtration of several different particulates. Head loss occurs at a lower rate with MgO, turbidities are lower, and filter runs can be longer. MgO could be used in place of sand in existing equipment, and regeneration of the filter can be accomplished by conventional backflushing.

Powdered MgO (magnesia) removes heavy metals from water to give a compact sludge that self-cements on standing. MgO precipitates metals as well or better than lime, and the MgO-hydroxide sludge is more easily filtered or dewatered. Several minutes reaction time is required for solid MgO. The cost of MgO is greater than the cost of lime but, for water containing low concentrations of dissolved metals, the savings in sludge handling may more than compensate for the cost difference. Future work should determine whether MgO can conveniently be used on a continuous basis for heavy metal removal.

LITERATURE CITED

1. Weber, W. J., "Physicochemical Processes for Water Quality Control," Wiley-Interscience, New York (1972), Chaps. 2 and 4.
2. Kirk-Othmer, "Encyclopedia of Chemical Technology," Wiley-Interscience, New York (1980), Vol. 10, pp. 284-337 and 489-523.

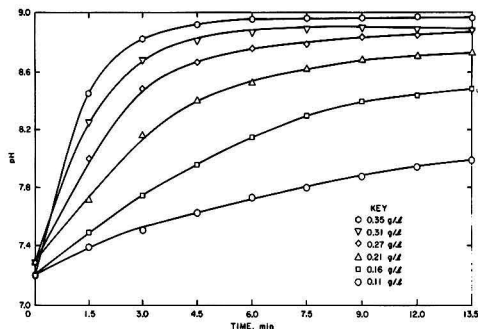


Figure 5. pH-time curves for the treatment of process water BM with various amounts of MgO.

3. Parks, G. A., "The Isoelectric Points of Solid Oxides, Solid Hydroxides, and Aqueous Hydroxo Complex Systems," *Chem. Reviews*, **65**, 177-208 (1965).
4. Oulman, C. S., D. E. Burns, and E. R. Baumann, "Effect on Filtration of Polyelectrolyte Coatings of Diatomite Filter Media," *Jour. AWWA*, **56**, 1233-1239 (1964).
5. Baumann, E. R. and C. S. Oulman, "Polyelectrolyte Coatings for Filter Media," *Proc. Filtration Soc.*, 682-690 (1970).
6. Knight, R. A. and P. Marinaccio, "Process for Producing Microporous Films and Products," U.S. Patent 3,876,738 (April 8, 1975).
7. Lanouette, Kenneth H., "Heavy Metals Removal," *Chem. Eng.* **84**, No. 22, 73-80.
8. Jorgensen, S. E., "Industrial Waste Management," Elsevier Scientific Publishing Company, New York, N.Y. (1979), pp. 187-214.



Joseph E. Schiller received his undergraduate training at Central Michigan University and a Masters degree in Chemistry in 1968 from Michigan State University. Following two years of junior college teaching, he returned to graduate school at the University of North Dakota when he received a Ph.D. in 1973. He is presently employed as Director of Refining Operations at Materials Processing Corporation, St. Paul, Minn.



Daniel N. Tallman received his B.A. in Chemistry in 1980 from Augsburg College, Minneapolis, Minn. He is a research chemist with the Twin Cities Research Center of the U.S. Bureau of Mines. His research interests involve treatment of mineral process waters, filtration, removal and detoxification of cyanides, and removal of heavy metals from mine waste streams. He is a member of the American Chemical Society.



Sanaa E. Khalafalla received his Ph.D. in Physical Chemistry from the University of Minnesota in 1953. His current research includes chemical and electrochemical aspects of drilling, dust physical chemistry and wettability, mineral process waters and spontaneous combustion. He is a member of AIME and past chairman of the Physical Chemistry Committee of TMS-AIME. He has authored over 120 publications and holds 15 U.S. Patents.

AIChE ENVIRONMENTAL DIVISION NEWSLETTER



Environmental Division (1970)

It shall (a) further the application of chemical engineering in the environmental field; (b) provide, in cooperation with the national Program Committee, suitable programs on environmental topics of current interest; (c) provide a communication medium for chemical engineers and other individuals to exchange nonconfidential information concerning all facets of environmental activity; (d) promote publication of papers of interest to chemical engineers in environmental activities; (e) coordinate the Institute's activities with other societies active in the environmental field; (f) act as a source of information for chemical engineers who are not actively engaged in the environmental field to bring to their attention the importance of concern for the environment, the need for its consideration in the design and operation of process plants, and opportunities in research and design of equipment and processes to solve environmental problems; (g) encourage chemical engineering educators to place suitable emphasis on protecting our environment and encourage excellence in courses in environmental engineering.

AIChE ENVIRONMENTAL DIVISION

EXECUTIVE COMMITTEE — 1984

CHAIRMAN	Theodore M. Fosberg Resources Conservation Co., P.O. Box 3766 Seattle, WA 98124206 / 828-2416
FIRST VICE CHAIRMAN	Alexander H. Danzberger Consultant, 13245 Willow Lane Golden, Colorado 80401303 / 238-4750
SECOND VICE CHAIRMAN	Louis J. Thibodeaux University of Arkansas, 227 Engineering Building Fayetteville, AR 72701501 / 575-4951
SECRETARY	Daniel L. Bensing Tennessee Eastman Co., P.O. Box 511 Kingsport, TN 37662615 / 229-5327
TREASURER	Richard Prober Havens and Emerson, Inc., 700 Bond Court Bldg. Cleveland, OH 44114216 / 621-2407
PAST CHAIRMAN	David L. Becker NUS Corporation, 1300 N. 17th Street Rosslyn, VA 22209703 / 522-8802
COUNCIL LIAISON	David B. Nelson Monsanto Research Corporation, Sta. B, Box 8 Dayton, OH 45407513 / 268-3411

DIRECTORS

DIRECTOR (1982-1984)	D. Bhattacharyya Dept. of Chemical Engr., University of Kentucky Lexington, KY 40506606 / 258-4958
-----------------------------------	--	-----------------

DIRECTOR (1982-1984)	Gary L. Leach 2210 South Memorial Pasadena, TX 77502713 / 946-9340
DIRECTOR (1983-1985)	Michael R. Overcash North Carolina State University, P.O. Box 5035 Raleigh, NC 27650919 / 737-2325
DIRECTOR (1983-1985)	Leo Weitzman Acurex Waste Technology, Inc., 8074 Beechmont Ave. Cincinnati, OH, 45230513 / 474-4420
DIRECTOR (1984-1986)	Jacoby A. Scher Resources Engr., Inc. N.E. Greenway Plaza Houston, TX 77046713 / 621-5900
DIRECTOR (1984-1986)	David G. Stephan U.S. Environmental Protection Agency Cincinnati, OH 45268513 / 684-7418

TECHNICAL SECTION CHAIRMEN

AIR SECTION	Richard D. Siegel Stone & Webster Engineering Corp., P.O. Box 2325 Boston, MA 02107617 / 589-7620
WATER SECTION	Robert L. Irvine Department of Civil Engineering, University of Notre Dame Notre Dame, IN 46556219 / 239-6306
SOLIDS SECTION	B. Tod Delaney Ground/Water Technology, Inc., 100 Ford Road Denville, NJ 07834201 / 625-5558

NEWSLETTER EDITOR	Marx Issacs 1513 Barbee Ave. Houston, TX713 / 523-6049
--------------------------------	--	-----------------

COMMITTEE CHAIRMEN

PROGRAMMING BOARD	D. Bhattacharyya	
Dept. of Chemical Eng., University of Kentucky		
Lexington, KY 40506		606/258-4958
AID/LIFE	Michael R. Overcash	
Chemical Engineering Department, No. Carolina State Univ.		
P.O. Box 5035, Raleigh, NC 27650		919 / 737-2325
AMERICAN ACADEMY OF ENVR. ENGRS.	C. J. Touhill	
Michael Baxter, Jr., Inc., Box 280		
Beaver, PA 15009		412 / 495-7711
AWARDS	Les Lash	
2877 Kentucky Avenue	(H) 801 / 277-9319	
Salt Lake City, UT 84117	(O) 801 / 566-7711	
CONTINUING EDUCATION	Michael R. Overcash	
Chemical Engineering Department, North Carolina State Univ.		
P.O. Box 5035, Raleigh, NC 27650		919 / 737-2325
PUBLIC RELATIONS & MEMBERSHIP	Marx Isaacs	

1513 Barbee, Houston, TX 77004		713 / 523-6049
NOMINATING	David L. Becker	
NUS Corporation, 1300 N. 17th Street		
Rosslyn, VA 22209		703 / 522-8802
WATER TASK FORCE	David B. Nelson	
Monsanto Research Corporation, Station B, Box 8		
Dayton, OH 45407		513 / 268-3411
SOLIDS & HAZARDOUS WASTE TASK FORCE		
	David P. Schoen	
Owens-Corning Fiberglas, Fiberglas Tower		
Toledo, OH 43659		419 / 248-8278
AIR TASK FORCE	John (Jack) F. Erdmann	
Union Carbide Corporation, P.O. Box 471		
Texas City, TX 77590		409 / 948-5126
INTERSOCIETY LIAISON	Robert A. Baker	
U.S. Geological Survey, Gulf Coast Hydroscience Center		
NSTL Station, MS 39529		601 / 688-3130
EDITOR - ENVIRONMENTAL PROGRESS	Gary F. Bennett	
Department of Chemical Engineering, University of Toledo		
Toledo, OH 43606		419 / 537-2520

AAEE PARTICIPATION AT PHILADELPHIA

Largely through the efforts of Robert T. Jaske, AIChE Trustee to the American Academy of Environmental Engineers (AAEE), the Academy will present a four-session mini-symposium at the Philadelphia AIChE Meeting, in cooperation with the officers and members of the Environmental Division. The sessions will be related to the general subject of risk assessment in decision-making involved in toxic and hazardous waste management.

APCA/AICHe ENVIRONMENTAL DIVISION COOPERATION

After two years of trying, progress has finally started on this cooperative effort. The APCA has provided us with a list of potential chairpeople for the Philadelphia meeting. To maintain the cooperation it will now be necessary to reciprocate by giving APCA a list of people who could co-chair APCA sessions.

In addition to the Annual Meetings, the APCA sponsors several Specialty Conferences as well as Sectional and Local Meetings. We can offer to reciprocate at the Annual Meeting or at a Specialty Conference.

The APCA suggested the following topics as possible areas of cooperation:

- Acid rain
- Hazardous air pollutants
- Innovative analytical techniques
- Mobile combustion
- Any session in cooperation with TS-3.1 Chemical, TS 3.4 Petroleum or TT Basic Science and Technology Technical Committees

There is a whole series of co-sponsored sessions between AIChE and APCA that seem to be natural. These would deal with the whole broad question of atmospheric chemistry, acid rain and transport, APCA could present the regulators' viewpoint to the AIChE at its meetings and AIChE could present the chemists' and scientists' viewpoints on these subjects to APCA.

Environmental Progress (Vol. 3, No. 2)

ENVIRONMENTAL DIVISION EMPLOYMENT/RESUME FILE

Last November at the Washington meeting of the Environmental Division Executive Committee, it was proposed that a file of resumes of unemployed, underemployed or about-to-be-unemployed members be kept by a Division member. The purpose would be to give members a central point of focus within the Division, with regard to the employment situation. Tom Goodgame agreed to retain the file. As of the latest report, five resumes of Division members were already in the file.

For this system to work to the best advantage for all concerned, cooperation by all members is a "must."

Tom needs the resumes of all members seeking employment. He prefers that they be sent to his home address: 120 Higman Park, Benton Harbor, MI 49022. Tom should be notified by anyone whose resume should be removed from the file.

Whenever a Division member hears of an opening that might be of interest to another member seeking employment, he should let Tom know about it. If called by an employment agency seeking job candidates, explain how this is handled and give Tom's name and telephone number (office, 616/926-5208; home, 616/927-2631). There will be no problem reaching him at whichever number the caller prefers.

MEMBER NEWS

THOMAS H. GOODGAME, Director Environmental Control, Whirlpool Corporation and former Chairman of the AIChE Environmental Division, has been designated an Arkansas Traveler by Arkansas Governor Clinton. This award is presented to outstanding citizens of other states who have traveled in Arkansas and distinguished themselves by their accomplishments. Tom has also received the Institute President's Award from the Porcelain Enamel Institute.

THEODORE M. FOSBERG, 1984 Chairman of the Division, is a new Diplomate of the American Academy of Environmental Engineers (AAEE).

ALEXANDER H. DANZBERGER, First Vice Chairman of the Division, has accepted the chairmanship of the Water Quality Subcommittee, reporting to the Government Programs Steering Committee (GPSC).

May, 1984

M6

**ENVIRONMENTAL SESSIONS
AIChE NATIONAL MEETING
PHILADELPHIA, PA.
AUGUST 19-22, 1984**

AIR

1. Environmental Aspects of Synfuel Industries - An Update (R. Mahalingham)
2. Reuse, Recovery & Recycling in Pharmaceutical & Biotechnology Industries, Parts I and II (S. M. Barnett)
3. Environmental Impact of Pharmaceutical & Biotechnology Industries (J. A. Phillips)
4. Process Modifications for Emissions Control in Plastics & Synthetics Industries (L. R. Roberts)
5. Reuse, Recovery, Recycling in Plastics & Synthetics Industries (R. E. Kenson)
6. Environmental Impact of Plastics & Synthetics Industries (T. A. Kittleman)
7. Monitoring at Hazardous Waste Sites-I (L. J. Thibodeaux)
8. Modeling at Hazardous Waste Sites-I (L. J. Thibodeaux)
9. Environmental Policy-Multimedia (W. J. Lacy, R. D. Siegel)
10. Hazardous Waste Incineration (E. Crumpler, L. J. Thibodeaux)

WATER

- 1,2. Tutorial on Genetic Engineering & Pollution Control-I, II (R. L. Irvine)
3. Monitoring of Hazardous Waste Sites-II (R. Evans)
4. Modeling of Hazardous Waste Sites-II (W. G. Gray)
5. Fundamentals of Biological Fixed-Film Processes for Hazardous Waste Treatment (B. E. Rittmann)
6. Use of Physical-Chemical Processes for Treatment of Hazardous Wastes (R. W. Peters)
7. Innovative Process for In-Situ Treatment of Hazardous Wastes (G. W. Dawson)
8. Heavy Metals Separation in Plating and Metal Processing Industries (B. M. Kim)

9. Oil Production Abatement: Onshore, Offshore, On the High Seas (E. I. Shaheen)
10. Liquid Phase Oxidation of Wastewaters Containing Hazardous Organics (D. Battacharyya)

SOLID WASTES

1. Considerations in Disposal of Solid/Hazardous Materials (Q. Todd)
2. Advanced Technology in Waste Treatment Fundamentals (M. Hunt)
3. Advanced Technology in Waste Treatment Design Considerations (W. Tambo)
4. Liability Questions/Hazardous Waste (B. T. Delaney)
5. Uncontrolled Hazardous Waste Sites - Case Studies (B. T. Delaney)
6. Remedial Action at Hazardous Waste Sites - Case Studies (D. Moon)
7. Reuse, Recovery, Recycling of Byproducts of Manufacturing (D. P. Schoen)

MINI-SYMPOSIUM

"Toxic & Hazardous Wastes: Multi-Media Considerations in Risk Assessment"

Sponsored by the American Academy of Environmental Engineers (AAEE) in cooperation with the officers and members of the AIChE Environmental Division.

1. Risk for Toxic and Hazardous Wastes - Their Nature and Their Threat to the Public Health and Welfare and its Assessment (H. T. Miller)
2. Toxic and Hazardous Wastes: Risk Management of Toxic Air Pollutants (W. Reilley)
3. Toxic and Hazardous Wastes: Considerations Involving Multi-Media Transport with Primary Routing Through Water (C. J. Touhill)
4. Toxic and Hazardous Wastes: Multi-Media Considerations in Risk Assessment Methodology and Decisionmaking Tools (W. H. Busch)

AICHE

Serving
Chemical Engineers
Since 1908

AICHE Symposium Series

ADVANCES IN PRODUCTION OF FOREST PRODUCTS

Andrew J. Baker, *Editor*

(*AICHE Symposium Series, Volume 79, No. 223*) The edited papers in this publication were presented at the Forest Products Division Symposium at the November 8-12, 1981 AIChE Meeting in New Orleans, Louisiana. *Contents:* A Review of Recent Developments in Debris Removal and Chemical Recovery from Pulp. Conversion of Cellulose Waste to Low-Cost Ethanol. Effect of Air on the Pulp Washer. Theory and Application of Horizontal Belt Type Filters for Pulp Washing and Recovery of Spent Cooking Liquors from Chemical Pulps. Ozone Mass Transfer Into Agitated Low Consistency Wood Pulp. Simulation Analysis Using Linear Techniques. Optimal Operation of Evaporators Subject to Rapid Fouling. Temperature Predictions for Closed Paper Machine Water Systems. Use of Computers in the Sawmill. Cogeneration in the Small Wood Products Plant. Trends in the Use of Chemicals for Preservative Treatment of Wood. Research Progress in Wood-Based Composite Products. Tables, figures, bibliographies.

(ISBN 0-8169-0247-X LC 83-8839)

Pub. #S-223 AICHE Members: \$15
87 pp. Others: \$30

PROBLEM SOLVING

J. T. Sears, D. R. Woods, and R. D. Noble, *Editors*

The purpose of this book is to assist practicing professionals by providing information to increase their awareness of how they solve problems, along with ideas for improvement. Educators and industrial training officers will find ideas on the development and incorporation of problem solving useful to their programs. Although the examples are presented in Chemical Engineering terms, they will also prove

useful in such disciplines as Chemistry, Physics, Fine Art, History, Nursing, Business and Psychology. *Contents:* Chemical Engineering Applications of a Problem-Solving Taxonomy. Incorporation of Problem-Solving Into Chemical Engineering Courses. Problem Solving and Chemical Engineering, 1981. Anxiety: Another Aspect of Problem Solving. Analysis of Student Mistakes, and Improvement of Problem-Solving on McCabe-Thiele Binary Distillation Tests. The Design of a Course in Problem Solving. Solving Problems in Industry. The Modeling Framework for Problem Solving.

(ISBN 0-8169-0255-0 LC83-15515)

Pub. # S-228 AICHE Members \$12
63 pp. Others \$24

UNDERGROUND COAL GASIFICATION: THE STATE OF THE ART

William B. Krantz and Robert D. Gunn, *Editors*

AICHE Symposium Series, Vol. 79 No. 226 contains papers presented at the 1982 Spring Meeting in Anaheim, June 6-10, 1982. *Contents:* Underground Coal Gasification. The Hanna Wyoming Underground Coal Gasification Field. Review of Underground Coal Gasification Field Experiments at Hoe Creek. ARCO's Research and Development Efforts in Underground Coal Gasification. The Large Block Experiments in Underground Coal Gasification. Research and Development on Underground Gasification of Texas Lignite. The Role of Instrumentation in UCG Process Development. Modeling the Underground Coal Gasification Process. An Analysis of Permeation Models for In Situ Coal Gasification. Sweep Efficiency Models for Underground Coal Gasification. Environmental Effects of In Situ Coal Gasification. Water Quality Monitoring at the Hoe Creek Test Site. Evaluation of the Use of UCG Gas to Produce Methanol.

(ISBN 0-8169-0251-8 LC 83-11741)

Pub. # S-226 AICHE Members: \$25
185 pp. Others: \$50

SEND YOUR BOOK ORDERS TO: Publications Sales Dept. E. American Institute of Chemical Engineers, 345 E. 47 St., New York, NY 10017. All orders must be accompanied by check or money order in U.S. dollars. No charge for postage or handling on U.S. orders. All foreign orders, regardless of quantity, must be accompanied by payment in U.S. dollars and must include \$2.00 per book to cover postage and handling. All books will be shipped bookrate. All sales are final.

Prices are subject to change

AMERICAN INSTITUTE OF CHEMICAL ENGINEERS

345 EAST 47 STREET
NEW YORK, N.Y. 10017

Environmental Progress (Vol. 3, No. 2)

May, 1984

M8



Serving
Chemical Engineers
Since 1908

Manual for Predicting Chemical Process Design Data

AICHe DESIGN INSTITUTE FOR PHYSICAL
PROPERTY DATA

DATA PREDICTION MANUAL

Ronald P. Danner and Thomas E. Daubert, Editors

AIChE and DIPPR are proud to announce the availability of this important research tool, which has been tested in the field for over one year and which has proven indispensable to the practicing engineer.

All material in the **DATA PREDICTION MANUAL** has been carefully selected and evaluated for accuracy, ease of use, and reliability. Literature sources, examples, and comments on reliability are included. To facilitate inclusion of new material and future revisions, the **DATA PREDICTION MANUAL** has been published in loose-leaf format.

Recommended methods which require simple input parameters for predicting physical and thermodynamic properties of chemicals are presented. Concentration is entirely on nonhydrocarbon materials. When feasible, requisite equations and procedures for calculation using a pocket calculator are provided. When more accuracy is required, alternate procedures for using a large computer are given. In most cases, property estimations methods are provided for pure compounds and mixtures of defined composition.

Chapters 1, 2, 3, 4, and 12

Contents:

Chapter 1. GENERAL DATA. Introduction. Units and Conversion Factors. Chemical Engineering Symbols. Miscellaneous Characterizing Parameters. General and Specific Property References.

Chapter 2. CRITICAL PROPERTIES. The Critical State of a Pure Compound. The Critical State of Mixtures. The Critical Locus. Excess Critical Properties. Pseudocritical Properties. References. Procedures.

Chapter 3. VAPOR PRESSURE. Procedures.
Chapter 4. DENSITY. Procedures.
Chapter 12. MEASURES OF ENVIRONMENTAL
MPACT. Procedures.

NOTE: Loose-leaf 7 hole binder is included with the above chapters.

Pub.# X98. Chapters 1, 2, 3, 4, 12.
(ISBN 0-8169-0233-X)

*Sponsor: \$75

AIChE Members: \$125 Others: \$150

(U.S. Postage is prepaid. Foreign orders add \$10 to cover postage and handling)

**Since this publication was, in part, made possible due to the support of sponsoring companies, we are offering this special discount to these organizations.*

When placing your order for the initial five chapters, please remember to request receipt of the remaining chapters on a Standing Order basis.

REMAINING CHAPTERS TO BE PUBLISHED

- Chapter 5. THERMAL PROPERTIES.
- Chapter 6. PHASE EQUILIBRIA.
- Chapter 7. SURFACE TENSION.
- Chapter 8. VISCOSITY.
- Chapter 9. THERMAL CONDUCTIVITY.
- Chapter 10. DIFFUSIVITY.
- Chapter 11. COMBUSTION.

These chapters will be available on a **Standing Order** basis. Standing Order Customers will automatically receive each chapter as soon as it becomes available, and will be billed with shipment. All will be seven-hole punched for easy insertion into materials previously received. Prices will vary according to length and complexity.

SEND YOUR BOOK ORDERS TO: Publications Sales Dept. A, American Institute of Chemical Engineers, 345 E. 47 St., New York, NY 10017. All orders must be accompanied by check or money order in U.S. dollars. All books will be shipped bookrate. All sales are final.

(Prices are subject to change)

AMERICAN INSTITUTE OF CHEMICAL ENGINEERS

345 EAST 47 STREET
NEW YORK, N.Y. 10017



Serving
Chemical Engineers
Since 1908

New Data Prediction Manual

AICHE DESIGN INSTITUTE FOR PHYSICAL PROPERTY DATA

DATA PREDICTION MANUAL

Ronald P. Danner and Thomas E. Daubert, Editors

AIChE and DIPPR are proud to announce the availability of this important research tool, which has been tested in the field for over one year and which has proven indispensable to the practicing engineer.

All material in the **DATA PREDICTION MANUAL** has been carefully selected and evaluated for accuracy, ease of use, and reliability. Literature sources, examples, and comments on reliability are included. To facilitate inclusion of new material and future revisions, the **DATA PREDICTION MANUAL** has been published in loose-leaf format.

Recommended methods which require simple input parameters for predicting physical and thermodynamic properties of chemicals are presented. Concentration is entirely on nonhydrocarbon materials. When feasible, requisite equations and procedures for calculation using a pocket calculator are provided. When more accuracy is required, alternate procedures for using a large computer are given. In most cases, property estimation methods are provided for pure compounds and mixtures of defined composition.

**Chapters 1, 2, 3, 4, and 12
will be available July 1, 1983**

Contents:

Chapter 1. GENERAL DATA. Introduction. Units and Conversion Factors. Chemical Engineering Symbols. Miscellaneous Characterizing Parameters. General and Specific Property References.

Chapter 2. CRITICAL PROPERTIES. The Critical State of a Pure Compound. The Critical State of Mixtures. The Critical Locus. Excess Critical Properties. Pseudocritical Properties. References. Procedures.

Chapter 3. VAPOR PRESSURE. Procedures.
Chapter 4. DENSITY. Procedures.
Chapter 12. MEASURES OF ENVIRONMENTAL
IMPACT. Procedures.

**NOTE: Loose-leaf 7 hole binder is
included with the above chapters.**

**Pub. # X98. Chapters 1, 2, 3, 4, 12.
(ISBN 0-8169-0233-X)**

***Sponsor: \$75**

AIChE Members: \$125

Others: \$150

**(U.S. Postage is prepaid. Foreign orders add \$10
to cover postage and handling)**

**Since this publication was, in part, made possible
due to the support of sponsoring companies, we are
offering this special discount to these organizations.*

**When placing your order for the initial five
chapters, please remember to request receipt of
the remaining chapters on a Standing Order
basis.**

REMAINING CHAPTERS TO BE PUBLISHED

Chapter 5. THERMAL PROPERTIES.
Chapter 6. PHASE EQUILIBRIA.
Chapter 7. SURFACE TENSION.
Chapter 8. VISCOSITY.
Chapter 9. THERMAL CONDUCTIVITY.
Chapter 10. DIFFUSIVITY.
Chapter 11. COMBUSTION.

These chapters will be available on a **Standing Order** basis. Standing Order Customers will automatically receive each chapter as soon as it becomes available, and will be *billed* with shipment. All will be seven-hole punched for easy insertion into materials previously received. Prices will vary according to length and complexity.

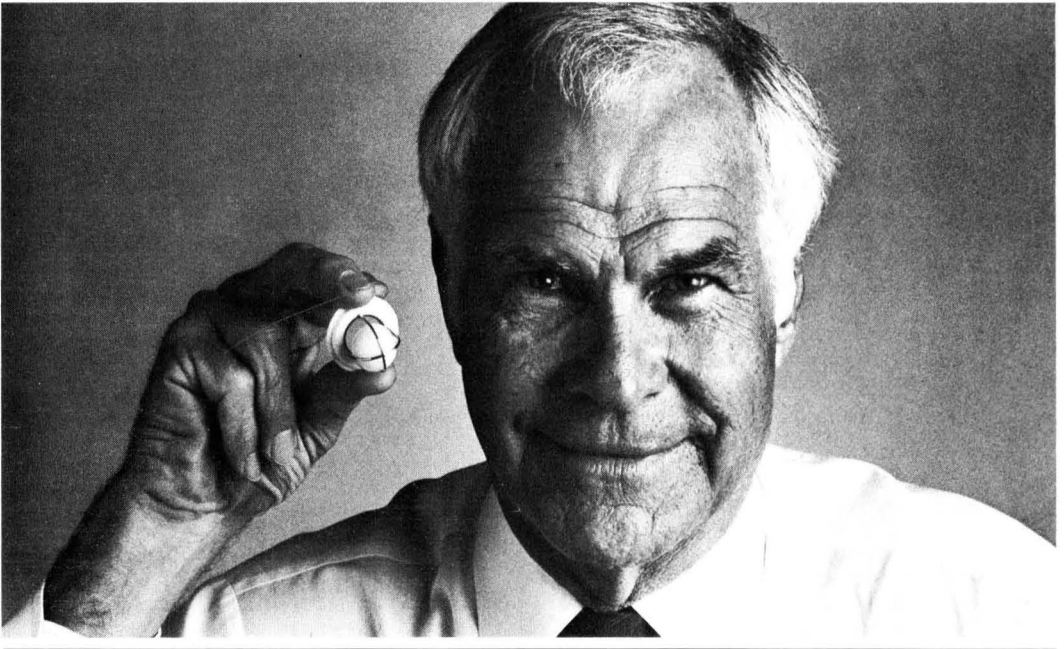
SEND YOUR BOOK ORDERS TO: Publications
Sales Dept. A. American Institute of Chemical
Engineers, 345 E. 47 St., New York, NY 10017. All
orders for less than 10 books must be accompanied by
check or money order in U.S. Dollars. All books will
be shipped bookrate. All sales are final.

Prices are subject to change.

AMERICAN INSTITUTE OF CHEMICAL ENGINEERS

**345 EAST 47 STREET
NEW YORK, N.Y. 10017**

In 1955, the artificial heart valve was just an idea. This year, it saved my life.



For over 30 years, The American Heart Association has invested research money in ideas. Lifesaving ideas like the artificial heart valve, cardiopulmonary resuscitation and drugs to control high blood pressure. Today, these ideas save lives.

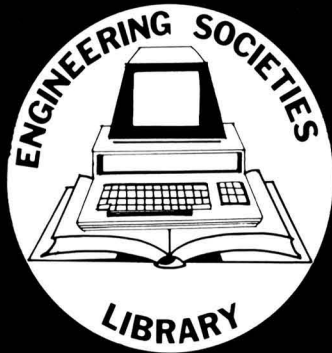
Despite this progress, one of every two American deaths is caused by diseases of the heart and blood vessels.

If today's ideas are to grow into the lifesaving techniques of tomorrow, the American Heart Association needs your support now.

American Heart Association, We're Fighting for Your Life.



WE'RE FIGHTING FOR YOUR LIFE



information for engineers

The Engineering Societies Library serves more than 100,000 readers and researchers a year, two thirds of whom make their requests by mail or telephone. The largest engineering library in the free world, its facilities are available to all those who need engineering information.

Photocopying is done on request. On-line ordering is available. Literature searches are made for all purposes. All inquiries are kept confidential. Services include both manual searches in the literature of engineering and technology and computer searches on the DIALOG, ORBIT, and BRS systems.

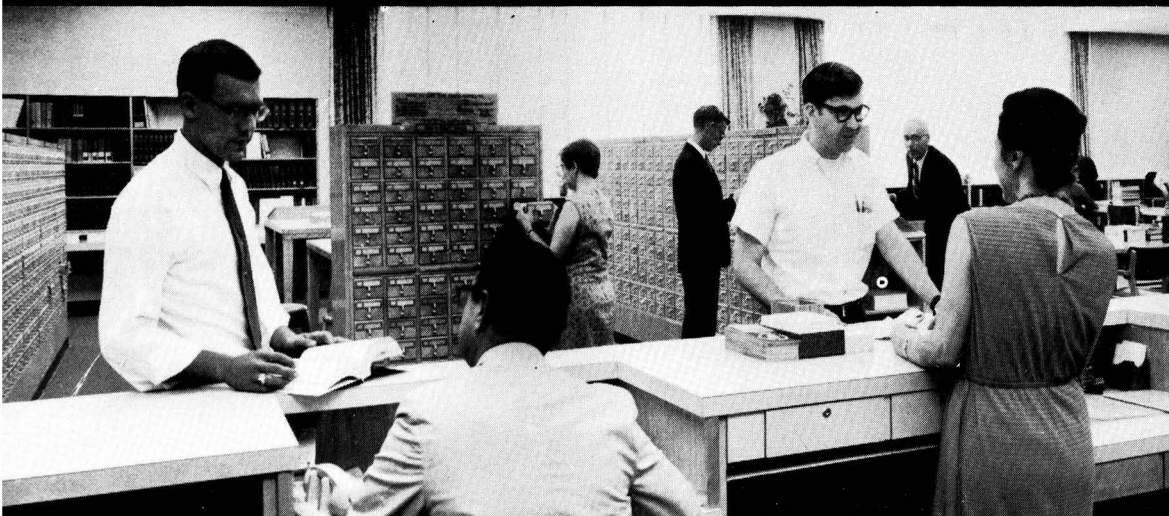
Books may be borrowed in person or by mail by members of ASME, IEEE, IES, SWE, ASCE, AIChE, and AIME within the continental U.S. and Canada. A member may have three books on loan at one time and may keep them up to two weeks, not counting time in transit.

Write for brochure detailing services and discounts to members of supporting societies.

ENGINEERING SOCIETIES LIBRARY, UNITED ENGINEERING CENTER

345 East 47TH St., New York, N.Y. 10017

Call (212) 705-7611



ENVIRONMENTAL[®] **PROGRESS**

May 1984
Volume 3, No. 2

25.11.84

2202/P